

https://dspace.org/

The deactivation of silico-aluminophosphate catalysts during methanol conversion reactions

Cornel, Veronica May

1993
https://hdl.handle.net/10539/24277

Downloaded from a DSpace repository. https://dspace.org/

THE DEACTIVATION OF SILICO-ALUMINOPHOSPHATE CATALYSTS DURING METHANOL CONVERSION REACTIONS

Veronica May Cornel

A dissertation submitted to the Faculty of Science,
University of the Witwatersrand, Johannesburg,
in fulfilment of the requirements for the degree of
Master of Science

Johannesburg, February, 1993

To my husband, Ant·n

DECLARATION

I declare that this dissertation is my own work and that any technical and industrial assistance has been acknowledged.

It is being submitted for the degree of Master of Science in the University of the Witwatersrand, Johannesburg. It has not been submitted before for any other degree or examination in this or any other University.



Veronica May Cornel

28th day of January 1993

ABSTRACT

This dissertation focusses on the deactivation of SAPO-34 and modified SAPOs during methanol conversion under various conditions, in comparison to H-ZSM-5.

SAPO-34 was found to deactivate rapidly during methanol conversion. This was shown by the decrease in activity, surface area and pore volume of the catalyst. The deposited "coke" was analysed by *in situ* diffuse reflectance infra-red Fourier Transform spectroscopy, solid-state magic angle spinning nuclear magnetic resonance, gas chromatography mass spectroscopy (GCMS) of the HF- and dichloromethane-extracted "coke", and GCMS of the organic species released during regeneration of the catalyst and trapped in resin in capillary inlet tubes. The "coke" consisted of alkylated aromatics and naphthalenes which probably formed on the surface or in the large cavities of SAPO-34.

The amount of "coke" deposited during methanol conversion increased with reaction temperature, decreased with dilution of the methanol with water or nitrogen, and decreased with increased pressure. Incorporation of Ni into the SAPO framework did not decrease the rate of deactivation, but the "coke" that was deposited was less bulky than that deposited in SAPO-34. Modification of the SAPO-34 with trimethyl silylchloride decreased the rate of deactivation of the catalyst.

ACKNOWLEDGEMENTS

I would like to thank my supervisor, Prof. Neil Coville, University of the Witwatersrand for his support, suggestions and guidance. Prof. Coville was very understanding about the difficulties experienced in conducting this study part-time.

Special thanks to Dr David Robinson for his inspiration in starting this study, as well as for his encouragement and guidance during the experimental stages. The novel technique for concentrating the organics released during regeneration of spent catalysts was inspired by Dr Robinson.

I would like to express my sincere appreciation to Dr Lawrence Jansen van Rensburg, Catalysis Research Group, AECI, for his encouragement, insights, and guidance throughout this study, as well as for reading and correcting the first draft of this dissertation.

I would like to thank Dr Richard Copperthwaite, Dr Ken Buchanan, Dr Roger Jones and Frank Fischer of AECI for allowing me to undertake this part time study while working at AECI. Special thanks to Dr Copperthwaite for his support, insights and helpful suggestions.

I would like to express my appreciation for the analytical work completed by the following people:

Marcel Brands, AECI, for the TGA analyses

Dr Tony Chalmers, CSIR, for the MAS NMR analyses

Marejke Ewen, AECI, for the XRF and XRD analyses

Clement Stander, AECI, for some of the mass spectroscopy analyses

Shadrack Shabangu, AECI, for the C and H analyses

Flo van Rooyen, AECI, for some of the mass spectroscopy analyses

Joe Wollbrandt for help with the DRIFTS analyses

Simon Yunes, Micromeretics, for the TPD spectra

LIST OF ABBREVIATIONS

ALPO	= Aluminophosphate
Atm	= Atmospheres
BET	= Brunauer-Emmett-Teller
"COKE"	= Carbonaceous Deposits
Conv.	= Conversion
CP	= Cross Polarization
DME	= Dimethylether
DRIFTS	= Diffuse Reflectance Infra-red Fourier Transform Spectroscopy
Ed	= Editor
EPR	= Electron Paramagnetic Resonance
ESR	= Electron Spin Resonance
FTIR	= Fourier Transform Infra-red
GC	= Gas Chromatography
GCMS	= Gas Chromatography Mass Spectroscopy
HPLC	= High Performance Liquid Chromatography
IR	= Infra-red
MAS NMR	= Magic Angle Spinning Nuclear Magnetic Resonance
MeAPO	= Substituted Aluminophosphate
MeAPSO	= Substituted Silico-aluminophosphate
MEOH	= Methanol
Ni-SAPO	= Nickel-substituted Silico-aluminophosphate
SAPO	= Silico-aluminophosphate
SBU	= Secondary Building Unit
Si-SAPO	= Silicon-substituted silico-aluminophosphate

STP	= Standard Temperature and Pressure
TEM	= Transmission Electron Microscopy
TEAOH	= Tetra-ethyl Ammonium Hydroxide
TGA	= Thermal Gravimetric Analysis
TG/DTA	= Thermal Gravimetric Differential Thermal Analysis
TMSC	= Trimethyl Silylchloride
TPD	= Temperature Programmed Desorption
WHSV	= Weight Hourly Space Velocity
XRD	= X-Ray Diffraction
XRF	= X-Ray Fluorescence
XPS	= X-Ray Photo-electron Spectroscopy
ZSM-5	= Zeolite Socony Mobil 5

CONTENTS

	Page
ABSTRACT	i
ACKNOWLEDGEMENTS	ii
LIST OF ABBREVIATIONS	iv
CONTENTS	vi
LIST OF FIGURES	xi
LIST OF TABLES	xiv
CHAPTER ONE : GENERAL INTRODUCTION	
1.1 INTRODUCTION	1
1.2 SCOPE OF DISSERTATION	3
1.3 ZEOLITE STRUCTURES	4
1.3.1 Zeolite Y	5
1.3.2 ZSM-5	6
1.3.3 Chabazite	7
1.3.4 Gmelinite	9
1.4 ZEOLITE ACIDITY	10
1.5 METHANOL TO OLEFINS AND GASOLINE	12
1.6 MECHANISM FOR "COKE" FORMATION	13
1.7 ZEOLITE DEACTIVATION	15
1.7.1 EFFECT OF PORE STRUCTURE	15
1.7.2 EFFECT OF ACID SITES	20
1.8 CHARACTERIZATION OF "COKE"	21
1.9 REGENERATION OF ZEOLITES	25
1.10 REFERENCES	26

Page

CHAPTER TWO : INTRODUCTION : DEACTIVATION OF SAPOs

2.1 SILICO-ALUMINOPHOSPHATE STRUCTURES 30

2.2 ACIDITY OF SAPOs 31

2.3 METHANOL CONVERSION OVER SAPOs 32

2.4 EFFECT OF PORE STRUCTURE ON THE DEACTIVATION OF SAPOs 36

2.5 EFFECT OF THE ACID SITES OF SAPOs ON DEACTIVATION 37

2.6 "COKE" FORMATION ON SAPOs DURING METHANOL CONVERSION 37

2.7 REGENERATION OF SAPO CATALYSTS 38

2.8 REFERENCES 39

CHAPTER THREE : CATALYST PREPARATION AND CHARACTERIZATION

3.1 INTRODUCTION 41

3.2 EXPERIMENTAL 41

3.2.1 Treatment of ZSM-5 41

3.2.2 Synthesis of SAPO-34 42

3.2.3 Synthesis of SAPO-5 43

3.2.4 Synthesis of Me-APSO 43

3.2.5 Modifications of SAPO-34 44

3.2.6 Characterization of the catalysts 44

3.3 RESULTS AND DISCUSSION 45

3.3.1 X-ray diffraction and X-ray fluorescence spectroscopy 45

3.3.1.1 H-ZSM-5 45

3.3.1.2 SAPO-34 47

3.3.1.3 SAPO-5 48

3.3.1.4 Ni-SAPO 50

3.3.1.5 Silicon-modified SAPO-34 51

Page

3.3.2 Solid state magic angle spinning – nuclear magnetic resonance spectra 53

3.3.3 Temperature programmed desorption studies 55

3.4 CONCLUSIONS 57

3.5 REFERENCES 58

CHAPTER FOUR : DEACTIVATION OF CATALYSTS DURING METHANOL CONVERSION – MEASUREMENT OF "COKE" DEPOSITION

4.1 INTRODUCTION 59

4.2 EXPERIMENTAL 62

4.2.1 Methanol conversion experiments 62

4.2.2 Surface area analysis 63

4.2.3 Pore volume analysis 64

4.2.4 Carbon and hydrogen analysis 65

4.2.5 Statistically designed experiments on methanol conversion over SAPO-34 65

4.2.6 Diffuse reflectance infra-red Fourier Transform spectroscopy of SAPO-34 during methanol conversion 67

4.3 RESULTS AND DISCUSSION 68

4.3.1 Methanol conversion experiments 68

4.3.2 Surface area analysis 69

4.3.3 Pore volume analysis 72

4.3.4 Carbon and hydrogen analysis 74

4.3.5 Statistically designed experiments 77

4.3.6 *In situ* diffuse reflectance infra-red Fourier Transform spectroscopy of SAPO-34 during methanol conversion 80

Page

4.3.7 *Ex situ* diffuse reflectance infra-red Fourier Transform spectroscopy of the deactivated SAPO-34 83

4.4 CONCLUSIONS 84

4.5 REFERENCES 86

CHAPTER FIVE : DEACTIVATION OF CATALYSTS DURING METHANOL CONVERSION - CHARACTERIZATION OF THE "COKE"

5.1 INTRODUCTION 88

5.2 EXPERIMENTAL 92

5.2.1 Mass spectroscopy after extraction 92

5.2.2 Solid state magic angle spinning - nuclear magnetic resonance spectroscopy 92

5.3 RESULTS AND DISCUSSION 93

5.3.1 Mass spectroscopy after extraction 93

5.3.2 Solid state magic angle spinning - nuclear magnetic resonance spectroscopy 94

5.4 CONCLUSIONS 96

5.5 REFERENCES 97

CHAPTER SIX : REGENERATION

6.1 INTRODUCTION 98

6.2 EXPERIMENTAL 99

6.2.1 Thermal gravimetric analysis during regeneration 100

6.2.2 Gas-chromatography-mass spectroscopy of "coke" 100

Page

6.2.3 Characterization of the catalyst after regeneration 102

6.3 RESULTS AND DISCUSSION 102

6.3.1 Thermo-gravimetric analysis during regeneration 102

6.3.2 Gas-chromatography-mass spectroscopy of "coke" constituents 103

6.3.3 Characterization of the catalysts after regeneration 110

6.4 CONCLUSIONS 116

6.5 REFERENCES 119

CHAPTER SEVEN : CONCLUSIONS 120

APPENDIX 1 : SURFACE AREA CALCULATIONS 123

APPENDIX 2 : PORE VOLUME CALCULATIONS 124

APPENDIX 3 : EQUIVALENT METHANOL CONVERSION 125

LIST OF FIGURES

		Page
1	: Secondary building units of zeolites	4
2	: Structure of zeolite Y (a) sodalite cage and (b) faujasite supercage	6
3	: Structure of pentasil H-ZSM-5 (a) SBU 5-1, (b) pentasil chain and (c) channel structure	6
4	: Structure of chabazite	7
5	: Structural arrangements of gmelinite	9
6	: Acid sites in zeolites (a) Brönsted acid sites and (b) Lewis acid sites	11
7	: Generalized mechanism for methanol conversion to hydrocarbons	12
8	: Mechanism for "coke" formation	13
9a	: "Coke" formation on small pore zeolites	16
9b	: Pore blockage in mono-dimensional pore zeolites	16
10a	: The deactivation of a zeolite with intersecting channels but no large cavities	17
10b	: Deactivation of zeolites with large cavities at the channel intersections	17
11	: The main components of the soluble "coke" isolated from various zeolites	24
12	: Nature of the "coke" formed externally on (a) zeolite Y (b) H-ZSM-5 during the cracking of *n*-heptane	25
13	: Acid sites on the SAPO framework	32

Page

14 : XRD pattern of H-ZSM-5 46

15 : XRD pattern of SAPO-34 47

16 : XRD pattern of SAPO-5 49

17 : XRD pattern of Ni-SAPO 50

18 : XRD pattern of silicon modified SAPO-34 52

19a: MAS-NMR spectra of SAPO-34 53

19b: MAS-NMR spectra of H-ZSM-5 54

20 : TPD spectra of (a) H-ZSM-5 (b) SAPO-34 and (c) SAPO-5 56

21 : Experimental Apparatus for methanol conversion reactions 62

22 : The DRIFTS cell used to study the surface of SAPO-34 during methanol conversion 66

23 : Conversion of methanol with reaction time 69

24 : Decrease in surface area of SAPO-34 during methanol conversion 70

25 : Decrease in surface area of H-ZSM-5 and SAPO-34 during methanol conversion 70

26 : Change in surface areas of the various catalysts after methanol conversion 72

27 : Decrease in pore volume of SAPO-34 and H-ZSM-5 during methanol conversion 73

28 : Carbon deposition on SAPO-34 during methanol conversion 75

29 : Cubic plot of the interacting effects of pressure, temperature, WHSV and dilution of the methanol with water on "coke" deposition 79

30 : DRIFTS of SAPO-34 during the conversion of pure methanol 80

Page

31 : DRIFTS of SAPO-34 during the conversion of methanol diluted with water 82

32 : DRIFTS of deactivated SAPO-34 83

33 : MAS-^{13}C-NMR spectra of spent (a) H-ZSM-5, (b) SAPO-34 and (c) Ni-SAPO 95

34 : TG/DTA spectrum of SAPO-34 during regeneration (a) mass change, (b) temperature and (c) differential of mass loss 103

35 : GC mass spectra of the organic species on the spiked capillary inlet tubes 104

36 : A comparison of the equivalent conversion of methanol over SAPO-34 and regenerated SAPO-34 111

37 : A comparison of the surface areas of the catalysts before the methanol conversion reaction and after regeneration 112

38 : XRD pattern of regenerated H-ZSM-5 113

39 : XRD pattern of regenerated SAPO-34 114

40 : XRD pattern of regenerated SAPO-5 114

41 : XRD pattern of regenerated Ni-SAPO 115

42 : XRD pattern of regenerated silicon modified SAPO-34 115

LIST OF TABLES

		Page
I	: Properties of chabazite	8
II	: "Coke" formation and deactivation during dimethylether conversion at 350°C	18
III	: XRD data for H-ZSM-5	46
IV	: XRD data obtained for SAPO-34	48
V	: XRD data for SAPO-5	49
VI	: XRD data for Ni-SAPO and other Me-SAPOs	51
VII	: XRD data for silicon-modified SAPO-34 and SAPO-34	52
VIII	: IR chemical shifts of species adsorbed on zeolite surfaces	61
IX	: Experimental design of methanol conversion reactions over SAPO-34	66
X	: C and H analysis of the carbonaceous deposit on SAPO-34 during methanol conversion	74
XI	: Carbon deposition in the statistically designed experiments	77
XII	: Effects of the variables in the statistically designed experiments on the C mass percent	78
XIII	: Conversion of methanol over SAPO-34 during the *in situ* DRIFTS experiment	81
XIV	: Chemical shifts reported for carbonaceous species	89
XV	: The carbon species extracted from SAPO-34 after methanol conversion	93
XVI	: Organic species released from H-ZSM-5 during regeneration	105

Page

XVII : Organic species released from SAPO-34 during regeneration 107

XVIII: Organics released from SAPO-5, Ni-SAPO and silicon-modified SAPO-34 during regeneration 108

XIX : XRF analysis of the fresh and regenerated catalysts 116

CHAPTER ONE : GENERAL INTRODUCTION

1.1 INTRODUCTION

Methanol, one of the largest commodity chemicals, is expected to have excellent growth potential as a fuel, fuel precursor, or building block for chemicals in countries where petroleum is scarce or becomes too expensive due to environmental constraints. Methanol is produced from synthesis gas which is in turn produced from natural gas, biomass or from coal [1.1].

Over the last twenty years a great deal of research has been carried out on the use of methanol as an alternative automotive fuel and as a building block for the production of olefins, aromatics and oxygenated chemicals [1.2]. One of the most remarkable discoveries in this latter area was made in the early 1970's by workers at Mobil Research and Development Corporation. They found that methanol could be converted to gasoline of high octane number, with excellent yields and catalyst lifetime, over the shape selective zeolite ZSM-5 [1.1]. Modifications of the catalyst operating conditions was shown to enhance the product selectivity [1.1].

Recently attention has been focussed on enhancing the selectivity of the product spectrum to light olefins (C_2 to C_4) which are used for the production of detergents, plasticizers, lubricants and a variety of chemicals [1.3, 1.4]. This has been achieved with zeolites which are less acidic than H-ZSM-5 and / or have small pores to restrict the formation and transport of bulky hydrocarbons. Small pore zeolites, such as erionite, zeolite T, chabazite, ZSM-34, FU-1 and ZK5 have been shown to be successful

in the conversion of methanol to light olefins [1.5, 1.6], but significant amounts of saturated hydrocarbons are also formed, methanol conversion is not complete and these catalysts deactivate rapidly due to formation of carbonaceous deposits [1.6]. Recently a novel class of crystalline microporous molecular sieves have been synthesized; the silico-aluminophosphates (SAPOs). These molecular sieves not only have the pore structures of zeolites, but also possess unique acidic properties which make them highly selective catalysts for the conversion of methanol to light olefins. This study focusses on two of these SAPO catalysts, viz. SAPO-34 and SAPO-5.

Reactions of organic compounds on zeolites, usually result in the formation of carbonaceous by-products, consisting mainly of fused ring aromatics, or bulky aliphatics, collectively called "coke" [1.7]. The "coke" is deposited on the surface of the catalyst or within the channels, limiting access to the active sites, which may ultimately lead to premature deactivation [1.9]. The rate of deactivation of the catalyst depends on the rate of formation of these by-products and the mode of deactivation [1.8].

The "coking" of zeolites is a shape-selective process as the rate of formation, nature and distribution of "coke" molecules depends on the pore structure of the zeolite [1.8]. The rate of "coke" formation also depends on the strength and density of the acid sites and on the operating conditions e.g. reaction time, temperature, pressure and reactants [1.8].

The rate, mechanism and nature of the "coke" deposited on two molecular sieves in the chabazite group, viz. SAPO-34 and SAPO-5, will be discussed in this dissertation. A better understanding of the "coking" process for these selective catalysts may lead to the retardation or prevention of "coke"

formation on these catalysts, thereby extending the useful catalyst lifetime.

1.2 SCOPE OF DISSERTATION

This dissertation focusses on the rate of "coke" formation on SAPO-34 and modified SAPO-34 during methanol conversion under various conditions, and compares the results to those obtained for H-ZSM-5 and SAPO-5. A general introduction to the structure and acidity of zeolites, as well as reports on the formation of "coke" on these zeolites, is described. The structures of SAPO-34 (chabazite structure) and SAPO-5 (gmelinite structure), as well as the acidity of silico-aluminophosphate catalysts, are also given. Very little information has been reported in the literature on the formation of "coke" on silico-aluminophosphate catalysts during methanol conversion, so this dissertation should provide some new information in this area of catalysis using these materials.

The change in surface area and pore volume of the vari catalysts after methanol conversion was determined. A statistically designed set of experiments was used to determine the effects of temperature, pressure and dilution of the methanol feed with water on the rate of "coke" formation on SAPO catalysts. The deactivation of SAPO-34 during the conversion of methanol was studied by *in situ* diffuse reflectance infra-red Fourier Transform spectroscopy.

The nature of the "coke" formed was analysed by currently available techniques such as infra-red spectroscopy, solid-state magic-angle spinning-nuclear magnetic resonance, breakdown of the zeolite framework using hydrofluoric acid and analysis of the extracted "coke" by gas

chromatography-mass spectroscopy (GCMS) as well as a novel technique whereby the organics released during regeneration are trapped and analysed by GC-mass spectroscopy.

1.3 ZEOLITE STRUCTURES

A zeolite is an aluminosilicate with a framework structure enclosing cavities occupied by large ion and water molecules, both of which have considerable freedom of movement, permitting ion-exchange and reversible dehydration.

Zeolites are crystalline aluminosilicates with an open three-dimensional framework structure consisting of silicate (SiO_4) and aluminate (AlO_4^-) tetrahedra, collectively denoted TO_4 tetrahedra. The T atoms in TO_4 tetrahedra of synthetic zeolites can be substituted by other atoms which can form oxide tetrahedra (e.g. phosphorous). The tetrahedra are linked together by common corner oxygen atoms to form various secondary building units (SBUs), some of which are shown in Fig 1 [1.9].

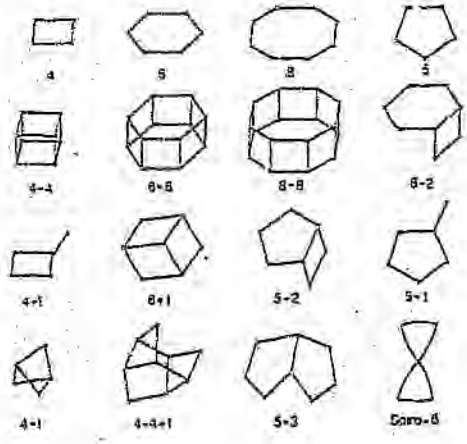


FIG 1 : SECONDARY BUILDING UNITS OF ZEOLITES [1.9]

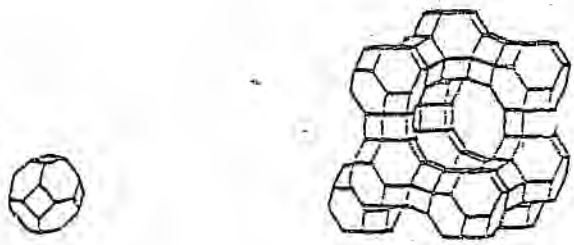
Different linking arrangements of these secondary building units gives rise to a large variety of zeolite structures with different channel networks.

It is estimated that at least 70 different zeolite structures have been identified [1.9]. The zeolite structures are classified into nine groups, namely analcime, natrolite, heulandite, phillipsite, mordenite, chabazite, faujasite, laumontite and pentasil groups [1.11]. Details of these structures have been described in many reviews [1.12, 1.13, 1.14]. Since in this dissertation processes occuring on a wide pore zeolite (zeolite Y), two medium pore zeolites (ZSM-5 and gmelinite which is topographically similar to SAPO-5) and a narrow pore zeolite (chabazite) will be discussed, the structures of these catalysts will be described in some detail.

1.3.1 Zeolite Y

The basic building blocks of zeolite Y (and other faujasite type zeolites) are sodalite units which are formed by eight 6-member rings linked together to form a truncated octahedron (Fig 2). The faujasite structure is formed from sodalite units linked together by their six-member rings, via oxygen atoms, in a tetrahedral array.

This arrangement results in channels, with a diameter of 7.8 A, interconnecting large cavities with a diameter of 12 A [1.16, 1.17]. The pore openings into the large cavity or supercage are sufficient to permit entry of aromatic compounds and some branched hydrocarbons [1.18].

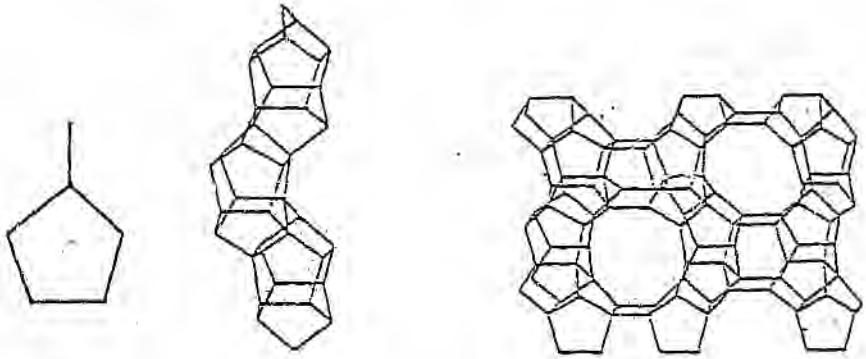


(a) (b)

FIGURE 2 : STRUCTURE OF ZEOLITE Y (a) SODALITE CAGE AND (b) FAUJASITE SUPERCAGE [1.15]

1.3.2 ZSM-5

ZSM-5 belongs to the pentasil group of zeolites. These zeolites are built up from 5-member ring SBUs linked together to form pentasil chains, which are in turn linked together to form pentasil layers (Fig 3) [1.17]. Linking of these pentasil layers by inversion gives the ZSM-5 structure, with both sinusoidal and straight channels (Fig 2) [1.17].



a) b) c)

FIGURE 3 : STRUCTURE OF PENTASIL ZSM-5 (a) SBU 5-1, (b) PENTASIL CHAIN AND (c) CHANNEL STRUCTURE [1.17]

The straight channels are elliptical in shape with dimensions of 5.1 x 5.5 Å, while the sinusoidal channels are nearly circular with dimensions of 5.4 x 5.6 Å [1.17, 1.19]. Unlike zeolite Y, ZSM-5 does not contain large cages at the channel intersections.

1.3.3 Chabazite

The crystal structure contains large ellipsoidal cavities (11Å long and 6.5 Å wide) [1.4] linked by a three-dimensional channel system [1.20]. The channels enter each ellipsoidal cavity through six small apertures (4.0 Å wide), formed by 8-membered rings [1.20]. The ellipsoidal cages are surrounded by eight double hexagonal ring units, six 4-membered rings, and six 8-membered rings which connect the ellipsoidal cages to six neighbouring cages [1.21]. A schematic structural diagram of chabazite is shown in Fig.4 [1.21]. The effective openings of the ellipsoidal cavities are shown by dotted lines, the interconnected channels are shown by rods and the stacking of the double hexagonal prisms indicated by "A", "B" and "C" [1.21]. The physical and structural properties, as reported by Breck [1.13], are listed in Table I.

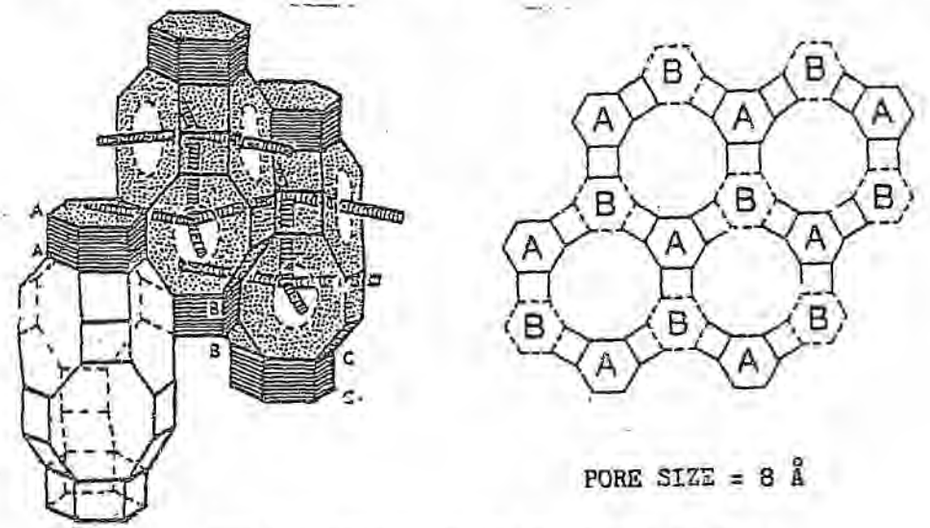


FIG 4 : STRUCTURE OF CHABAZITE [1.21]

The straight channels are elliptical in shape with dimensions of 5.1 x 5.5 A, while the sinusoidal channels are nearly circular with dimensions of 5.4 x 5.6 A [1.17, 1.19]. Unlike zeolite Y, ZSM-5 does not contain large cages at the channel intersections.

1.3.3 Chabazite

The crystal structure contains large ellipsoidal cavities (11A long and 6.5 A wide) [1.4] linked by a three-dimensional channel system [1.20]. The channels enter each ellipsoidal cavity through six small apertures (4.0 A wide), formed by 8-membered rings [1.20]. The ellipsoidal cages are surrounded by eight double hexagonal ring units, six 4-membered rings, and six 8-membered rings which connect the ellipsoidal cages to six neighbouring cages [1.21]. A schematic structural diagram of chabazite is shown in Fig.4 [1.21]. The effective openings of the ellipsoidal cavities are shown by dotted lines, the interconnected channels are shown by rods and the stacking of the double hexagonal prisms indicated by "A", "B" and "C" [1.21]. The physical and structural properties, as reported by Breck [1.13], are listed in Table I.

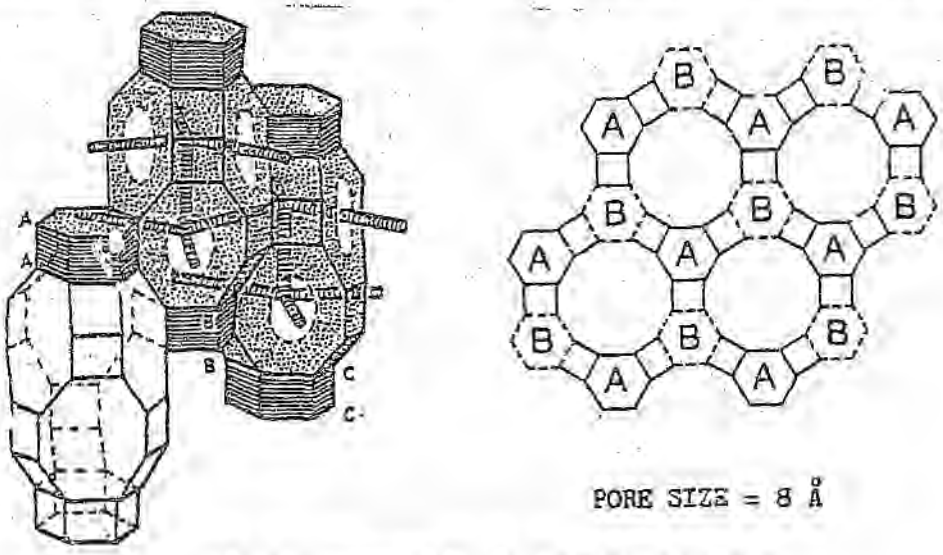
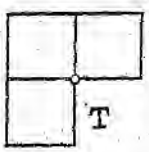


FIG 4 : STRUCTURE OF CHABAZITE [1.21]

TABLE 1 : PROPERTIES OF CHABAZITE [1.13]

Secondary building units:	single 6-rings in AABBCC sequence (double 6- or single 4-rings)
Framework density:	14.6 T/1000 A^3
Loop configuration of T-atoms:	
Coordination sequence:	T(36) 4 9 17 29 45 64 85 110 140 173
Channels:	⊥ [001] 8 3.6 x 3.8 variable due to considerable flexibility of framework[1]
Fault planes:	(001)
Type species:	Chabazite $Ca_6[Al_{12}Si_{24}O_{72}] \cdot 40\ H_2O$ trigonal, $R\bar{3}m$, a=13.2, c=15.1 A[2,3]
Isotypic framework structures:	CoAPO-44[4] CoAPO-47[4] LZ-218[5] Linde D[6] Linde R[7] MeAPO-47[4,8] MeAPSO-47 SAPO-34 Willhendersonite ZK-14 ZYT-6
Alternate designations:	Acadialite (obsolete) Haydenite (discredited) Herschelite (discredited) Seebachite (obsolete)

1.3.4 Gmelinite

Gmelinite belongs to the chabazite group of zeolites as its structure contains stacked double hexagonal rings (denoted "A" and "B") although these rings are arranged differently to the natural zeolite chabazite [1.21]. In chabazite the hexagonal rings are arranged in the sequence ...ABCABC... whereas in gmelinite they are arranged in the sequence ...ABAB...[1.21]. In the gmelinite structure the double ring units are connected by inclined four-membered rings so as to generate polyhedral cages which are smaller in size and contain fewer faces than those of chabazite [1.21].

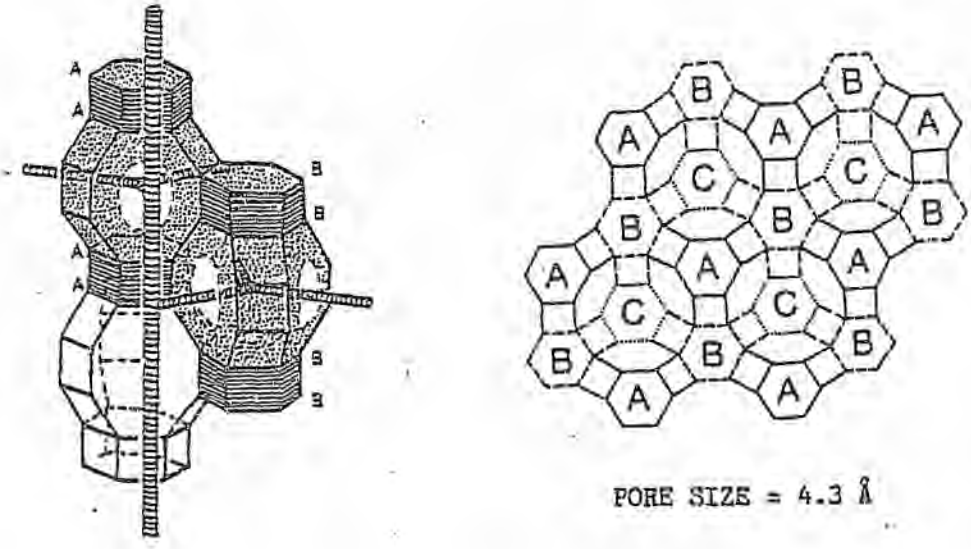


FIG 5 : STRUCTURAL ARRANGEMENTS OF GMELINITE [1.21]

The openings to the polyhedral cages are larger (7.0 Å) than those of chabazite (4 Å) and the channels parallel to the c-axis are continuous, non intersecting and wide (defined by 12-membered rings) [1.21]. Each of the polyhedral cages has three 8-membered rings which connect them to the wide channels parrallel to the c-axis. The gmelinite structure contains another set of narrow (less than 4.0 Å) intersecting channels normal to the c-axis.

The spatial T-model (tetrahedron-centre-model) of gmelinite is shown in Fig 5 [1.21]. The effective openings of the cages are shown by dotted lines and the interconnected channels are shown by rods. Stacking of the double hexagonal prisms is also indicated.

1.4 ZEOLITE ACIDITY

In aluminosilicate zeolites the negative charge created by the tetrahedral Al is balanced by the presence of cations or by protons [1.22]. Zeolites contain many Brönsted acid sites which are formed by surface hydroxyls associated with the tetrahedrally co-ordinated Al (see Fig.6) [1.23]. The strength of these acid sites depends on the concentration of tetrahedral Al atoms and of exchangeable cations [1.24, 1.25]. Above 500°C these Brönsted acid sites may be dehydrated to Lewis acid sites without the crystal structure being changed [1.24, 1.25]. An interaction between the Lewis acid sites and the Brönsted acid sites reduces the Brönsted hydroxyl group's electron density, making the proton more acidic [1.26]. Recently there has been evidence that extremely strong acid sites are produced when Al-O species are leached from the zeolite framework of mordenite and this may be true for all zeolites [1.2].

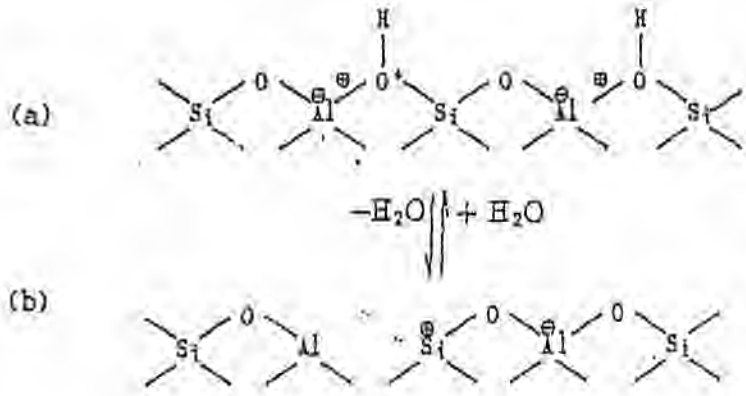


FIGURE 6 : ACID SITES IN ZEOLITES (a) BRÖNSTED ACID SITE AND (b) LEWIS ACID SITE

The hydoxyl groups of Brönsted acid sites have been observed by Fourier Transform Infra-red (FTIR) spectroscopy in the 3500-3600 cm^{-1} region [1.26, 1.27]. The decrease in intensity of the hydrogen bonded silanol stretching band, but not the terminal silanol stretching band, after treatment with sodium hydroxide, was used to show that the former acid sites are stronger than the latter [1.28]. Brönsted acidity can be separated from Lewis acidity by using probe molecules such as pyridine [1.29]. The hydroxyl stretching frequency has been shown to shift according to the electronegativity of surrounding atoms and to the framework structure, as electrostatic interactions are influenced by the geometry of the channels [1.29]. The frequency of the hydroxyl stretch can only be used as an approximate indication of the acid strength [1.29].

Temperature programmed desorption (TPD) of chemisorbed ammonia on zeolites Y and ZSM-5 (which have the same Al content and therefore the same number of acid sites) has shown that both zeolites have a fairly weak type of acid site due to surface hydroxyl groups, but ZSM-5 has an additional, stronger type of acid site (as shown by a second desorption peak at a higher temperature) [1.30] due to Si-OH-Al groups.

Acidic forms of zeolites (denoted H-zeolite) can be prepared by ion-exchanging the zeolite with ammonium ions e.g. treating the catalyst with an ammonium nitrate solution and subsequently deammoniating at elevated temperatures [1.11].

1.5 METHANOL TO OLEFINS AND GASOLINE

Chang, Lang and Silvestri proposed that the conversion of methanol to hydrocarbons may be simplified into a three step process [1.5]. The first step is the dehydration to dimethylether (DME), the second step the conversion of DME into olefins and the third step the conversion of olefins into higher hydrocarbons as shown in Fig 7 [1.3]. With increasing reaction time the yield of DME increases while the yield of hydrocarbons decreases [1.20].

$$2\ CH_3OH \xrightarrow{-H_2O} CH_3OCH_3 \xrightarrow{-H_2O} \underset{\text{OLEFINS}}{C_2\text{–}C_5} \longrightarrow \underset{\text{PARAFFINS, AROMATICS CYCLOPARAFFINS}}{C_5^{+}\ \text{OLEFINS}}$$

FIG 7 : GENERALIZED MECHANISM FOR METHANOL CONVERSION TO HYDROCARBONS

The course of catalytic reactions on molecular sieves has been quantitatively studied using *in situ* ^{13}C and ^{1}H Magic Angle Spinning Nuclear Magnetic Resonance (MAS-NMR) spectroscopy [1.4]. Aromatic and aliphatic species were observed on the surface of ZSM-5 after it was used for the conversion of methanol [1.4].

1.6 MECHANISM FOR "COKE" FORMATION

The oligomerization, cyclization and dehydrogenation reactions catalysed by acid sites on zeolites can lead to the formation of "coke", as illustrated in Fig 8 [1.7].

Paraffins can undergo dehydrocyclization reactions to form cycloparaffins, or be converted to olefins by dehydrogenation and cracking reactions [1.7]. Olefins can also be formed directly from oxygenates [1.7]. The olefins can undergo oligomerization (e.g. Diels-Alder reactions), cyclization and dehydrogenation reactions to form cycloparaffins, aromatics and naphthenes [1.7]. Alkylation and dehydrocyclization of these cyclic structures results in fused aromatic rings which can undergo dehydrogenation. The "coke" which causes deactivation in catalysts can consist of fused ring aromatics, alkylaromatics, naphthalenes, aromatics, cycloparaffins and even bulky or branched aliphatics which are unable to diffuse out of the channels.

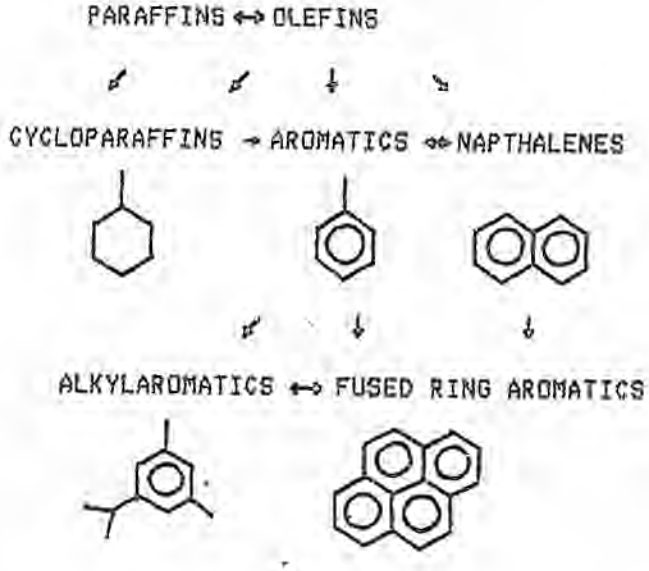


FIG 8 : MECHANISM FOR "COKE" FORMATION

Bulky transition state intermediates are necessary for the alkylation of aromatics and aromatization of polyalkylaromatics. These reactions thus occur mainly in zeolites with large pores (12-membered ring pores) or with large cavities (e.g. erionite and chabazite) or on the external surface of zeolites [1.7].

In small pore zeolites and certain medium pore zeolites, "coke" cannot form internally due to spatial constraints [1.7]. Deactivation results from acid site occupancy and pore blockage by high molecular weight oligomers [1.7]. Studies of methanol conversion over H-ZSM-5 at various temperatures from 270-400°C have shown that the pore system of H-ZSM-5 is blocked by the accumulation of bulky one or two ring aromatics at low temperature, whereas at high temperature the aromatics undergo isomerization reactions and the less bulky "coke" constituents leave the pores. At temperatures above 400°C the selectivity to "coke" increases.

Catalytic sites for "coke" formation can also be present in the "coke" itself e.g. carbenium ions [1.7]. These acid sites can lead to the continued growth of "coke" outside of the zeolite pores or channels, or to reorganization of the "coke", even after the zeolite acid sites have been covered [1.7]. The additional "coke" is formed directly from methanol, while methane and water are released, as indicated by the following equation [1.31]:

$$2\ CH_3OH \rightleftharpoons C_{\text{-coke-}} + CH_4 + 2\ H_2O$$

Experimental studies on the formation of "coke" on zeolite Y during methanol conversion have shown that methane formation can be used as a measure of the amount of "coke" formed [1.31].

1.7 ZEOLITE DEACTIVATION

All acidic zeolites deactivate during organic reactions due to the deposition of carbonaceous deposits. The rate of deactivation is dependant on the pore structure and acidity of the zeolites. The "coke" deposits can cause deactivation by covering of the acid sites, or by blocking access to the pores in which the acid sites are found [1.7]. These two aspects of deactivation will be discussed in some detail here.

1.7.1 Effect of pore structure

It is difficult to evaluate the effect of pore structure on the "coking" rate as it is not easy to obtain a range of catalysts with different pore structures but with the same acidity [1.8]. However, it has been found that catalysts with large cavities or channel intersections (in which bulky "coke" molecules can form) and with structures that limit diffusion of the "coke" precursors, have greater "coking" rates [1.8]. Catalysts with structures which limit diffusion prevent the "coke" from forming uniformly throughout the catalyst [1.32] and deactivate rapidly when certain regions are blocked off by "coke".

Small pore zeolites e.g. erionite and ferrierite, have channel dimensions which are too small for the formation of bulky "coke" precursors e.g. cycloparaffins or naphthenes [1.7]. The "coke" is deposited in the outer zone of the catalyst while the inner zone remains "coke"-free [1.8, 1.32]. Blockage of the outer pores causes deactivation of the catalyst as access to the internal area and hence to the active sites is decreased (Fig 9a) [1.8, 1.32].

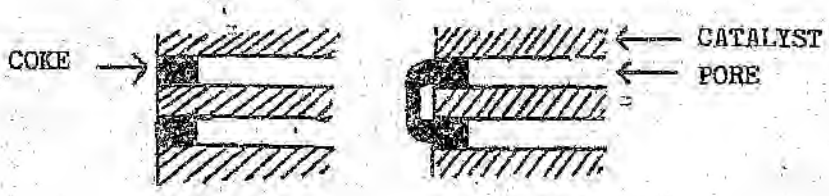


FIG 9a : "COKE" FORMATION ON SMALL PORE ZEOLITES [1.8]

Catalysts with monodimensional pore structures e.g. mordenite, deactivate when aromatic "coke" forms anywhere along the channel as access to the active sites in the rest of the channel is blocked (see Fig 9b) [1.7].

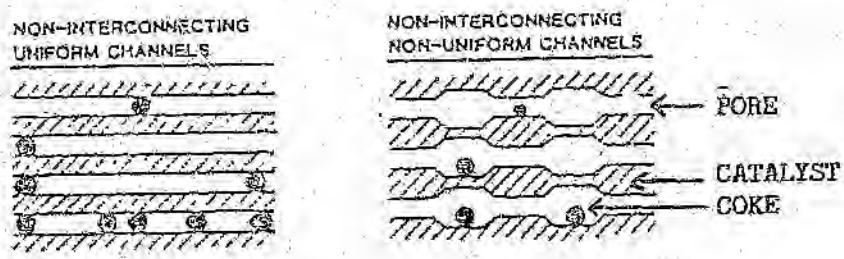


FIG 9b : PORE BLOCKAGE IN MONODIMENSIONAL PORE ZEOLITES [1.7]

Medium pore zeolites with interconnecting channels but no large cavities (e.g. ZSM-5) deactivate initially through limitation of access to the active sites [1.8]. Only at high "coke" contents is access to all the active sites blocked by "coke" deposited on the surface of the crystallites (Fig 10a) [1.8].

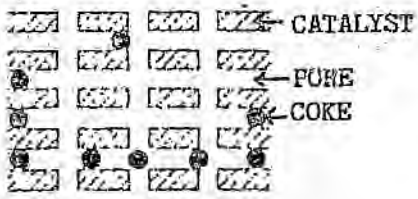


FIG 10a : THE DEACTIVATION OF A ZEOLITE WITH INTERSECTING CHANNELS BUT NO LARGE CAVITIES [1.8]

The mode of deactivation of zeolites with large cavities at the channel intersections, e.g. chabazite and zeolite Y, is shown in Fig 10b [1.8]. These large cavities facilitate the formation of "coke" precursors, but the narrower pore network limits the diffusion of "coke" molecules out of the zeolite [1.8]. The "coke" forms initially in the cavities and then protrudes into the channels. The blockage of the channel intersections limits the access of reactants to the active sites and diffusion of products out of the zeolite, so deactivation occurs [1.8].

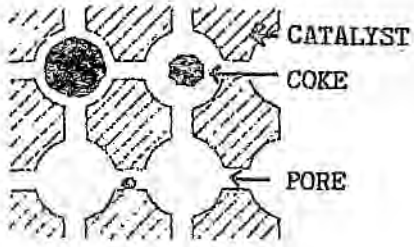


FIG 12b : DEACTIVATION OF ZEOLITES WITH LARGE CAVITIES AT THE CHANNEL INTERSECTIONS

Medium and large pore zeolites can accomodate bulky "coke" precursors and therefore "coke" up rapidly [1.33]. The deactivation is directly related to the amount of "coke" deposited, which is indicated by the change in weight of the catalyst [1.33].

The relative amounts of "coke" formed on ZSM-5, zeolite Y, chabazite and mordenite, during the conversion of dimethyl ether, as determined by Cormerais *et al* [1.34] are shown in Table II.

TABLE II : "COKE" FORMATION AND DEACTIVATION IN DIMETHYL ETHER CONVERSION AT 350°C [1.34]

CATALYST	RESIDUAL ACTIVITY (%)	WT % "COKE"	"COKE" / HYDROCARBONS X 10^4
H-ZSM-5	90.00	1.5	0.3
H-Y	8.00	8.3	40
H-CHABAZITE	0.15	8.6	90
H-MORDENITE	0.15	6.8	200

The rate of deactivation, as indicated by the residual activity (ratio of the activity after 7.5 h to the initial activity, the selectivity to "coke" are inversely correlated [1.34].

A greater percentage of "coke" was deposited on zeolie H-Y, H-Chabazite and H-mordenite than on H-ZSM-5 as the pore diameters (H-Y and mordenite) and/or channel intersections (H-Y and chabazite) of these catalysts are sufficiently large to accomodate the formation of bulky "coke" precursors.

At a given percentage of "coke" the catalytic activities of mordenite and erionite were decreased more than that of zeolite Y, which in turn was decreased more than that of H-ZSM-5 [1.34]. The difference in "coke" sensitivity of the zeolites was probably due to the nature and/or distribution of the "coke", differing from one zeolite to another, as a result of different pore structures [1.34].

The "coke" formation on zeolite Y during the conversion of *n*-heptane has been studied by Guisnet *et al* [1.8]. The initial "coke" molecules which were deposited consisted of mainly 5-ring aromatics with a volume of about 200 A^3, which corresponds to a quarter of the volume of the supercage [1.8]. This "coke" had a moderate deactivating effect. The diffusion of nitrogen into the pores of the catalyst was not limited so a decrease in pore volume V_A corresponded to the volume of "coke" deposited V_R (as determined by the ratio of the mass of "coke" deposited per gram of zeolite to the density of the "coke" as estimated from its composition). The ratio of V_A / V_R decreased when the "coke" content increased due to pore blockage. When the "coke" content exceeded 7 wt % the V_A / V_R ratio remained constant which indicated that the increase in "coke" was no longer due to "coke" deposited in the pores, but on the surface of the catalyst or protruding from the micropores [1.8].

The adsorption capacity of trimethylamine (TMA) has been used to study the mode of "coke" formation in ZSM-5 [1.35]. The initial decrease in TMA adsorption was slow as ZSM-5 has an extensively interconnected pore network and thus a substantial amount of "coke" is required before access to certain regions is completely sealed off. If the "coke" was preferentially deposited on the outer surface one would expect the blocking effect to be very abrupt. If the "coke" was laid down randomly throughout the zeolite, without blocking

off regions, one would expect a gradual decrease in TMA adsorption. The adsorption capacity decreased more than expected from a consideration of the volume of deposit, thus certain regions were blocked off by the "coke".

X-ray photoelectron spectroscopy (XPS) has been used to show that "coke" forms predominantly inside the pores of ZSM-5 during methanol conversion as the C/Si ratio increased steadily until 15 wt % "coke" had been deposited [1.36]. When the level of "coke" deposited exceeded 15 wt % the C / Si ratio increased dramatically which indicated that external "coke" was formed, probably by the thermal cracking of methanol [1.36].

Transmission electron microscopy (TEM) was also used to study the distribution of "coke" in a zeolite cut with an ultramicrotome [1.37]. Filaments of "coke" in the micropores and protruding from the surface of Zeolite Y after heptane cracking have been observed by TEM [1.37]. Controlled atmosphere electron microscopy has been used *in situ* to study the formation of "coke" on catalysts [1.38] e.g. the filamentous carbon formation from acetylene on nickel, iron and cobalt at 700°C. The resolution was not as good as obtained with post-reaction TEM, but changes in the catalyst and appearance of the "coke" can be observed.

1.7.2 Effect of acid sites

The density and strength of the acid sites of a catalyst also affects the rate of "coking" [1.8]. There is a linear relationship between the number of strong acid sites and the initial "coking" rate, which shows that the strong acid sites are the main active centres for the "coking" of zeolites during methanol conversion [1.39].

McLellan *et al* studied the decrease in acid sites in ZSM-5 during the conversion of methanol using chemisorption of ammonia and pyridine and IR spectroscopy [1.40]. They found that initial "coke" formation caused a rapid decrease in the number of acid sites. Approximately 1 acid site was deactivated for every 5 carbon atoms deposited. A C_5 molecule would have been flushed out from the catalyst at the reaction temperature, so larger "coke" molecules had probably formed on more than one acid site e.g. a C_{10} molecule adsorbed onto 2 acid sites. This indicates that initial "coke" formation may occur at channel intersections where there are several acid sites in close proximity. At higher "coke" levels (9.5 wt %) the active sites of ZSM-5 were still detected by ammonia desorption, but not by pyridine adsorption. About 100 carbon atoms were deposited per acid site. This indicates that "coke" formed on the outer surface, partially blocked the access to the internal acid sites.

1.8 CHARACTERIZATION OF THE "COKE"

"Coke" is difficult to recover from the zeolite, therefore *in situ* analytical methods are often used in an attempt to characterize the carbonaceous deposits. However, the distribution of the "coke" cannot be determined using these methods [1.8].

The atomic hydrogen-to-carbon ratio can be used to determine if the carbonaceous deposit is polyaromatic or aliphatic [1.8]. The amount of "coke" deposited on ZSM-5 during methanol conversion has been determined by quantifying the hydrogen and carbon released during combustion [1.41]. The C / H ratio was observed to decrease from 2 to 0.5 when the amount of "coke" increased from 1 to 17 % [1.36]. The results are often ambiguous as internal and external "coke" deposits could have different compositions, thus an

average of these compositions is always obtained [1.8].

Infra-red (IR) studies have been used to identify the nature of the surface "coke" (olefinic, saturated or aromatic), to monitor the changes in the concentration of Brönsted OH sites and to quantify the "coke" by the intensity of the so-called "coke" band at 1585 cm^{-1} [1.8]. *In situ* IR spectroscopy has been used, but most of the studies have been performed on zeolites after reaction [1.8].

UV-VIS spectroscopy has also been used to investigate the type of "coke" formed e.g. the "coke" formed on dealuminated H-mordenite during ethene oligomerisation was found to be polyaromatic [1.8].

^{1}H - ^{13}C cross polarization (CP) and magic angle spinning (MAS) ^{13}C-NMR spectroscopy have been used to investigate the "coke" on zeolites [1.8, 1.42] and can be used to discriminate between molecular species trapped inside the zeolite and other species adsorbed onto acid sites, rendering them insensitive to basic probe molecules. For example ZSM-5 and mordenite have been analysed by CP - ^{13}C - MAS-NMR after methanol conversion reactions. ^{13}C-enriched methanol was adsorbed onto the zeolites in a NMR cell and after a period of contact with air (one day or more) volatile fractions were removed. The spent catalysts were transferred into the MAS spinner and analysed [1.42]. The carbonaceous deposits on the spent ZSM-5 and mordenite catalysts were compared semiquantitatively. Aliphatics (mainly isoparaffins) and alkyl benzenes were found to form on ZSM-5, whereas mainly polyaromatics were formed on mordenite [1.42]. Mordenite has larger pore dimensions than ZSM-5, and can therefore accomodate the bulky intermediates required for the formation of polyaromatics. Surface methoxy groups, produced by the alkylation of acidic sites and bound to the framework of both catalysts, were observed. These

species are thought to have been trapped in the zeolite intracrystalline volume due to pore blockage or very low diffusion rates [1.42].

Electron paramagnetic resonance (EPR) has been used to study the radicals formed that accompany the formation of "coke" on zeolites. Thus the amount and type of "coke" on zeolites can be determined [1.8]. Two types of EPR signals were observed in "coked" ZSM-5 zeolites [1.43]. The broad signal was reported to be due to the free radicals of weakly condensed "coke" with a low C / H ratio. The narrow signal was assigned to highly condensed "coke" with a high C / H ratio i.e. polyaromatic planar networks of carbon with mobile electrons (graphitic carbon).

A small part of the carbonaceous compounds in the zeolite pores has been recovered by treating the "coked" zeolite with an organic solvent or flushing with an inert gas at high temperatures [1.8]. Guisnet *et al* [1.44] found that no organics were desorbed from zeolite Y, which had been deactivated during phenol alkylation reactions, under nitrogen at 200°C [1.37]. Higher temperatures and / or longer desorption periods may have been required. This method of "coke" desorption will be discussed in chapter 6.

Magnoux *et al* reported a solvent extraction technique for investigating the chemical nature of the "coke" [1.37, 1.8]. The zeolite structure was destroyed in hydrofluoric acid, or by ballmilling, and the organics were leached out with methylene chloride. The soluble "coke" compounds were analysed by gas chromatography, high performance liquid chromatography (HPLC), ^{1}H-NMR, IR and mass spectroscopy [1.8]. The methylene chloride soluble "coke" component was found to possess low polyaromatic character and was thought to be deposited in the micropores. The insoluble "coke" component was thought to be polyaromatic in nature and was deposited within the large zeolite cages,

mesopores or as an external envelope which can retain the shape of the granule after the zeolite granule has been dissolved [1.37]. The insoluble "coke" was filtered and analysed by TEM [1.37]. This method was used to study the "coke" deposited in zeolites Y, mordenite, H-ZSM-5 and erionite during *n*-heptane cracking [1.8]. The main components of the soluble "coke" isolated from the various zeolites is shown in Fig. 11 [1.8]. Insoluble "coke" was formed on the zeolites after different amounts of "coke" had been deposited (2 % "coke" on zeolite Y and erionite and 4 % "coke" on H-ZSM-5) [1.8]. The atomic H to C ratio of the insoluble "coke" was found to be between 0.4 and 0.5 on zeolite Y, H-ZSM-5 and erionite and 0.6 on mordenite [1.8]. This shows that the insoluble "coke" was polyaromatic [1.8].

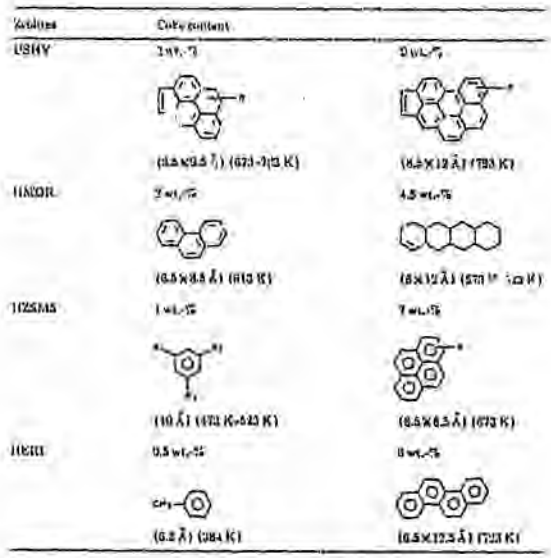


FIG 11 : THE MAIN COMPONENTS OF THE SOLUBLE "COKE" ISOLATED FROM VARIOUS ZEOLITES [1.8]

Electron energy loss spectroscopy has shown that the external "coke" formed on zeolite Y during the cracking of *n*-heptane consisted of linear aromatic chains as shown in Fig. 12 (a) [1.37]. The filaments of "coke" were observed bundled together at the mouth of mesopores and protruding out of the zeolite

micropores [1.37]. By contrast, the "coke" formed on the external surface of H-ZSM-5 was shown to consist of fused aromatic rings as shown in Fig. 14 (b) [1.37].



(a) (b)

FIG 12 : NATURE OF THE "COKE" FORMED EXTERNALLY ON a) ZEOLITE Y AND b) H-ZSM-5 DURING THE CRACKING OF *n*-HEPTANE [1.37]

Some controversy exists as to the best technique with which to identify the actual components of the "coke" deposited in deactivated zeolites. A novel technique of releasing and analysing the "coke" deposited in zeolites will be described in this dissertation.

1.9 REGENERATION OF ZEOLITES

It has been shown that ZSM-5 does not return to its original state after oxidative regeneration, even though thermogravimetric analysis and EPR show no residual form of "coke" on the regenerated zeolites [1.45]. The change in acidity of ZSM-5 during methanol conversion and oxidative regeneration has been studied by Bibby *et al* [1.46]. They measured the change in intensity of the silanol and Brönsted acid site IR bands at 3740 and 3610 cm^{-1} respectively as well as the chemisorption of pyridine [1.46]. Only 91 % of the original Brönsted acidity and 55 % of the acidity due to silanol groups was regained after regeneration [1.46].

The zeolites are thermally stable up to temperatures of 900°C and therefore would not be expected to be affected by the regeneration temperature of 600°C. The ^{27}Al NMR data has shown that dealumination occurs during regeneration, probably as a result of steam produced during the combustion of the carbonaceous products [1.45]. Dealumination has been shown to cause a change in the nature of the "coke" deposited, i.e. the "coking" rate decreases and a more condensed "coke" is formed [1.45].

During oxidative regeneration the major products are CO and CO_2, but small traces of other organics may be present. To date there has been no analysis of these "other" organics released during the regeneration of zeolites.

1.10 REFERENCES

1.1] Chang, C.D.; Hydrocarbons from Methanol, Marcel Dekker, Inc., New York, (1983)

1.2] Mizodatcs, C. and Barthomeuf, H.K.; *J. Chem. Soc. Chem. Commun.*, 1, (1981), 39

1.3] Chang, C.D. and Silvestri, A.J. *J. Catal.*, 47 (1977), 249

1.4] Anderson, M.W., Sulikowski, B., Barrie, P.J. and Klinowski, J.; *J. Phys. Chem.*, 94, (1990), 2730

1.5] Chang, C.D., Lang, W.H. and Silvestri, A.J., U.S. Patent 4 062 905 (1977).

1.6] Kaiser, S.W., *Arab J. Sci. Eng.*, 10, (1985), 361

1.7] Derouane, E.G.; Catalysis by Acids and Bases, Imelik *et al* (eds), Elsevier Science Publishers, Amsterdam (1985)

1.8] Guisnet, M and Magnoux P; *Applied Catal.*, 54, (1989), 1

1.9] Meier, W.M. and Olson, D.H., Atlas of Zeolite Structures, Butterworths, London (1987), 5

1.10] Meier, W.M. and Olson, D.H.; Zeolites for the nineties, Jansen, J.C., Moscou, L. and Post, M.F.M. (Eds), 8th International Zeolite Conference proceedings, Amsterdam, (1989)

1.11] Rabo, J.A.; ACS Monograph 171, American Chemical Society, Washington D.C. (1976)

1.12] Barrer, R.M., Zeolites and clay minerals as sorbents and molecular sieves, Academic Press, London, (1978)

1.13] Breck, D.W., Zeolite molecular sieves, John Wiley and Sons, New York, (1974).

1.14] Smith, J.V., in "Zeolite Chemistry and Catalysis", Rabo, J.A. (Ed.), Am. Chem. Soc. Monograph, 171, (1976), 1

1.15] Kerr, T.; *Scientific American*, July (1989), 82

1.16] Whan, D.A., *Chem. in Britain*, 17, (1981), 11

1.17] Dwyer, J and Dyer, A., *Chemistry and Industry*, 2, (1984), 237

1.18] Leach, H.F.., *Annual Rept. Progr. Chem. A*, (1971), 68, 195

1.19] Olson, D.H., Kerr, G.T., Lawton, S.L. and Meier, W.M., *J. Phys. Chem.*, 85, (1981), 2238.

1.20] Singh, B.B.; Doctor of Philosophy Dissertation entitled "Catalytic Conversion of Methanol to Low Molecular Weight Hydrocarbons", Dec. (1979), Texas University.

1.21] Chatterjee, M., Ganguli, D. and Saha, P.; *Transaction of the Indian Ceramic Society*, 35 (5). (1976), 99

1.22] Pines, H.; The Chemistry of Catalytic Hydrocarbon Conversions, Academic Press, New York, (1981), 1

1.23] Jacobs, P.A. and von Ballmoos, R., *J. Phys. Chem*, 86, (1982), 3050

1.24] Chen, N.Y., Degnam, T.F., *Chem. Eng. Prog.*, (1988), 2, 32

1.25] Ward, J.W.; Zeolite Chemistry and Catalysis, (Ed. Rabo, J.A.) ACS Monograph 171, Washington D.C. (1976), 118

1.26] Blackmond, D.G. and Goodwin, J.G; *J. Catalysis*, 78, (1982), 34

1.27] Dong, Q.N., Anderson, J.R. and Mole, Y.; *Applied Catal.*, 72, 99 (1991)

1.27] Moser, W.R., Chiang, C.C. and Thompson, R.W.; *J. Catal.*, 115, (1989), 552

1.29] Rabo, J.A. and Gajda, G.J., *Catal. Rev. Sci. Eng.*, 31 (4), (1990), 385

1.30] Jacobs, P.A., Martens, J.A., Weitkamp, J and Beyer, H.K.; *Faraday Discuss. Chem. Soc.*, 72, (1981), 353

1.31] Schulz, H., Barth, D. and Siwei, Z.; Catalyst Deactivation 1991, Bartholomew, C.H. and Butt, J.B. (Eds.), Elsevier Science Publishers, Amsterdam (1991), 783

1.32] Chinchen, G.C.; *Crit. Rep. Appl. Chem.*, 12, (1985), 1-29

1.33] Delmon, B. and Froment, G.F.; Catalyst Deactivation, Elsevier Scientific Publishing Co., Amsterdam, (1980)

1.34] Cormerais, F.X., Perot, G. and Guisnet, M., *Zeolites*, 1 (1), (1981), 141

1.35] Bibby, D.M. and Pope, C.G.; *J. Catal.*, 116, (1989), 407

1.36] Sexton, B.A., Hughes, A.E. and Bibby, D.M.; *J. Catal.*, 109, (1988), 126

1.37] Gallezot, P., Leclercq, C., Guisnet, M. and Magnoux, P.; *J. Catal.* 114, (1988), 100

1.38] Baker, R.T.K and Harris, P.S.; *J. Phys. E.*, 5, (1970), 793

1.39] Liu, Z., Chen, G., Liang, J, Wang, Q. and Cai, G.; Catalyst Deactivation 1991, Bartholomew, C.H. and Butt, J.B. (Eds.), Elsevier Science Publishers, Amsterdam (1991), 815

1.40] McLellan, G.D., Howe, R.F., Parker, L.M. and Bibby, D.M.; *J. Catal*, 99, (1986), 486

1.41] Meier, W.M.; Molecular Sieves, Society of the Chemical Industry, London, (1968)

1.42] Derouane E.G., Gilson, J. and Nagy J.B., *Zeolites*, 2, (1982), 42

1.43] Echevskii, G.V., Kharlamov, G.V., Kalinina, N.G., Poluboyarov, V.A., Pashis, A.V. and Anufrienko, V.F.; *Kinet. Katal.*, 28 (6), (1987), 1456

1.44] Guisnet, M., Neves, I., Ribeiro, F.R., Canaff, C., Magnoux, P. and Perot, G.; Catalyst Deactivation 1991, Bartholomew, C.H. and Butt, J.B. (Eds.), Elsevier Science Publishers, Amsterdam (1991), 735

1.45] Ryabov, Y.V., Echevskii, G.V., Antonova, N.V., Antsiburova, E.A., Kalinina, N.G., Poluboyarov, V.A., Erofeev V.I. and Anufrienko, V.F.; *Kinet. Katal.*, 28 (5), (1987), 1217

1.46] Bibby, D.M., McLellan, G.D. and Howe, R.F.; Catalyst Deactivation 1987, Delmon, B and Froment, G.F. (Eds.), Elsevier Science Publishers, Amsterdam, (1987), 657

CHAPTER TWO : DEACTIVATION OF SAPOs DURING METHANOL CONVERSION

2.1 SILICO-ALUMINOPHOSPHATE STRUCTURES

Recently a new class of molecular sieves have been synthesized from aluminium and phosphorous oxide tetrahedra, viz. aluminophosphates (ALPOs) [2.1]. Pure aluminophosphate frameworks are electroneutral, but can be modified by isomorphous substitution of either aluminium or phosphorus (or both) during synthesis to produce a negatively charged framework [2.2]. These substituted aluminophosphate molecular sieves are called MeAPOs. More specifically the silicon substituted ALPOs are called SAPOs. The specific structure of the molecular sieve is indicated by a number e.g. SAPO-34 which is topographically similar to the natural zeolite chabazite [2.3] discussed in section {1.2.3} and SAPO-5 which has a structure similar to the natural zeolite gmelinite [2.4] discussed in section {1.2.4}.

The synthesis of SAPO molecular sieves has been further modified in order to produce metal-ion-containing SAPO catalysts, which are denoted MeAPSOs. The incorporation of a metal ion into the catalyst is thought to decrease the acid strength of the catalyst thereby improving the selectivity for C_2 and C_3 olefins [2.5]. Incorporation of a metal into SAPO-34 has been shown to change the distribution and strength of acid sites, but not the geometry of the channel apertures [2.2], so the selectivity to light olefins is not affected by changes in the pore structure. The incorporation of a metal is also thought to help retard the deactivation process by cracking "coke" precursors [2.6]. A further advantage of the presence of transition metals (from 1 ppm

to 20 wt %) is the reported promotion of the oxidation during regeneration [2.6]. Inui has patented the synthesis of Ni-SAPO-34 [2.7] and shown that this catalyst can produce high selectivities (nearly 90 % at 450°C) of ethylene during methanol conversion [2.5].

2.2 ACIDITY OF SAPOs

The ALPO framework consists of alternating positively charged aluminium and negatively charged phosphorous tetrahedra, which result in overall neutrality of the framework [2.8]. Substitution of Si into the framework in the place of P creates an acid site as the positively charged tetrahedral aluminium is not neutralized, as shown in Fig 13. Surface hydroxyls also impart weak Brönsted acidity to the zeolite.

Temperature-programmed desorption and thermogravimetric analysis (TPD-TGA) using isopropylamine as a probe molecule has been used to show that there is one acid site per framework Si in SAPOs with a low silicon content (0.48 mol % Si) [2.9]. Isopropylamine was shown to decompose to propene and ammonia at the same temperature (between 300 and 375°C) on H-ZSM-5 and SAPOs, but not on ALPOs. The number of propene and ammonia molecules that desorbed from H-ZSM-5 corresponded to one molecule per framework Al, whereas for the SAPOs it was close to the number of silicon atoms incorporated into framework. This confirms that the acid sites in low silica SAPOs are formed by isolated Si atoms. In SAPOs with high Si contents (>16 mol % Si) the number of propene and ammonia molecules desorbed was less than the number of Si atoms incorporated into the framework. Therefore some of the Si may have been incorporated as Si-Si pairs in the place of Al-P pairs [2.9].

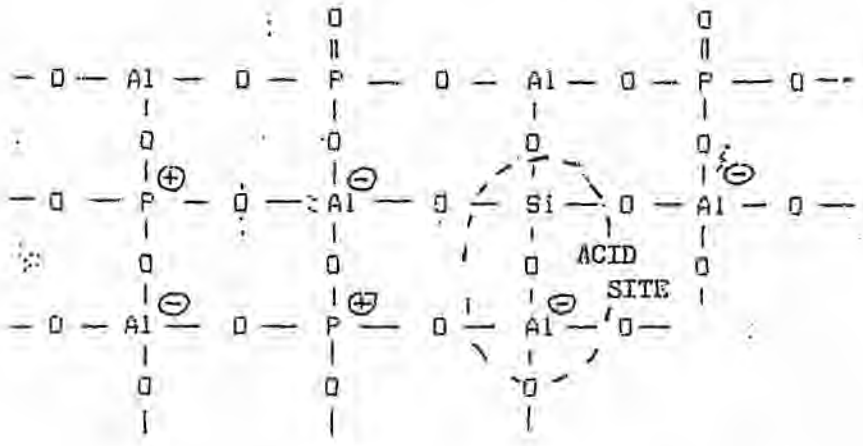


FIG 13 : Acid sites on the SAPO framework

2.3 METHANOL CONVERSION OVER SAPOs

Weisz and Frilette first used the term "shape-selective catalysis" in their report on the selective dehydration of *n*-butanol over the narrow pore zeolite A [2.10]. *Iso*-butanol was shown to be too large to react within the pores [2.10]. This concept has been shown to be extremely important to the petroleum and petrochemical industries e.g. methanol can now be converted selectively to light olefins or gasoline depending on the catalyst used [2.11]. The specific diameter of the molecular sieve channels limits both the entry of certain reactants and the exit of large products into and out of the crystal structure. SAPO-34 is a small pore molecular sieve, so the products of methanol conversion over this molecular sieve are limited to light olefins [2.12]. SAPO-5 has a medium pore structure, so the selectivity for C_4 products is greater than over SAPO-34 [2.8] and larger molecules like hexamethylbenzene are formed [2.8].

The conversion of methanol over silico-aluminophosphates has been patented

Union Carbide [2.13]. Methanol conversion over SAPO-34 in particular is reported to give selectivities to light olefins (C_2 -C_4) of greater than 88 % with 100 % conversion of methanol [2.12, 2.14, 2.15]. However relatively short useful catalytic lifetimes were reported. The need for frequent regenerations led workers at Union Carbide to develop a SAPO-34 catalyst which could be used in a fluidized bed reactor which was cycled between reaction and regeneration modes [2.12]. The small-pore framework of SAPO-34 constrains the product distribution to the C_2 -C_4 range [2.12]. Very low levels (4-7 %) of saturated hydrocarbons (methane, ethane, propane and butane) have been detected [2.12] which shows that there is insufficient surface reactivity in silico-aluminophosphates for hydride transfer to occur for the conversion of olefins to saturated hydrocarbons. Within the C_4 fraction only 1-butene, *cis*-butene, *trans*-butene and no isobutene or isobutane have been detected [2.15]. This would show that there is a steric constraint on the production and/or desorption of branched hydrocarbons. No aromatics were observed in the gaseous effluent which may indicate that either the acid sites are too weak for aromatization to occur, or that aromatics are formed but the pore size is too small to permit them to diffuse out of the pore structure. Methane (4 %) and CO_2 (4.5 %) were detected in the product stream, but 75 % of the methane and CO_2 was shown to result from the reaction of methanol on the walls of stainless steel reactors [2.12]. The selectivity to ethylene was shown to increase with temperature, while the selectivity to butene decreased [2.12]. An ethylene selectivity of 61 % has been achieved at 450°C, using a methanol WHSV of 0.8 h^{-1}, a water WHSV of 2.0 h^{-1} and a nitrogen carrier gas flowrate of 5 ml/min [2.12]. The SAPO-34 was active (100 % methanol conversion) for 5 to 11 hours depending on the reaction temperature [2.12]. The molar ratio of ethylene to propylene in the hydrocarbon product was shown to increase when aromatic diluents with molecules with kinetic diameters greater than the average pore size of SAPO-34 were used (e.g.

benzene and toluene) [2.13].

Marchi and Froment have also studied the conversion of methanol over SAPO-34 [2.15]. In their study the yield of olefins was found to increase at higher reaction temperatures, at lower silicon/aluminium ratios and greater percentages of water in the feed [2.15]. They suggested that water competed with oxygenated and hydrocarbon molecules for the strong acid sites, thereby limiting further reactions of the olefins [2.15]. The number of acid sites decreases during deactivation, as less olefins were converted into paraffins [2.15].

Hydrocarbon formation from methanol on SAPO-34 has been investigated by Anderson *et al* [2.16] and Xu *et al* [2.17] in a closed static system by MAS-NMR. Samples of SAPO-34 and methanol were sealed in Pyrex glass tubes, heated to various temperatures for various periods of time and subsequently quenched in liquid nitrogen. The samples were then analysed by ^{13}C MAS-NMR and the adsorbed products were compared to gaseous products obtained under the same conditions in a flow through reactor [2.16].

Anderson *et al* [2.16] showed that more C_3 species were present in the adsorbed products than C_1 and C_2, but in the gaseous products C_1 species were the most abundant, followed by C_2 and C_3. Only 5 to 10 % of the C_3 species found in the adsorbed phase were observed in the gas-phase. Above 270°C the diffusion coefficients for methane, ethane and propane can be expected to be of the same order in chabazite type structures, therefore additional constraints on diffusion of the C_3 fraction must have been present. Branched aliphatics up to C_4 were observed in the adsorbed phase, but not in the gaseous phase [2.16]. These branched aliphatics must have formed inside the SAPO-34 cavities and were incapable of leaving the cavities even at 370°C. Anderson

et al [2.16] suggested that branched hydrocarbons partially block the pore system and therefore retard the diffusion of the C_3 species. It is therefore not sufficient to only consider crystallographic pore dimensions in order to predict shape-selectivity of a catalyst. Furthermore, this interference of the diffusion of C_3 products by branched hydrocarbons indicates that the catalyst could be made more selective for C_2 and C_3 species if occluded material or large cations are incorporated into the catalyst [2.16]. These occluded species could prevent branched hydrocarbons from forming and impose some constraint so that only C_2 and C_3 species diffuse out of the intracrystalline spaces [2.16].

Higher olefin selectivity was obtained in the flow through reactor system due to shorter residence times [2.17]. The olefins were flushed out of the zeolite before they reacted further. The concentration of C_4 paraffins in the static system decreased when the temperature increased above 400°C. It was thought that the C_4 paraffins were converted into aromatics by dehydrogenation and disproportionation reactions [2.17]. Aromatics were observed in the adsorbed phase after methanol conversions at temperatures above 400°C [2.17]. SAPO-34 has weaker acid sites than ZSM-5, therefore the conversion of alkanes to aromatics is expected to be lower [2.17]. An increase in the residence time and reaction temperature increased the proportion of aromatics observed in the adsorbed phase, but no aromatics were detected in the gaseous phase as they were too bulky to diffuse out of the SAPO-34 cavities [2.17]. The concentration of ethane increased when the temperature increased above 450°C, which indicates that ethane could be a side product during the formation of aromatics or cracking reactions.

The ^{13}C-MAS NMR signals from methanol and DME adsorbed on SAPO-34 were broad, indicating that methanol and/or DME are strongly bound on SAPO-34. After

conversion into hydrocarbons the aliphatic resonances were much narrower which indicated that the non-polar hydrocarbons were less strongly bound than the polar oxygenates [2.16].

The catalytic conversion of methanol over SAPO-5 has been studied by Das *et al* [2.8] in a fixed bed continuous flow reactor at 350°C and a methanol WHSV of 0.6 h^{-1}. The gaseous products consisted of 33 to 57 wt % olefins, while the liquid products comprised hydrocarbons in the boiling range 98-320°C. The selectivity to C_4 products (30 to 50 wt %) [2.8] was enhanced compared to SAPO-34 (21 wt %) [2.18] under the same conditions, due to the wider pore dimensions. A significant amount of solid hexamethylbenzene was also formed (7 wt %).

2.4 EFFECT OF PORE STRUCTURE ON THE DEACTIVATION OF SAPOs

The structure of SAPO-34, with small pore openings into the large supercages, restricts the transport of reactants and products to only straight chain paraffins and olefins [2.11]. The large cages are sufficiently large to facilitate the formation of "coke" precursors, but deactivation is expected to occur when diffusion of aromatics out of the cages is restricted.

SAPO-5 has larger pores than SAPO-34 which allows the intermediates for hexamethylbenzene branched hydrocarbons to form, and does not inhibit the diffusion of the hexamethylbenzene out of the zeolite [2.8]. The pores are therefore large enough for the initial "coke" precursors to form too. Deactivation by "coke" deposition only occurs when "coke" molecules become too bulky to diffuse out of the pores.

2.5 EFFECT OF THE ACID SITES OF SAPOs ON DEACTIVATION

Temperature programmed desorption (TPD) of dimethyl ether (DME) and ethene from SAPO-34, metal substituted SAPOs (MeAPSOs) and H-ZSM-5 after methanol adsorption has been used to show that the acid strength of SAPO-34 is lower than that of MeAPSOs which in turn is lower than H-ZSM-5 [2.2]. The temperature of the DME desorption peaks showed that the Me-(OH)-P group in MeAPSO-34 samples were more acidic than the Si-(OH)-Al groups in SAPO-34 and MeAPSO-34, but less than the Si-(OH)-Al groups in H-ZSM-5 [2.2]

Diffuse Reflectance Infrared Fourier Transform spectroscopy of some SAPOs have shown that bridging Si-(CH)-Al groups are present [2.19]. Only aluminium hydroxyls are present in SAPO-34, whereas in other SAPOs (e.g. SAPO-11 [2.15]) silicon and phosphorous hydroxyls are also present [2.15]. The silicon and phosphorous hydroxyls are less acidic than aluminium hydroxyls.

The formation of hexamethylbenzene during methanol conversion over SAPO-5 requires the catalyst to have dehydrogenation activity and weak acidic properties, so that the intermediate can proceed through an allyl intermediate [2.8]. Electron transfer between the weak acid centres and the allyl group generates a radical-like species which undergoes dimerization, cyclization, oxidative dehydrogenation and alkylation to form hexamethylbenzene [2.8] in the same way that "coke" is formed.

2.6 "COKE" FORMATION ON SAPOs DURING METHANOL CONVERSION

There has been only one report to date on the deactivation of SAPO catalysts during the conversion of methanol [2.15]. Marchi and Froment stated that the deactivation of SAPO-34 occurs in two stages [2.15]. Initially there is slow

deactivation of the acid sites as oligomers and "coke" precursors adsorb onto them. In the second stage there is a drastic deactivation caused by pore blockage with bulky hydrocarbons. They suggested that the linear compounds e.g. light olefins, paraffins and oligomers, can migrate from the small pores to the large cavities and subsequently interact with the strong acid sites. The light olefins and oligomers can react together in the cavities to form heavier oligomers which grow to be too bulky to leave the cavities [2.15]. However, no study on the characterization of the "coke" responsible for the deactivation of SAPOs has been published.

Increasing the reaction temperature above 427°C, lowering the silicon/aluminium molar ratio (from 0.15 to 0.05) and increasing the water content of the feed (from 0 to 70 wt %) were all found to decrease the rate of "coke" formation on SAPO-34 during methanol conversion [2.15]. The strength and concentration of acid sites was reduced by the water adsorbed onto them, and this decreased aromatisation and "coke" formation [2.15]. The concentration of acid sites also decreased when the silicon/aluminium ratio decreased [2.15]. The deactivation of SAPO-34 was found to be more strongly affected by the strength of the acid sites and the pore structure, than the concentration of acid sites [2.15].

2.7 REGENERATION OF SAPO CATALYSTS

Deactivated SAPO-34 catalysts have been regenerated by burning off the carbonaceous deposit in flowing air at 500°C for 1 to 2 h [2.12]. The conversion of methanol over SAPO-34 which had been used for 55 reaction/regeneration cycles was slightly lower than over fresh SAPO-34, but the selectivity to light olefins was the same [2.20]. XPS studies on the SAPO-34 catalyst regenerated 55 times showed that some of the aluminium had

migrated to the surface. Therefore the number of acid sites had decreased [2.20]. This could have been due to hydrothermal dealumination [2.20]. The catalytic activity of the lower part of the catalyst bed was slightly higher than at the top of the catalyst bed which indicates that there was sequential deactivation along the catalyst bed [2.20]. The crystallinity of the catalyst framework, as determined by X-ray diffraction (XRD), was shown to be unaffected after fifteen conversion / regeneration cycles [2.12].

2.8 REFERENCES

2.1] Anderson, M.W., Sulikowski, B., Barrie, P.J. and Klinowski, J.; *J. Phys. Chem.*, 94, (1990), 2730

2.2] Hocevar, S. and Levec, J.; *J. Catal.*, 135, (1992), 518

2.3] Singh, B.B.; Doctor of Philosophy Dissertation entitled "Catalytic Conversion of Methanol to Low Molecular Weight Hydrocarbons", Dec. (1979), Texas University.

2.4] Chatterjee, N., Ganguli, D. and Saha, P.; *Transaction of the Indian Ceramic Society*, 35 (5), (1976), 99

2.5] Inui, T., Phatanasri, S. and Matsuda, H.; *J. Chem. Soc. Commun.*, (1990), 205

2.6] Lewis, J.M.O.; *Catalysis*, (1987), 199

2.7] Inui, T.; Showa Shell Sekiyu Kabushiki Kaisha, EP 0 418 142 A1, (1991)

2.8] Das, J., Bhattacharya, A., Goswami, T.K. and Roy, S.K.; *J.Chem.Tech. Biotechnol.*, 50, (1991), 13

2.9] Biaglow, A.I., Adamo, A.T., Kokotailo, G.T. and Gorte, R.J.; *J.Catal.*, 131, (1991), 252

2.10] Weisz, P.B. and Frilette, V.J.; *J. Phys. Chem.*, 64, (1960), 382

2.11] N.Y. Chen and W.E. Garwood; *Catal. Rev. Sci. Eng*,28,(1986),185

2.12] Kaiser, S.W.; *Arab J. Sci. Eng.*, **10**, (1985), 361

2.13] Kaiser, S.W., U.S. Patent 4524 234, (1985)

2.14] Lewis, J.M.O. in Catalysis 1987, Ward, J.W. (ed), Elsevier Science Publishers, Amsterdam, (1988)

2.15] Marchi, A.J. and Froment, G.F.; *Applied Catalysis*, 71, (1991), 139

2.16] Anderson, M.W., Sulikowski, B., Barrie, P.J. and Klinowski, J.; *J. Phys. Chem.*, 94, (1990), 2730

2.17] Xu, Y., Grey, C.P., Thomas, J.M. and Cheetham A.K.; *Catal. Letters*, 4, (1990), 251

2.18] Inui, T., Matsuda, H., Okamura, H. and Miyamoto, A.; *Appl. Catal.*, 58, (1990), 155

2.19] Zibrowlus, B., Löffler, E., Finger, G., Sonntag, E., Hunger, M. and Kornatowski, J.; Catalysis and Adsorption by Zeolites, Öhlmann *et al* (Eds.), Elsevier Science Publishers, Amsterdam, (1991), 537

2.20] Liang, J., Li, H., Zhao, S., Guo, W., Wang, R. and Ying, M.; *Appl. Catal.* 64 (1990), 31

CHAPTER THREE : CATALYST PREPARATION AND CHARACTERIZATION

3.1 INTRODUCTION

In order to study the deactivation due to "coke" formation on SAPO catalysts during methanol conversion, batches of SAPO-34, SAPO-5, Ni-SAPO and silicon-modified SAPO-34 were prepared. The formation of "coke" on H-ZSM-5 during methanol conversion experiments has been studied and reported in great detail [e.g. 3.1], and was therefore studied in conjunction with the SAPOs for comparison purposes.

The integrity of the prepared SAPO-34, SAPO-5, Ni-SAPO and silicon-modified SAPO-34, as well as the treated ZSM-5, was determined by X-ray diffraction (XRD) and X-ray fluorescence (XRF) spectroscopy. The atomic frameworks of the SAPO-34 and H-ZSM-5 were analysed by magic angle spinning nuclear magnetic resonance (MAS-NMR) spectroscopy. The acid sites on the catalysts were analysed by temperature programmed desorption (TPD) of ammonia.

3.2 EXPERIMENTAL

3.2.1 Treatment of ZSM-5

Powdered ZSM-5 was ammonium ion-exchanged with 1M NH_4NO_3 (250 ml per 200 g of ZSM-5) at room temperature for 15 hours. The ZSM-5

was subsequently rinsed three times with distilled, deionized water and then dried (100°C, 4h) and calcined (650°C, 4h) to leave the ZSM-5 in the acid form (H-ZSM-5). The H-ZSM-5 was pelletized using a Specac hydraulic press, 5 tons pressure and a 20 mm die. The pelletized catalyst was then crushed, sieved and the particles between 850 and 1150 μm in size were retained.

3.2.2 Synthesis of SAPO-34

The SAPO-34 catalyst was prepared according to a method described by Inui *et al* [3.2]. Aluminium isopropoxide (0.20 mol) was added to 3.88 mol of distilled, deionized water, under nitrogen, with vigorous stirring. *Ortho*-phosphoric acid (0.283 mol) and finely divided silica (0.06 mol) were similarly added. The template, tetraethylammonium-hydroxide (TEAOH) (0.10 ml) was then added and the mixture homogenized in an ultrasonic bath. The gel was charged to a teflon lined stainless steel autoclave (Parr) using 5.55 mol of extra water to transfer the last part of the gel. The autoclave was purged with nitrogen, heated to 160°C at 1.5°C / min, then to 200°C at 12°C/h, and held there for 4 to 15 hours under autogenous pressure (400 psi). The catalyst was recovered by centrifugation, washed three times with distilled, deionized water, dried (120°C, 15h) and calcined in air (600°C, 6 h). The SAPO-34 was pelletized, crushed and sieved, as described in section (3.2.1), to give particle sizes between 850 μm and 1150 μm.

3.2.3 Synthesis of SAPO-5

SAPO-5 was prepared using the same method as for SAPO-34, using one quarter of the water and twice as much TEAOH template. Aluminium isopropoxide (2.203 mol) was hydrolysed with distilled, deionized water (23.3 mol). *Ortho*-phosphoric acid was added slowly (2.285 mol) followed by finely divided silica (0.657 mol) and TEAOH (0.11 mol). The mixture was placed in an 800 ml autoclave which was subsequently purged with nitrogen. The autoclave was heated to 160°C at 1.5°C / min, then to 200°C at 12°C / h, and held there for 15 hours under autogenous pressure (400 psi). The catalyst was recovered by centrifugation, washed 3 times in distilled, deionized water, dried (100°C, 4 h) and calcined (550°C, 6 h). The SAPO-5 catalyst was pelletized, crushed and sieved to give particle sizes between 850 μm and 1150 μm, as described in section (3.2.1).

3.2.4 Synthesis of Ni-SAPO

Nickel hydroxide was prepared by dissolving nickel sulphate (30.0 g) in water (60 ml) followed by the addition of 3 M sodium hydroxide (90 ml). The nickel hydroxide was recovered by centrifugation and washed three times in distilled, deionized water. The nickel hydroxide was converted into nickel acetate by the addition of acetic acid (13.7 g) and subsequent evaporation of the excess acetic acid. A 87.3 % yield of nickel acetate was obtained and this salt was used in the synthesis of Ni-SAPO, using a method described by Inui [3.3]. The molar ratios of the synthesis mixture were

0.2 Ni : 1.0 Al : 0.2 Si : 1.0 P : 0.5 TEAOH.

The synthesis mixture was crystallized for 2 days at 150°C under autogenous pressure, washed three times in distilled, deionized water, dried (100°C, 4h) and calcined (550°C, 15h). The Ni-SAPO was pelletized, crushed and sieved to give particle sizes between 850 μm and 1150 μm, as described in section (3.2.1).

3.2.5 Modification of SAPO-34

A portion of the SAPO-34 (prepared by the method described in section 3.2.2) was modified with trimethyl-silylchloride in an attempt to decrease the activity, and hence "coke" formation, on the surface of the catalyst. This silylating agent is t ılky to enter the pores of SAPO-34 and therefore does not deactivate the hydroxyl sites within the pores of catalyst. Trimethyl silylchloride (0.80 g) was dissolved in 7.20 g of xylene and the mixture was added to 10.0 g of SAPO-34. The xylene was evaporated off at room temperature for 4 hours and then the catalyst was dried at 110°C for 15 hours.

3.2.6 Characterization of the catalysts

The crystallinity of the catalysts was analysed by XRD using a Philipps PW1050 XRD spectrometer. The molar composition of each of the catalysts was determined on a Phillips 1410 XRF spectrometer.

The atomic framework of the SAPO-34 catalyst was analysed by MAS-

NMR spectroscopy at the Council for Scientific and Industrial Research (CSIR), Pretoria, using a Brüker AM300 MAS-NMR spectrometer, using spectroscopically pure oxides of Al, Si and P as the reference materials

The acid sites on the catalysts were also analysed by ammonia TPD analysis. The catalyst sample was degassed under a stream of helium, heating to 700°C at 10°C / min and maintaining this temperature for 30 minutes before cooling under helium. The sample was then saturated with ammonia at room temperature and then heated to 100°C to desorb any condensed or partially adsorbed ammonia. The temperature was then raised to 700°C at 10°C / min and the ammonia which desorbed was monitored by a thermal conductivity detector.

3.3 RESULTS AND DISCUSSION

3.3.1 X-ray diffraction and X-ray fluorescence spectroscopy

3.3.1.1 H-ZSM-5

The XRD pattern obtained for the H-ZSM-5 is shown in Fig. 14 and the XRD data is listed in Table III. The molar ratios of Al and Si in the ZSM-5 were found to be 1.0 Al : 18.3 Si (95 % Si), using XRF spectroscopy.

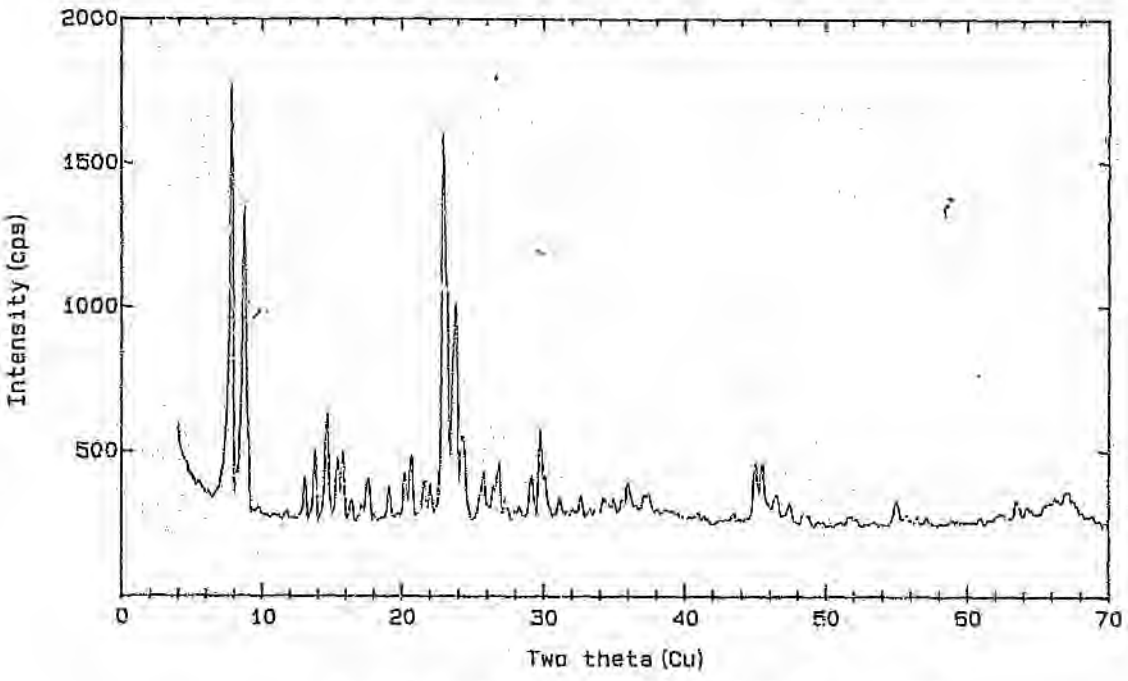


FIGURE 14 : XRD PATTERN OF H-ZSM-5

TABLE III : XRD DATA FOR H-ZSM-5

TREATED H-ZSM-5		REPORTED H-ZSM-5 [3.9]	
2θ	INTENSITY	2θ	INTENSITY
7.8	100	7.8	98
8.7	73	8.9	91
		13.0	21
13.8	19	13.8	32
14.7	28	14.7	38
15.4	18	15.4	25
15.8	19	15.8	34
		16.2	16
		17.5	21
		19.0	17
20.3	15	20.1	18
20.7	19	20.8	26
		22.0	17
23.0	90	23.0	100
23.2	54		
23.8	53	23.6	51
24.3	23	24.2	5
25.8	15	25.8	20
26.9	17	26.3	22
29.8	24	29.1	21
		29.9	25
45.0	17	45.1	19
45.4	17		

3.3.1.2 SAPO-34

The XRD pattern of the synthesized SAPO-34 (Fi. 15) closely matched the XRD data reported for SAPO-34 [3.2] as shown in Table IV.

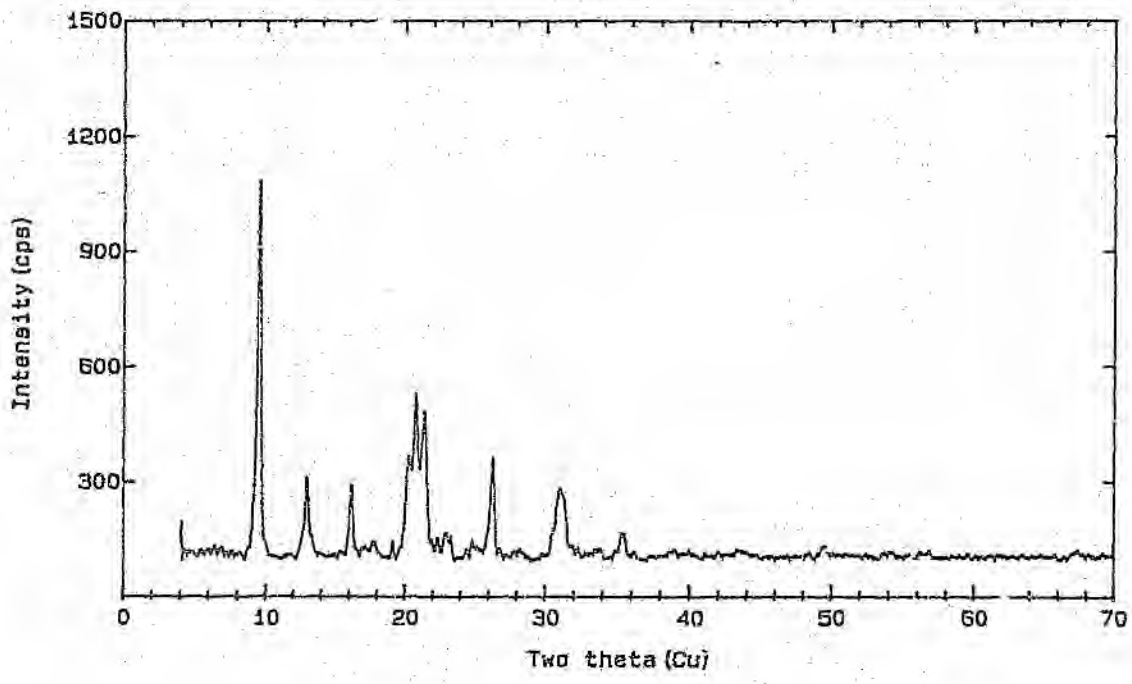


FIGURE 15 : XRD PATTERN FOR SAPO-34

The molar ratios of the synthesized SAPO-34 were found to be 1.00 Al : 0.27 Si : 0.86 P which corresponds to the range of molar ratios reported for SAPO-34 (1.00 Al : 0.10-0.30 Si : 0.9-0.70 P) [3.4].

TABLE IV : XRD DATA OF SAPO-34

SYNTHESIZED SAPO-34		REPORTED SAPO-34	
2θ	INTENSITY	2θ	INTENSITY
9.7	100	9.5 - 9.7	100
13.1	21	12.8 - 13.0	8- 20
		14.0 - 14.2	8- 23
16.3	10	16.0 - 16.2	25- 54
17.9	6	17.9 - 18.2	11- 76
20.4	17	20.6 - 20.9	44-100
20.9	24		
21.5	13		
23.2	6	23.0 - 23.2	2- 10
23.7	4		
25.1	5	25.0 - 25.4	12- 87
26.2	7	25.8 - 26.0	14- 26
28.	3	28.1 - 28.4	1- 12
29	1	30.5 - 30.7	19- 75
31.0	34	31.1 - 31.4	15- 28
32.0	3		
34.9	3	34.4 - 34.7	4- 15
35.6	2		
49.2	2	48.8 - 49.2	4- 7

3.3.1.3 SAPO-5

The XRD data obtained for the synthesized SAPO-5 corresponded to the data reported in the literature [3.4], as shown in Table V. The XRD pattern is shown in Fig 16. The molar ratios of the synthesized SAPO-5 were found to be 1.00 Al : 0.22 Si : 0.93 P which is within the range of ratios reported for SAPO-5 (1.00 Al : 0.1-0.6 Si : 0.9-1.0 P) [3.4].

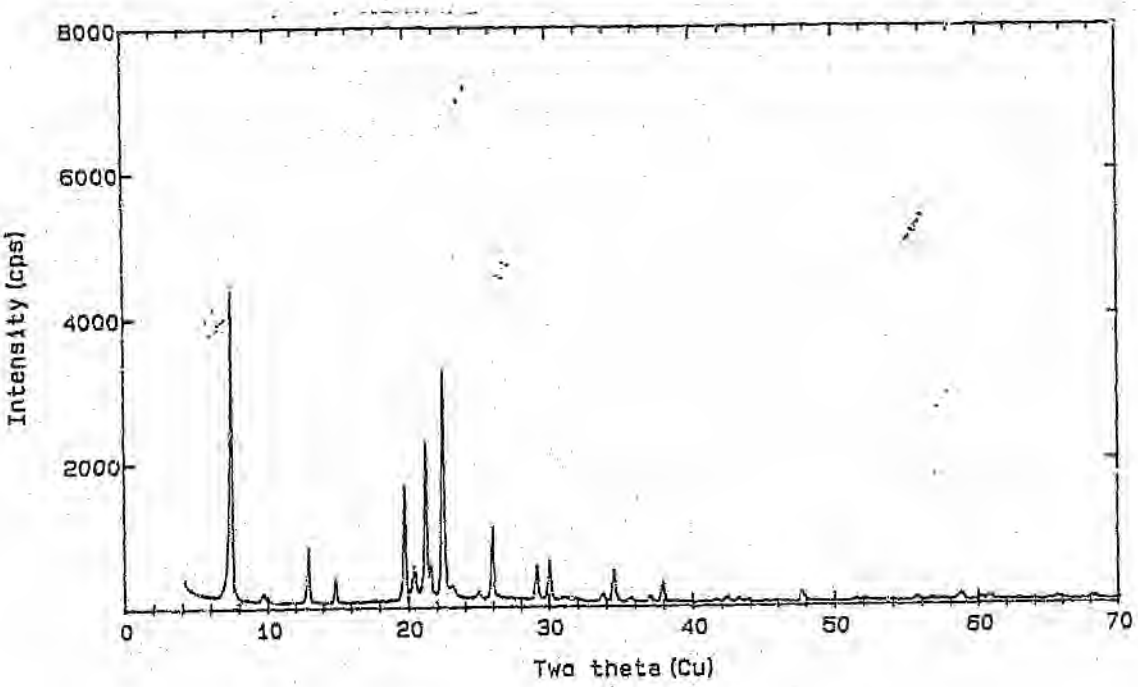


FIGURE 16 : XRD PATTERN OF SAPO-5

TABLE V : XRD DATA OF SAPO-5

SYNTHESIZED SAPO-5		REPORTED SAPO-5	
2θ	INTENSITY	2θ	INTENSITY
7.5	100	7.5	100
9.7	4		
12.9	15	13.0	12
14.9	4	15.0	23
19.8	28	19.9	56
21.2	75	21.0	52
22.5	79	22.5	68
24.9	1	24.7	2
25.9	22	26.2	29
29.1	8	28.9	8
30.0	7	30.3	17
33.6	2	33.8	3
34.6	8	34.8	12
37.1	1	37.1	2
37.9	6	37.7	7
41.5	1	41.8	1
42.4	2	42.6	2
47.7	3	48.1	2
58.7	3	52.1	2

3.3.1.4 Ni-SAPO

The molar ratios of the Ni-SAPO catalyst were found to be 0.2 Ni : 1.0 Al : 0.2 Si : 0.8 P, which is consistent with the reported data [3.5]. The XRD pattern and data obtained, along with the reported data for Me-SAPO-5 and Me-SAPO-34, are shown in Fig 17 and Table VI. The synthesized catalyst was found to be Ni-SAPO-5.

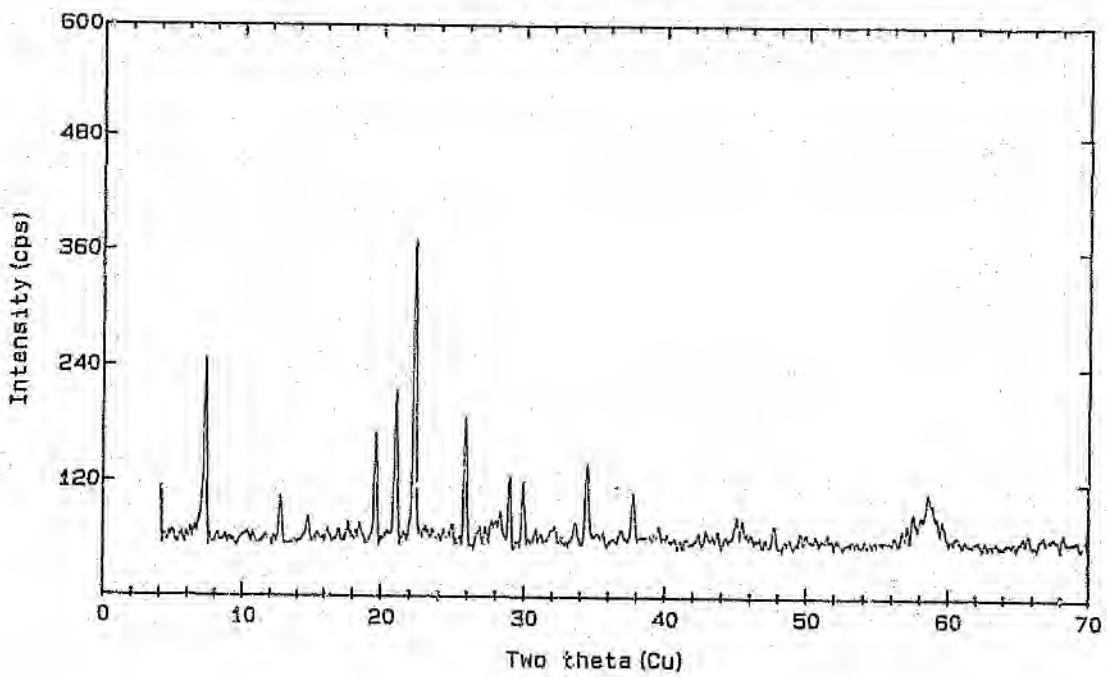


FIG 17 : XRD PATTERN OF Ni-SAPO-34

TABLE VI : XRD DATA OF Ni-SAPO AND OTHER Me-SAPOs

Ni-SAPO		REPORTED Me-SAPO-34		REPORTED Me-SAPO-5	
2θ	INTENSITY	2θ	INTENSITY	2θ	INTENSITY
7.3	61			7.3	m-vs
		9.5	m-vs		
12.8	17	12.9	w-m		
		16.0	vw-m		
19.6	37			19.6	w-m
		20.8	w-vs		
21.0	50			21.2	w-vs
				22.3	m-vs
		25.1	vw-m		
25.8	43			25.8	vw-m
29.0	23				
30.0	22	30.5	vw-m		
34.5	28				
37.8	18				
58.6	19				

3.3.1.5 Silicon-modified SAPO-34

The XRD data obtained for the silicon modified SAPO-34 was similar to that obtained for SAPO-34 as shown in Table VII. The XRF analysis showed that the molar ratios of the silicon-modified SAPO-34 were 1.0 Al : 0.1 Si : 0.8 P which shows that the silicon content did not increase during the modification as expected, or that the Si content increased by such a small amount that the difference could not be detected by XRF analysis. The XRD pattern, as shown in Fig 18, was the same as for SAPO-34, except the peak at 2θ = 20.05 had decreased.

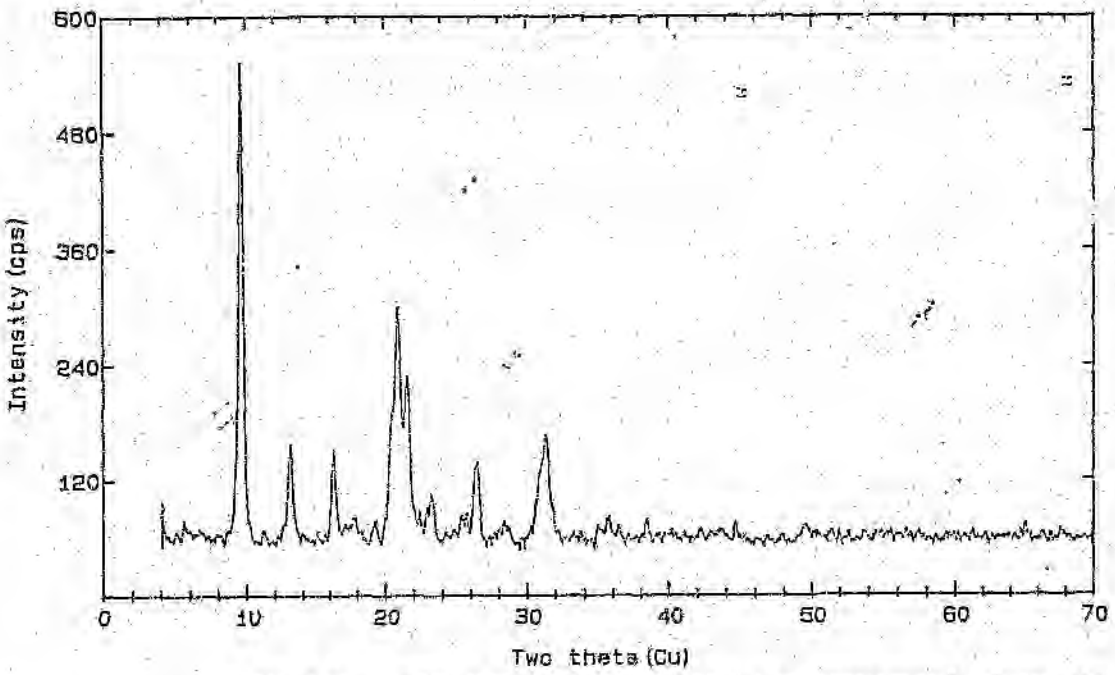


FIG 18 : XRD PATTERN OF SILICON-MODIFIED SAPO-34

TABLE VII : XRD DATA OF SILICON-MODIFIED SAPO-34 AND SAPO-34

SILICON MODIFIED SAPO-34		UNMODIFIED SAPO-34	
2θ	INTENSITY	2θ	INTENSITY
9.7	100	9.7	100
13.1	25	13.1	21
16.3	20	16.3	10
		17.9	6
20.5	shoulder	20.4	17
20.9	50	20.9	24
21.6	36	21.5	13
22.1	6		
23.0	8		
23.3	10	23.2	6
		23.7	4
		25.1	5
26.4	18	26.2	7
		28.3	3
		29.9	1
31.3	23	31.0	34
31.9	6	32.0	3
		34.9	3
35.7	6	35.6	2
38.4	6		
44.6	5		
		49.2	2

3.3.2 Solid state magic angle spinning - nuclear magnetic resonance spectra

The ^{27}Al, ^{31}P and ^{29}Si MAS-NMR spectra of SAPO-34 are shown in Fig 19a and the ^{27}Al and ^{29}Si MAS-NMR spectra of H-ZSM-5 are shown in Fig 19b.

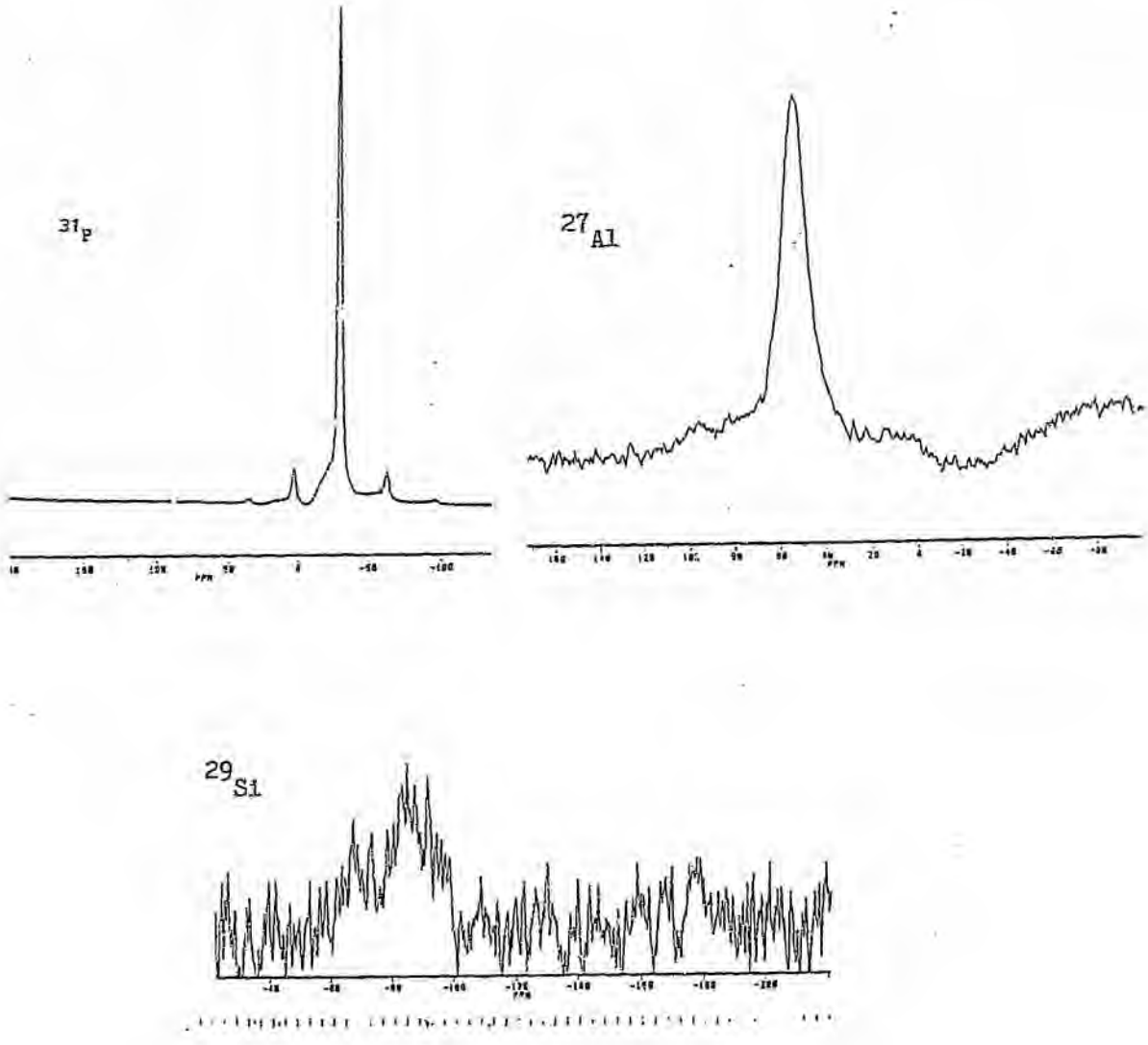


FIG 19a : MAS-NMR SPECTRA OF SAPO-34

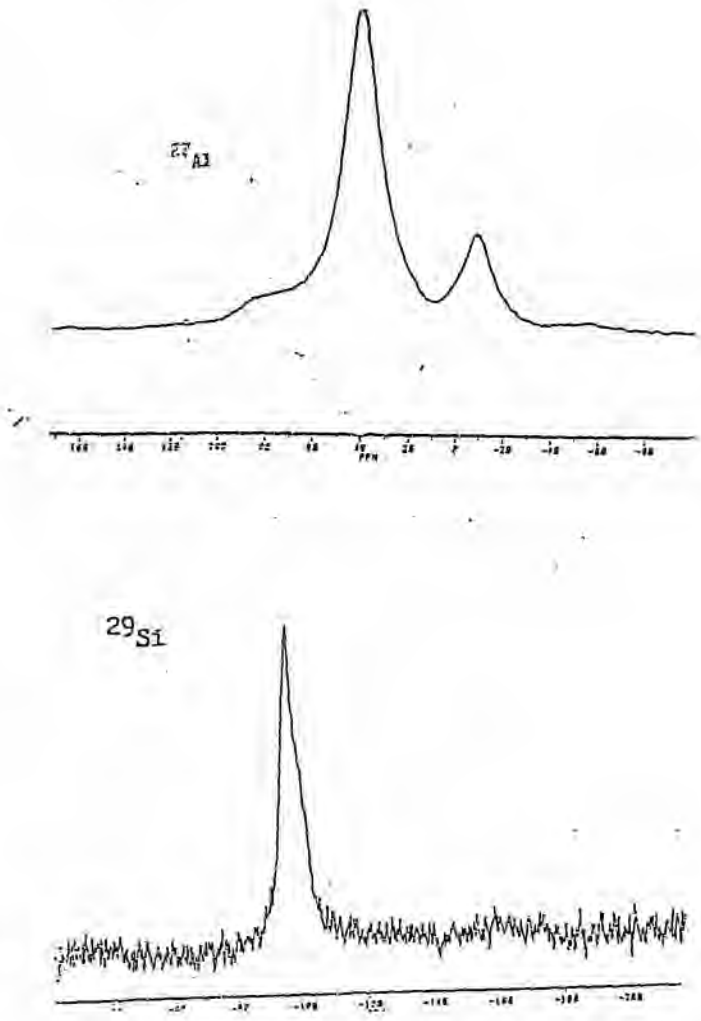


FIGURE 19b : MAS-NMR SPECTRA OF H-ZSM-5

The ^{27}Al signals obtained for H-ZSM-5 at -9 ppm and 40 ppm relative to aluminium trichloride hexahydrate show that Al was present in both octahedral and tetrahedral environments respectively. The octahedral Al is due to non-framework Al [3.8]. The ratio of tetrahedral to octahedral sites was 3:1 respectively. In SAPO-34 only a ^{27}Al signal at 58 ppm due to tetrahedrally co-ordinated Al was observed.

A strong ^{31}P signal at -30 ppm relative to $CaHPO_4$ and two sidebands was observed for SAPO-34. This is typical of P(4Al) environments in $AlPO_4$ [3.6].

A ^{29}Si single peak of very low intensity was observed at -84 ppm relative to tetramethylsilane which corresponds to Si(4Al) units [3.7]. The absence of a ^{29}Si signal in the -110 region shows that no amorphous silica was present [3.7]. A ^{29}Si peak at -96 ppm relative to tetramethylsilane, with a shoulder in the -100 ppm region, was observed for H-ZSM-5. This corresponds to Si in Si(2Al) and Si(1Al) environments [3.8]

The framework of SAPO-34 was therefore shown to be a matrix of aluminium and phosphorous oxide tetrahedra, with occasional silicon oxide tetrahedra substituting the phosphorous oxide tetrahedra, as shown in Fig 13 of section [2.2]. This model is in accordance with Loewenstein's rule in that no Al-O-Al linkages were observed [3.8].

3.3.3 Temperature programmed desorption studies

Spectra of the temperature programmed desorption of ammonia from H-ZSM-5, SAPO-34 and SAPO-5 are shown in Fig 20. Desorption of physisorbed ammonia, which was not evacuated off, was found at 208°C, 218°C and 200°C for H-ZSM-5, SAPO-34 and SAPO-5 respectively. Desorption of ammonia adsorbed onto the acid sites of H-ZSM-5, SAPO-34 and SAPO-5 was observed at 425°C, 350°C and 268°C respectively. This shows that strong acid sites were present in H-ZSM-5, weaker acid sites were present in SAPO-34 and the weakest acid sites were present in SAPO-5.

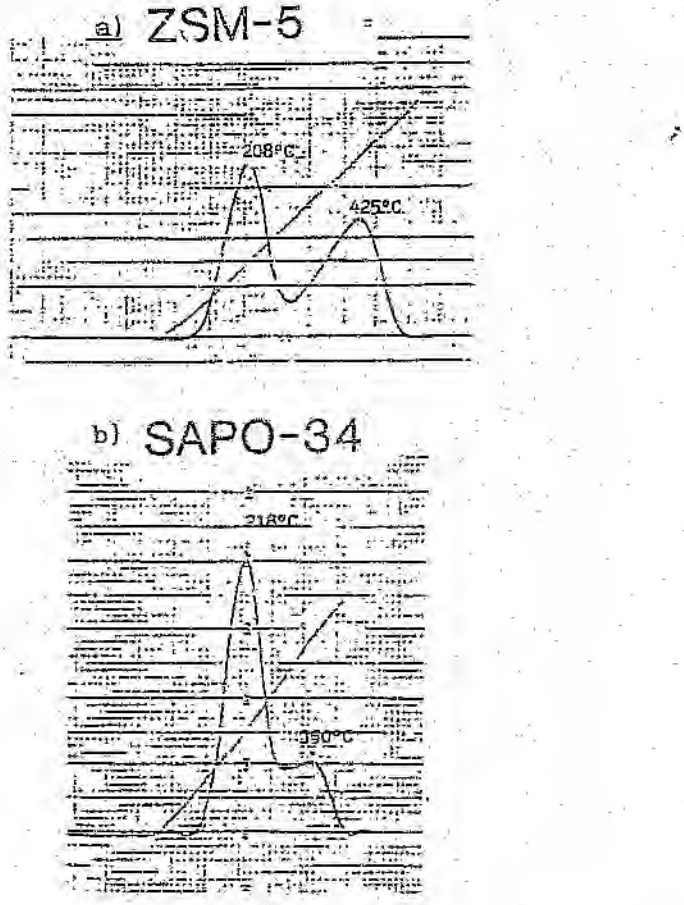


FIG 20 : TPD SPECTRA OF a) H-ZSM-5, b) SAPO-34 AND c) SAPO-5

The weak acid sites are probably due to surface hydroxyls, while the stronger acid sites are most likely bridging Si-OH-Al groups. Only one type of weak acid site was observed in SAPO-34, due to aluminium hydroxyls according to studies discussed in section {2.5} by Marchi *et al* [3.10]. Marchi *et al* reported that phosphorous and silicon hydroxyls were found in SAPO-11, so the additional weak Brönsted acid site observed in SAPO-5 was most likely due to one or both of these hydroxyl groups.

3.4 CONCLUSIONS

Authentic batches of H-ZSM-5, SAPO-34, SAPO-5, Ni-SAPO and silicon modified SAPO-34 were prepared. The framework of SAPO-34 was shown to consist of isolated Si atoms substituting phosphorous in a network of phosphorous and aluminium tetrahedra. The Si atoms in ZSM-5 were shown to be in Si(2Al,2Si) or Si(1Al,3Si) tetrahedral environments. Strong Brönsted acid sites were only observed in H-ZSM-5, while weak Brönsted acid sites were observed in H-ZSM-5, SAPO-34 and SAPO-5 due to bridging Si-OH-Al groups. Additional weak Brönsted acid sites were observed in SAPO-5, possibly due to P-OH or OH groups.

3.5 REFERENCES

3.1] Bibby, D.M , Milestone, N.B., Patterson, J.E. and Aldridge, L.P.; *J. Catal.*, **97**, (1986), 493

3.2] Inui, T., Matsuda, H., Okaniwa, H. and Miyamoto, A.; *Appl. Catal.*, **58**, (1990), 155

3.3] Inui, T., Phatanasri, S. and Matsuda, H.; *J. Chem. Soc. Chem. Commun.*, (1990), 205

3.4] Lok, B.M., Messina, C.A., Patton, R.L., Gajek, R.T., Cannan, T.R. and Flannigan, E.M., U.S. Patent 4 440 871

3.5] Inui, T.; Showa Shell Sekiyu Kubushiki Kaisha, EP 0 418 142 A1, (1991)

3.6] Kornatowski, J., Baur, W.H. and Pieper, G.; *J. Chem. Soc. Faraday Trans.*, **88** (9), (1992), 3033

3.7] Anderson, M.W., Sulikowski, B., Barrie, P.J. and Klinowski, J.; *J. Phys. Chem*, **94**, (1990), 2730

3.8] Engelhardt, G. and Michel, D.; High resolution solid-state NMR of silicalites and zeolites, John Wiley and Sons, New York, (1987), 218-229

3.9] Argauer, R.J., Olson, D.H. and Landoli, G.R.; U.S. Patent 630 993, (1967)

3.10] Marchi, A.J. and Froment, G.F.; *Appl. Catal.*, **71**, (1991), 139

CHAPTER FOUR - DEACTIVATION OF CATALYSTS DURING METHANOL CONVERSION : MEASUREMENT OF "COKE" DEPOSITION

4.1 INTRODUCTION

There have been many reports on the conversion of methanol over SAPO catalysts [4.1, 4.2, 4.3, 4.4, 4.5, 4.6] but to date there has been only one report on the deactivation of SAPOs during methanol conversion [4.3], and no report on the characterization of the deposited "coke".

The ZSM-5, SAPO-34, SAPO-5, Ni-SAPO and silicon-modified SAPO-34 catalysts were all used in methanol conversion reactions under the same conditions so that a comparative study on the deactivation rate due to "coke" formation could be assessed.

The relative effects of the carbonaceous deposits on the surface areas and pore volumes of the various catalysts were determined to investigate the mode and rate of deactivation due to "coke" formation. A steady decrease in surface area and pore volume would indicate that the "coke" was deposited uniformly through the catalyst. Alternatively, a rapid decrease in both surface area and pore volume would indicate that the deactivation was due to pore blockage. If the rate of loss of activity decreased more rapidly than the surface area and pore volume, the deactivation could be ascribed to the poisoning of acid sites [4.7].

A statistically designed series of eight methanol conversion experiments was conducted to investigate the degree of "coke" formation on SAPO-34 during methanol conversion reactions under various conditions. The effects of temperature, reaction pressure and degree of dilution of the methanol feed with water, on the formation of "coke", were investigated. The amount of carbon as well as the densities of the spent catalysts were determined in order to investigate the formation of "coke" on the catalyst under the various conditions.

The oxygenates and hydrocarbons adsorbed onto the surface of SAPO-34 during methanol conversion were observed by *in situ* diffuse reflectance infra-red spectroscopy (DRIFTS). The effect of methanol conversion on SAPO-34 has previously been investigated using *ex situ* and *in situ* DRIFTS [4.8 and 4.4 respectively]. The weakly acidic AL-OH and P-OH groups on the outer surface of the crystallites were observed at 3795, 3740 and 3680 cm^{-1} [4.8]. The more intense bands at 3625 and 3600 cm^{-1} have been assigned to Si-OH-Al groups arising from the isomorphous substitution of Si for P in the framework [4.8]. These bands have also been observed in SAPO-5 [4.8]. The band at 3625 cm^{-1} corresponds to Si-OH-Al groups which form weak complexes with hydrogen (a weak base), whereas the Si-OH-Al groups which give a stretching vibration band at 3600 cm^{-1} do not interact with hydrogen [4.8]. The former hydroxyl group is probably located in the inner spaces of the hexagonal prisms where they are hydrogen bonded to the neighbouring oxygen anions of the framework [4.8]. Both types of hydroxyl groups interact with stronger bases and have the same acidity as the Si-OH-Al

hydroxyls in SAPO-5 [4.8]. A band at 3950 cm^{-1} was detected and was assigned to the out-of-plane bending of the bridged hydroxyl groups [4.8]. No aromatics were visible [4.4], although their presence has been observed by MAS NMR [4.4].

The stretching and bending vibrations of various oxygenates and hydrocarbons on the surface of zeolites, as reported by numerous authors [4.7, 4.8, 4.9, 4.10, 4.11, 4.12, 4.13, 4.14 and 4.15], are summarized in Table VIII.

TABLE VIII : IR CHEMICAL SHIFTS OF SPECIES ADSORBED ON ZEOLITE SURFACES

CHEMICAL SHIFT (cm^{-1})	CHEMICAL LINKAGES
< 1200	Si-O and Al-O linkages
1315-1410	C-H vibrations of unsaturated compounds
1460	Asymmetric methyl bend of adsorbed MEOH
1410-1620	Aromatic rings
1550-1700	C=C stretching of olefins
1625	Adsorbed water
1550-1900	C=O stretching of carbonyl compounds
2700-3000	Aliphatic methyl or methylene groups or C-H vibrations of surface methoxy species
3000-3100	C-H stretching vibrations (olefinic and aromatic)
3500	Stretch vibrations of H-bonded OH groups
3600-3625	Si-OH-Al stretching
3680-3800	P-OH and Al-OH stretching
3950	Out-of-plane Si-OH-Al bending

4.2 EXPERIMENTAL

4.2.1 Methanol conversion experiments

Methanol conversion studies were carried out in a stainless steel fixed bed reactor as shown in Fig 21. Pelletized catalyst between 500 and 850 μm in size was used. The methanol feed was diluted with water (30 wt % dilution unless stated otherwise) and pumped into the reactor via an electrically heated evaporator, at a methanol WHSV of 0,5 h^{-1}, unless otherwise stated. The reaction temperature was 400°C unless otherwise stated. Nitrogen was used as a carrier gas at a flow rate of 10 ml/min. The gaseous and liquid products were analysed by gas chromatography using both a flame ionisation detector (FID) and a thermal conductivity detector (TCD). A blank methanol conversion reaction was conducted at 400°C and no significant reactions due to the stainless steel reactor were observed. Full mass balances were completed for every reaction and the accountability of carbon was above 80% in all cases.

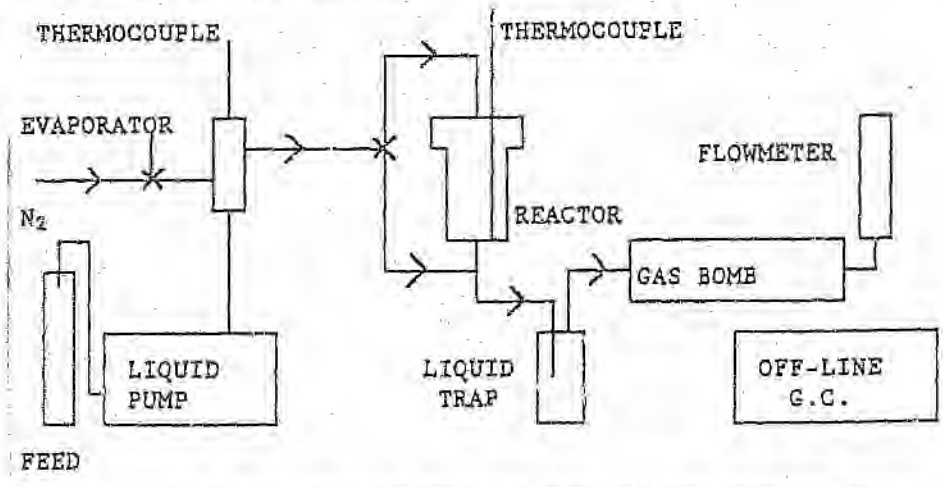


FIG 21 : EXPERIMENTAL APPARATUS FOR METHANOL CONVERSION REACTIONS

A standard time on-line of 5 h was used for comparison of the percentage "coke" deposition on SAPO-34, SAPO-5, ZSM-5, and Ni-SAPO-5 during methanol conversion. A second batch of H-ZSM-5 was used on-line for 112 h. The SAPO-34 catalyst previously modified with trimethyl-silylchloride showed no deactivation after 5 h at a methanol WHSV of 0.7 h^{-1}, so it was used to convert methanol into hydrocarbons for 18.5 h.

A batch of pelletized SAPO-34 catalyst was used to convert methanol into hydrocarbons under conditions described above (180, 215, 250, 280 and 310 min), so that the change in surface area, pore volume and amount of C and H deposited could be monitored *ex situ*.

4.2.2 Surface area analysis

The surface areas of the fresh and spent catalysts were determined by the Brunauer-Emmett-Teller (BET) method on a Micromeretics chemisorptometer 2700. The pulse chemisorptometer was calibrated using the method in Appendix 1 based on the theory that 1.0 cm^3 of nitrogen gas at 22°C and 638 mmHg pressure corresponds to a monolayer of nitrogen molecules adsorbed onto a surface of 2.39 m^2.

About 0.3 to 1.0 g of catalyst (predried at 110°C for 15 h) was placed in a glass U-tube and dried at 200°C under nitrogen for 30 minutes and then cooled to room temperature. A 30:70 N_2:He mixture was passed over the catalyst sample at room temperature

and then at liquid nitrogen temperature to adsorb a monolayer of nitrogen onto the sample. The helium does not adsorb onto the surface at liquid nitrogen temperature and flushed excess nitrogen away from the surface of the sample.

The sample was heated back to room temperature and the amount of nitrogen desorbed was detected by a TCD. The adsorption and desorption of a monolayer of nitrogen was repeated until 2 consistent values of desorption were recorded. The mass of the catalyst sample was then determined and used to calculate the surface area per 1.0 g of sample.

4.2.3 Pore volume analysis

The pore volumes of the zeolites were measured by determining the volume of nitrogen, at 98 % saturation vapour pressure, which condensed in the pores. A 98 % nitrogen in helium mixture was used as any pure gas held at its condensation temperature would continue to accumulate on the zeolite surface unless sufficient inert sweep gas was present [4.16].

The pore volumes of the zeolites were determined using a Micromeretics chemisorptometer 2700. The instrument was calibrated by injecting 10 ml of nitrogen, into the bypass loop before the TCD, while the instrument was purged with the 98 % N_2 : 2 % He stream at ambient conditions. The instrument was set to indicate the true volume of this gas when condensed as a liquid (0.012 ml; as shown in Appendix 2), the state in which it exists when filling the pores of a sample under these conditions.

The samples were dried at 110 C for 15h prior to analysis and then heated at 200°C under dry nitrogen for 30 minutes. The sample was allowed to cool to liquid nitrogen temperature under nitrogen in order to fill the pores with condensed nitrogen. The nitrogen stream was then substituted with a 98 % N_2 : 2 % He mixture to flush excess condensate away. The total pore volume was obtained by bringing the sample back to room temperature and determining the amount of nitrogen desorbed per 1.0 g of sample.

4.2.4 Carbon and hydrogen analysis

The compositions of the carbonaceous deposits on all of the spent catalysts were analysed using a LECO-932 C,H,N analyser. The carbon content was determined by mass loss during oxidation, and the H content by the formation of water.

4.2.5 Statistically designed experiments on methanol conversion over SAPO-34

A half fraction 2^4 experimental design, as set out in Table IX, was used to establish the effects of changing the catalyst bed temperature, reaction pressure and degree of dilution of the methanol feed with water, on the formation of "coke" on SAPO-34.

TABLE IX: EXPERIMENTAL DESIGN OF METHANOL CONVERSION REACTIONS OVER SAPO-34

EXPERIMENT	TEMPERATURE (°C)	PRESSURE (atm)	DILUTION OF METHANOL (wt % H_2O)
1	350	1	30
2	400	1	50
3	400	1	30
4	350	1	50
5	400	4	30
6	400	4	50
7	350	4	50
8	350	4	30

The carbon deposited on the catalysts after each of the experiments was determined on a LECO 932 C,H,N analyser, as described in section (4.2.4).

The relative effects of the individual variables on the amount of carbon deposited was determined using the following equation:

Effect on carbon deposition = $C_h - C_l$

Where C_h = the sum of the carbon mass percentages for the experiments conducted at the higher value of that variable

and C_l = the sum of the C mass percentages for the experiments conducted at the lower value of that variable.

The absolute values of the effects of the various parameters on the carbon deposition gave an indication of the magnitude of the

effect of that parameter on the amount of "coke" deposited. The sign indicated whether the higher or lower value of the parameter gave a higher percentage of carbon.

4.2.6 Diffuse reflectance infra-red fourier transform spectroscopy of SAPO-34 during methanol conversion

The build-up of carbonaceous and organic species on the surface of SAPO-34 during the conversion of pure methanol, and methanol diluted with 30 wt % water, was studied using *in situ* DRIFTS on a Brucker IFS 85 FTIR spectrometer. The methanol WHSV in both experiments was 1.0 h^{-1} and the flowrate of the nitrogen carrier gas was 10 ml/min. The SAPO-34 catalyst was placed in a DRIFTS cell with a zinc sulphide window and heated to 400°C. A schematic of the drifts cell is shown in Fig 22.

The product spectrum was analysed simultaneously on a Pye Unicam series 204 gas chromatograph (G.C using a Porapak Q column and a FID.

A Fourier Transform IR (FTIR) spectrum of the SAPO-34, after use in converting methanol into hydrocarbons for 4 h at a methanol WHSV of 0.5 h^{-1}, was obtained on a Perkin Elmer 1725X FTIR spectrometer.

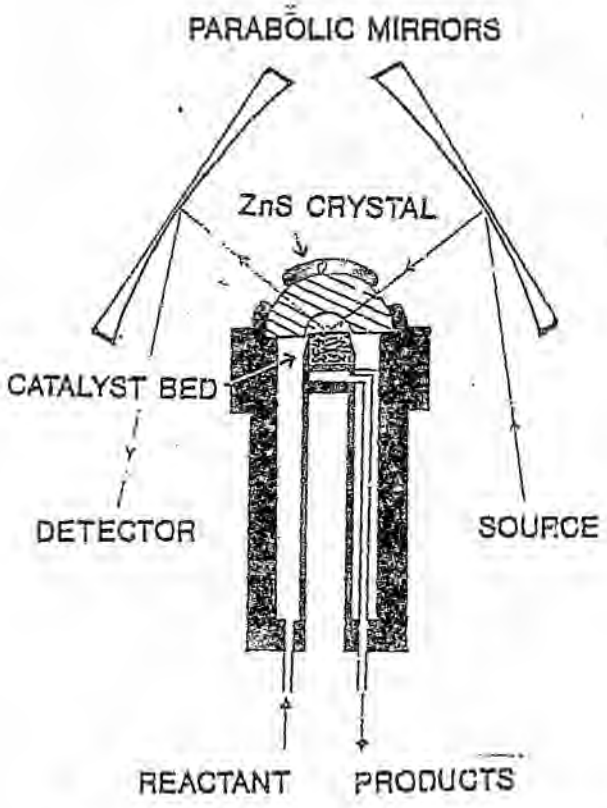


FIG 22 : THE DRIFTS CELL USED TO STUDY THE SURFACE OF SAPO-34 DURING METHANOL CONVERSION

4.3 RESULTS AND DISCUSSION

4.3.1 Methanol conversion experiments

The equivalent conversions of methanol (as defined in Appendix 3) with reaction time over SAPO-34, SAPO-5, ZSM-5, Ni-SAPO-34 and Si-SAPO-34 are shown in Fig 23.

The activity of SAPO-5 and Ni-SAPO (which has the SAPO-5 structure) decreased faster than that of SAPO-34. The silicon modification increased the active lifetime of the SAPO-34, but it was still much shorter than that of H-ZSM-5.

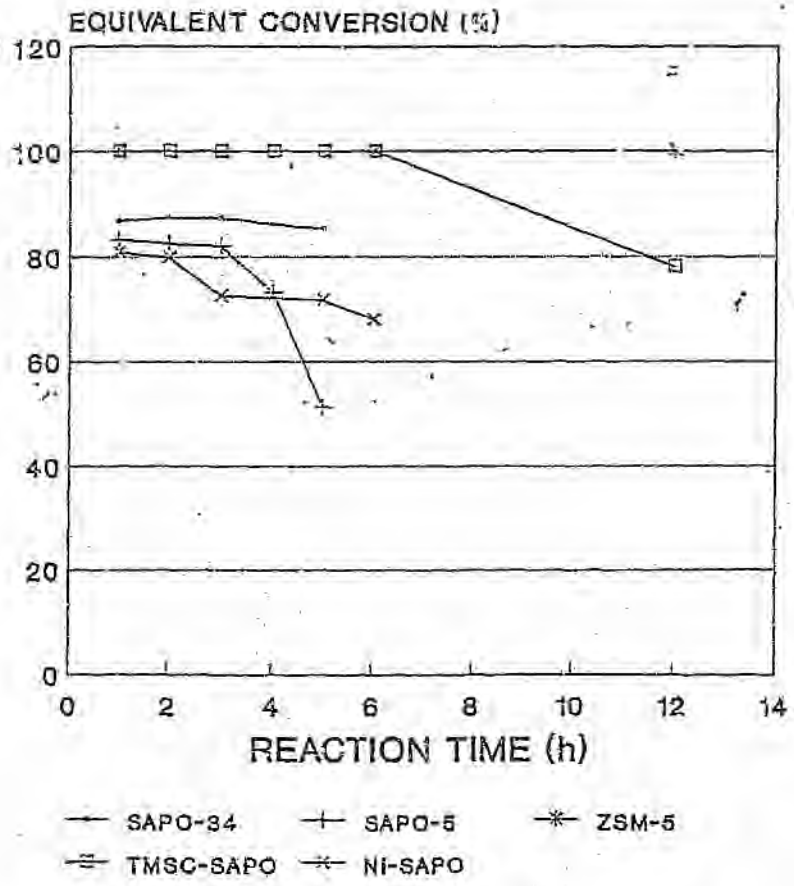


FIG 23 : CONVERSION OF METHANOL WITH REACTION TIME

4.3.2 Surface area analysis

The decrease in surface areas of SAPO-34 during the conversion of methanol is shown in Fig 24.

The decrease in surface area of SAPO-34 during methanol conversion compared to H-ZSM-5 is shown in Fig 25. The rate of decrease in surface area was shown to be much greater for SAPO-34 than for H-ZSM-5. There was a sharp decrease in surface area in both catalysts initially as carbonaceous species formed on the acid sites. The deposition of carbonaceous deposits could have decreased exponentially as the number of available acid sites decreased.

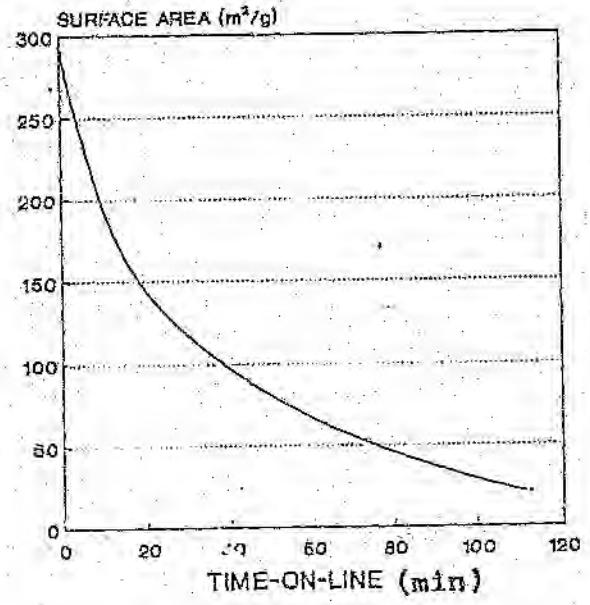


FIG 24 : DECREASE IN SURFACE AREA OF SAPO-34 DURING METHANOL CONVERSION

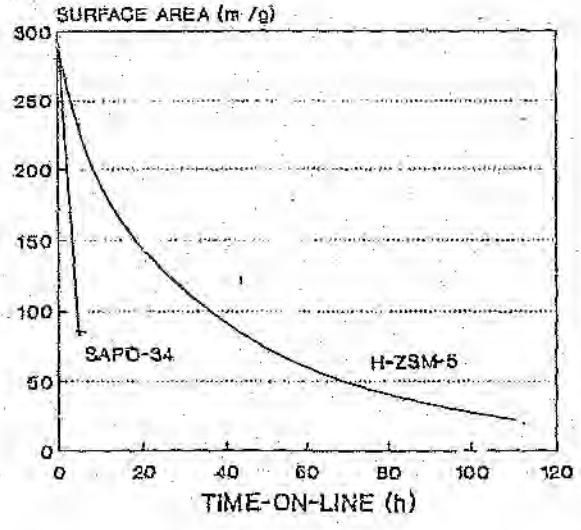


FIG 25 : DECREASE IN SURFACE AREA OF H-ZSM-5 AND SAPO-34 DURING METHANOL CONVERSION

The "coke" which was deposited within the first 5 h caused significant blockage in the SAPO-34 framework, so the activity of the catalyst decreased significantly, whereas in ZSM-5 reactants and products diffused through the pores for 112 h before significant deactivation by "coke" occurred. The bulk of the "coke" is thought to form at the surface of H-ZSM-5 [4.17], and a significant amount of "coke" is required before the medium pores are blocked. However, the "coke" is thought to build up in the ellipsoidal cavities in SAPO-34 and protrude into the narrow pores, rapidly causing blockage.

The change in surface areas of H-ZSM-5, SAPO-34, SAPO-5 and Ni-SAPO after being used for 5 h in the conversion of methanol under conditions described in section 4.2.1] are shown in Fig 26. The change in surface area of the silicon modified SAPO-34 after 18.5 h is also shown in Fig 26.

The decrease in surface areas of the SAPO-34, SAPO-5 and the Ni-SAPO catalysts were significantly greater than for H-ZSM-5 after the same time-on-line. The lower "coking" rate on H-ZSM-5 was due to the steric constraints exerted by the medium pore structure on the bimolecular reactions involved in the formation of "coke" [4.18]. To counteract this rapid deactivation of SAPO-34 by "coke" deposition, some workers use SAPO-34 in a circulating fluidized bed reactor with continuous regeneration [4.3]. The decrease in surface area of the silicon modified SAPO-34 was less severe than with SAPO-34, which indicates that the silicon decreased the rate at which "coke" was deposited. The percentage of methanol converted was also significantly

higher with the silicon modified SAPO-34 than unmodified SAPO-34 (Fig 23). This could indicate that the silicon adhered to the strong acid sites on the surface of the catalyst, or within the ellipsoidal cavities, thus limiting "coke" formation reactions, but permitting methanol conversion reactions on the weaker acid sites.

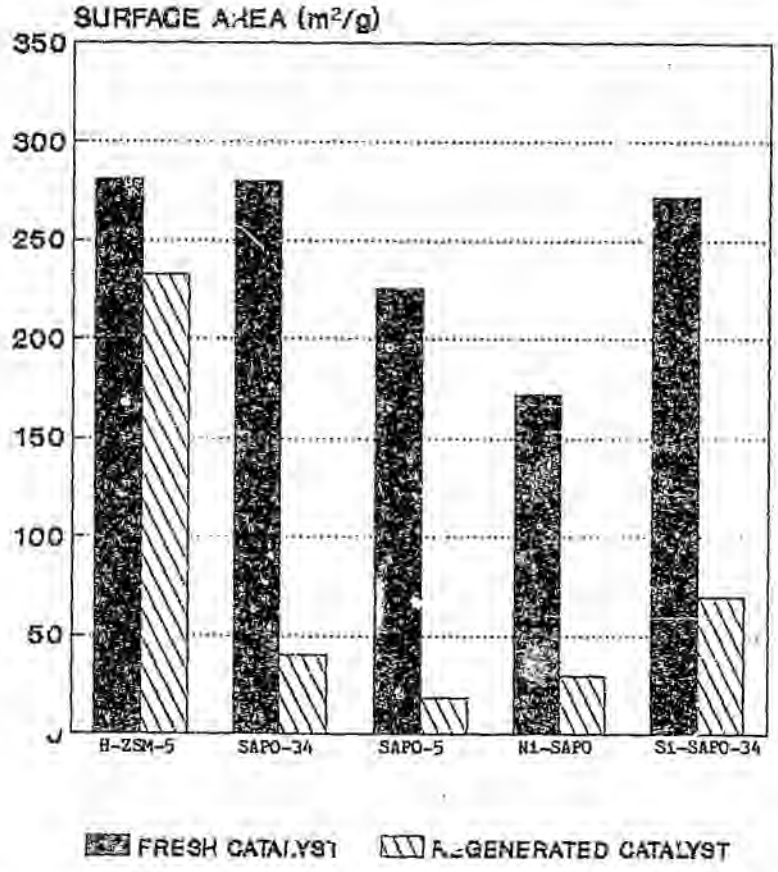


FIG 26 : CHANGE IN SURFACE AREAS OF THE VARIOUS CATALYSTS AFTER METHANOL CONVERSION

4.3.3 Pore volume analysis

The decrease in pore volume of H-ZSM-5 and SAPO-34 are shown in Fig 27. The initial pore volume of SAPO-34 was the same as that of H-ZSM-5. The bulk of the pore volume of H-ZSM-5 is due to the medium sized pores, while in SAPO-34 it is due to the large

ellipsoidal cavities at the channel intersections.

The pore volume of SAPO-34 decreased rapidly during the first hour of methanol conversion, due to the deposition of "coke" in the large ellipsoidal cavities, as reported for chabazite catalysts [4.18]. After the first hour the pore volume of SAPO-34 remained constant at about 80 % of the initial pore volume, but the surface area continued to decrease. A possible explanation is that after the initial deposition of "coke" in the cavities, the formation of bulky "coke" precursors was sterically hindered [4.18].

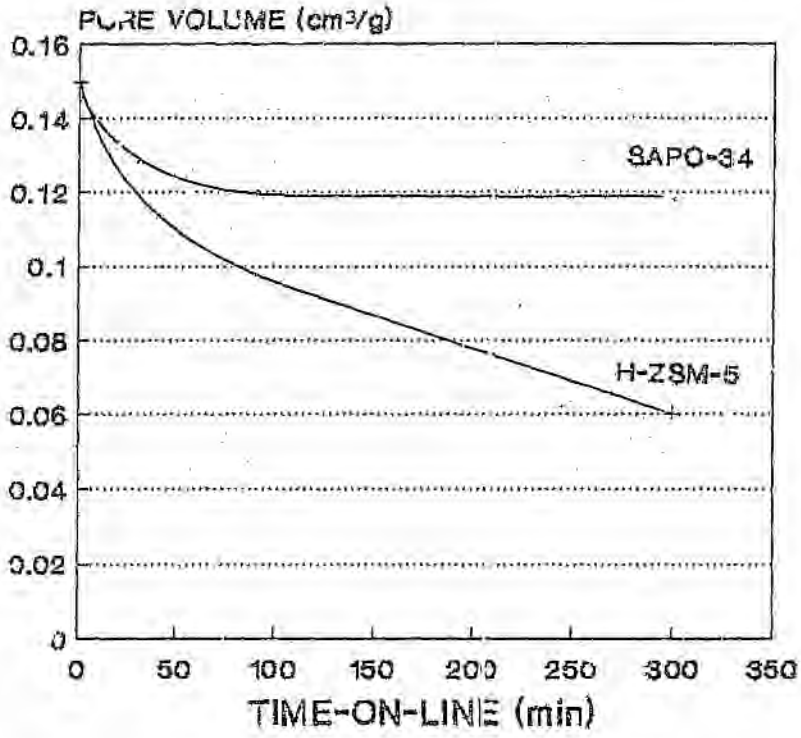


FIG 27 : DECREASE IN PORE VOLUME OF SAPO-34 AND H-ZSM-5 DURING METHANOL CONVERSION

The initial decrease in pore volume of H-ZSM-5 was also rapid, probably due to the formation of light "coke" molecules in the

The initial decrease in pore volume of H-ZSM-5 was also rapid,probably due to the formation of low molecular weight "coke" molecules in the channel intersections. After the initial 5 h the pore volume decreased slowly, over the next 107 h, to 0.012 cm^3 / g as the formation of bulky "coke precursors was also sterically hindered in the pores, but did occur on the surface [4.18].

4.3.4 Carbon and hydrogen analysis

The percentage of "coke" (C mass %) deposited on SAPO-34 after various reaction times is shown in Table X. The hydrogen mass percent in the fresh catalyst is assumed to be due to water. The hydrogen mass percent remained constant with time-on-line, but the carbon mass increased steadily as shown in Fig 28. The amount of H deposited in the form of "coke" was therefore too small to be determined relative to the background hydrogen from the adsorbed water. The carbonaceous deposit was therefore assumed to be graphitic or polyaromatic in nature.

TABLE X : C AND H ANALYSIS OF THE CARBONACEOUS DEPOSIT ON SAPO-34 DURING METHANOL CONVERSION

REACTION TIME (h)	mass % C	mass % H
0.0	0.3	2.7
0.5	2.6	2.5
1.5	4.4	2.7
3.0	5.8	2.6
5.0	7.2	2.7

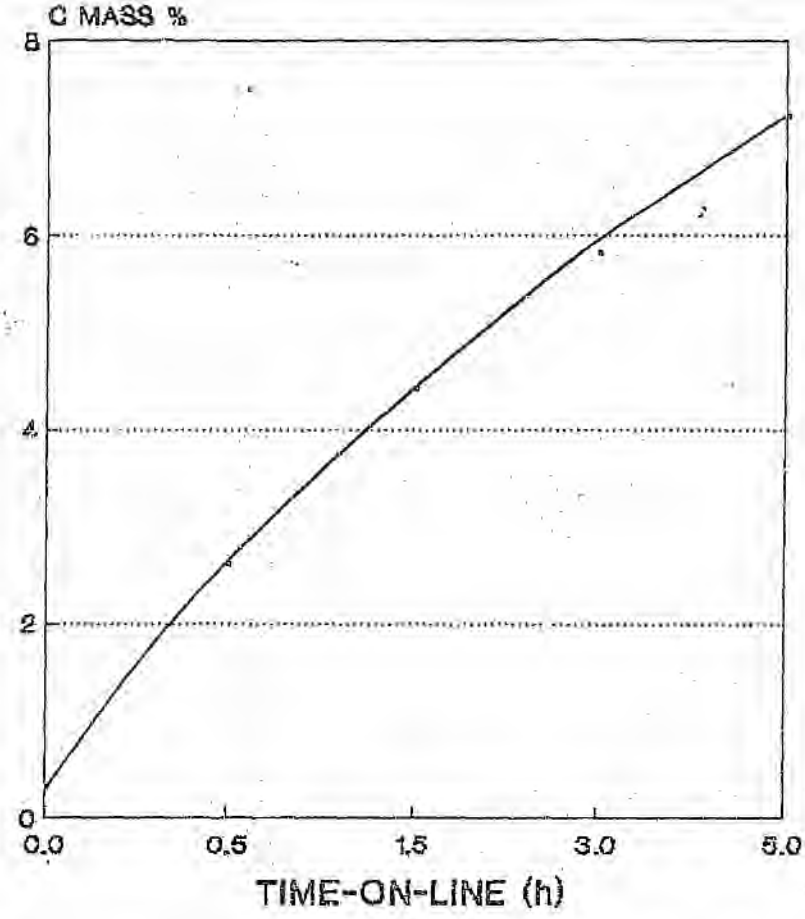


FIG 28 : CARBON DEPOSITION ON SAPO-34 DURING METHANOL CONVERSION

A second methanol conversion experiment was conducted on SAPO-34 using the same conditions at a lower methanol WHSV (0.25 h^{-1}). After 410 minutes the same amount of methanol had been converted over the catalyst as after 205 minutes at a WHSV of 0.50 h^{-1}. However, the catalyst contained 4.0 mass % C due to the carbonaceous deposit as opposed to 6.2 mass % C at a WHSV of 0.5 h^{-1}. This shows that less "coke" is deposited at a low methanol WHSV. This could be due to a greater dilution of the methanol as 10 ml / min nitrogen was used in all the experiments.

The amount of carbon deposited on SAPO-34, SAPO-5 and Ni-SAPO

after 5 h of methanol conversion was found to be 7.2 %, 8.3 %, 2.8 % respectively, while the equivalent conversion of methanol had dropped to 88 %, 52 % and 69 % respectively (Fig 23). After 5 h on-line the equivalent conversion of methanol over H-ZSM-5 was still 100 % and only 3.3 % carbon had been deposited. After 112 h of methanol conversion over H-ZSM-5 the equivalent conversion had decreased to 55 % and the mass percent carbon deposited had increased to 10.3 %. Only 3.3 % carbon was deposited on the silicon modified SAPO-34 after 18.5 h on-line, and the equivalent conversion had decreased to 79 % (Fig 23). This shows that the rate of carbonaceous deposition on SAPO-34 and SAPO-5 was rapid compared to H-ZSM-5 and that the Ni and Si modifications decreased the rate at which "coke" was deposited.

Incorporation of Ni into SAPO-5 decreased the amount of "coke" deposited, possibly by decreasing the distribution and strength of the acid sites, as reported by Inui [4.19] for SAPO-34. A second explanation for the decrease in "coke" deposition on the Ni-SAPO compared to SAPO-5 is that the nickel cracked "coke" precursors as they formed [4.20].

In section (3.3.1.5) the silicon treatment was shown not to affect the amount of silicon present in the SAPO-34 catalyst. The silicon treatment has been shown to affect the activity of the catalyst, therefore the silicon was probably deposited on the surface of the catalyst and retarded the formation of "coke" on the surface of the catalyst.

4.3.5 Statistically designed experiments

The mass percent carbon deposited on SAPO-34 during each of the statistically designed experiments is shown in Table XI.

TABLE XI : CARBON DEPOSITION IN THE STATISTICALLY DESIGNED EXPERIMENTS

EXPERIMENT	MASS % C	ACCURACY
1	9.98	± 0.18
2	6.33	± 0.18
3	8.48	± 0.20
4	4.72	± 0.41
5	5.90	± 0.23
6	9.05	± 0.35
7	7.96	± 0.29
8	5.29	± 0.28

The mass percent of hydrogen was also determined by C and H analysis, but inaccuracies occurred due to the strong absorbance of water by the catalysts. The amount of water on each of the spent catalysts was determined by Karl Fischer analysis, but these results were too inaccurate to be used in the statistically designed experiments. Thus only the carbon mass percentages recorded in Table XI were used for the statistical calculations.

The effects of temperature, pressure, WHSV and dilution of methanol with water on the C mass % is shown in Table XII. The relative effects were calculated as described in section (4.2.5) e.g. the effect of temperature on the amount of C deposited was estimated as follows :

$$= [\ Exp(2) + Exp(3) + Exp(5) + Exp(6)\ ] - [\ Exp(1) + Exp(4) + Exp(7) + Exp(8)\ ]$$

$$= [\ 6.833 + 8.479 + 5.895 + 9.047\ ] - [\ 9.984 + 4.723 + 7.959 + 5.285\ ]$$

$$= 1.803$$

TABLE XII : EFFECTS OF THE VARIABLES IN THE STATISTICALLY DESIGNED EXPERIMENTS ON THE C MASS %

	TEMPERATURE	PRESSURE	METHANOL WHSV	DILUTION WITH WATER
MASS % C	1.80	-1.33	2.64	-1.58

The methanol WHSV had the greatest effect on the mass of "coke" deposited. The greater the methanol WHSV (and hence more methanol passing over the catalyst in the 5 h), the more "coke" was deposited. In section (4.3.4) it was shown that more "coke" was deposited at a lower methanol WHSV than at a higher WHSV if the reactions are stopped after the equivalent amount of methanol had passed over the catalyst. This was due to the greater dilution of the methanol with nitrogen.

The amount of "coke" deposited was shown, by the statistical result in Table XII, to increase with temperature (350°C to 400°C). Marchi and Froment [4.3] found that the amount of "coke" deposited in a quartz reactor decreased if the reaction temperature was raised above 427°C. Temperatures above 400°C could not be used in the stainless steel reactor as "coke" would have formed on the walls of this reactor at these temperatures [4.1].

The statistical result in Table XI showed that slightly less "coke" was deposited when the partial pressure of water (via

methanol dilution) was increased. Marchi and Froment also found that the amount of "coke" deposited decreased when the dilution of methanol was increased on addition of 0 to 70 % water [4.3]. They suggested that the water suppressed aromatisation and chain growth reactions by competing with the alkene molecules for the strongest acid sites [4.3].

The effect of reaction pressure was also small i.e. more "coke" was deposited at the lower pressure. The effect of pressure was shown to interact with the effect of water partial pressure. Maximum "coke" was deposited at low pressure and low partial pressure of water, or at high pressure and high partial pressure of water (Fig 29).

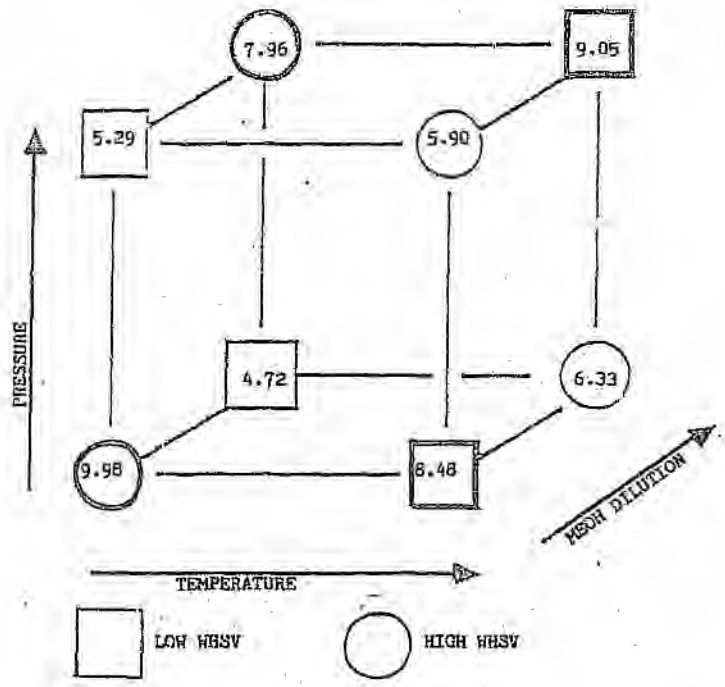


FIG 29 : CUBIC PLOT OF THE INTERACTING EFFECTS OF PRESSURE, TEMPERATURE, WHSV AND DILUTION OF THE METHANOL WITH WATER ON "COKE" DEPOSITION

This shows that the formation of "coke" decreased when the methanol molecules were concentrated by pressure or when the dilution with water was lower. This effect is probably due to the lower conversion of methanol, or the decrease in oligomerization reactions due to le Chatelier's principle.

4.3.6 *In situ* Diffuse reflectance infra-red fourier transform spectroscopy of SAPO-34 during methanol conversion

The Kubelka-Munk IR spectra of the differences between the surface of the used and original catalyst, obtained at various times during the conversion of methanol and diluted methanol over SAPO-34, are shown in Figs 30 and 31 respectively. Data for the conversion of pure methanol at various times is shown in Table XIII.

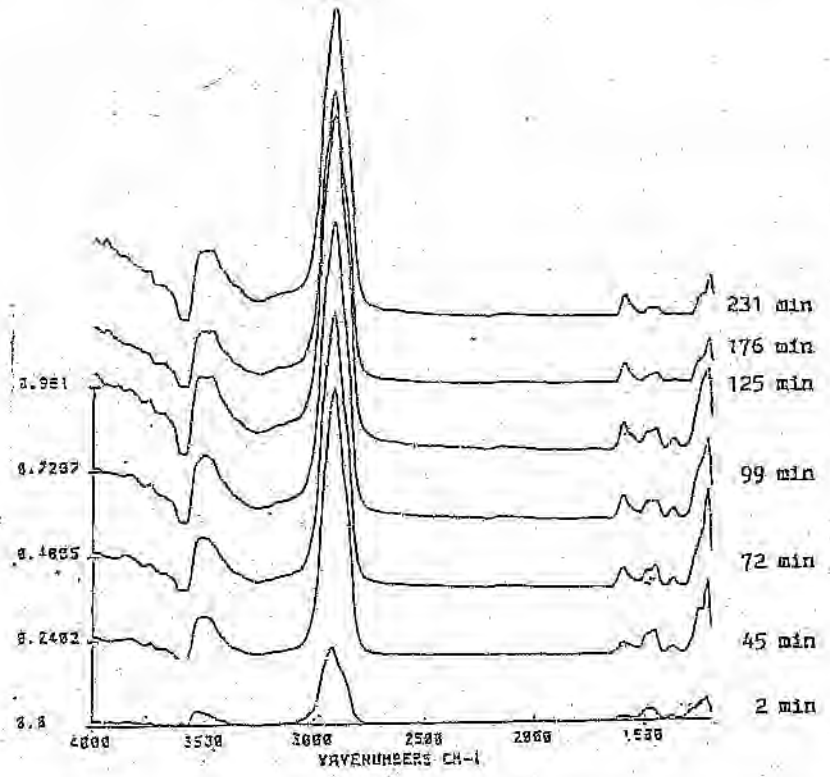


FIG 30 : DRIFTS OF SAPO-34 DURING THE CONVERSION OF UNDILUTED METHANOL

TABLE XIII : CONVERSION OF METHANOL OVER SAPO-34 DURING THE *in situ* DRIFTS EXPERIMENT

TIME-ON-LINE (min)	EQUIVALENT CONVERSION (%)
2	89
45	91
72	82
99	68
125	53
176	6
231	3

During the conversion of pure methanol the catalyst deactivated within 2.5 h but no aromatic "coke" was observed (bands expected at 3050 and 1585 cm^{-1} [4.21]). Initially all the hydroxyl groups disappeared on exposure to methanol due to the formation of methoxy species, as observed by Xu *et al* [4.4]. The hydroxyl groups reappeared as the hydrocarbons started to form [4.4]. Aliphatic carbonaceous deposits built up during the first hour of the reaction but did not seem to increase thereafter (appearance of methyl and methylene asymmetric stretches between 2860 and 2970 cm^{-1} [4.7, 4.9, 4.21]). The absorbance at 1630 cm^{-1}, assigned to C=C symmetric vibrations [4.22] also increased during the first hour and then remained constant. The shoulder at 1500 cm^{-1} has been assigned to C-OH bending. The absorbance at 1450-1470 cm^{-1}, which decreases with reaction time, could be due to the deformation of the methyl groups [4.7, 4.9] or aliphatic C-H deformations. The absorbance at 1390 cm^{-1} assigned to a C-H symmetric bending mode [4.9] also decreased

with time on line, especially after two hours of reaction. The bands at 1220-1250 cm^{-1}, assigned to methyl and methylene scissor deformations, increased during the first two hours on-line, and then decreased as the catalyst deactivated rapidly. The methylene, C=C, C-H and C-OH stretches could just be due to the methanol and initial products, and not due to "coke".

During the conversion of methanol diluted with water (30 % water m/m) the same absorbance bands were observed. However, the bands at 1390 to 1600 cm^{-1} (paraffins and olefins) did not decrease with time-on-line as was observed with pure methanol over SAPO-34. This shows that the water competed with the methanol and the products for adsorption on the acid sites.

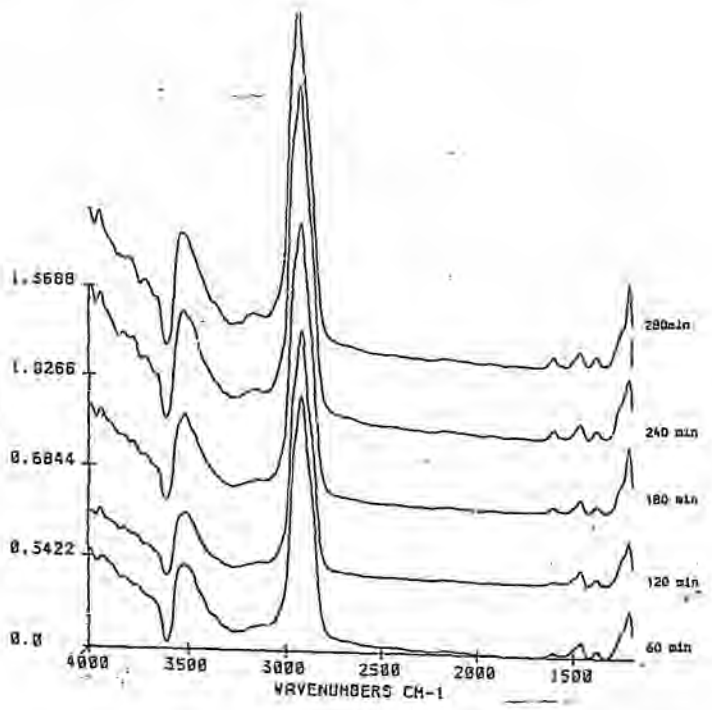


FIG 31 : DRIFTS OF SAPO-34 DURING THE CONVERSION OF METHANOL DILUTED WITH WATER

4.3.7 *Ex situ* diffuse reflectance infra-red Fourier Transform spectroscopy of the deactivated SAPO-34

DRIFTS was used to study the deactivated SAPO-34 after methanol conversion under conditions described in section {4.2.1}. The spectrum of the deactivated catalyst is shown in Fig 32.

The band from 3450 to 3600 cm^{-1} was assigned to the stretching vibrations of H-bonded OH groups on the SAPO surface (due to water, Brönsted acid sites or methanol) [4.7 and 4.9]

The band at 2959 cm^{-1} was probably due to the stretching vibrations of methyl groups of aliphatics, while the bands at 2922 and 2852 cm^{-1} was most likely due to the asymmetric and symmetric stretches of aliphatic methylene groups [4.12 and 4.21].

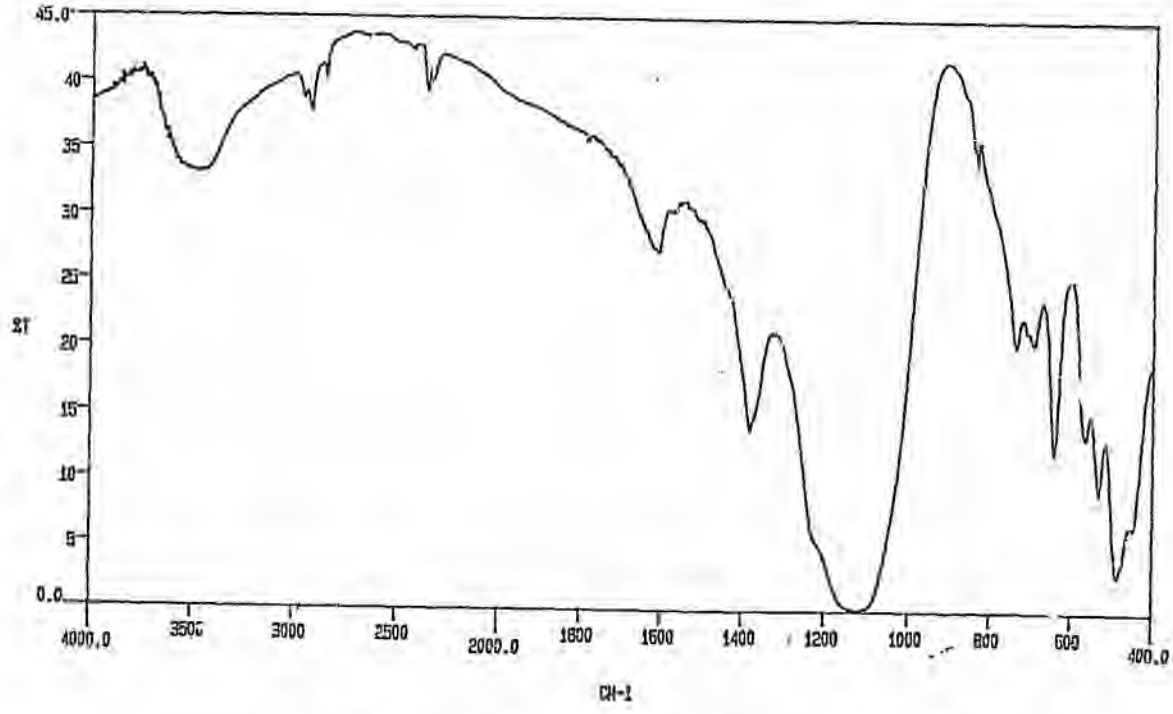


FIG 32 : DRIFTS OF DEACTIVATED SAPO-34

The broad band at 1611 cm^{-1} was assigned to the O-H vibration of adsorbed water [4.22], although a C=C symmetric vibration at 1630 cm^{-1} could also have been present [4.9 and 4.22]. The band at 1384 cm^{-1} could have been due to a C-H symmetric bending mode [4.12 and 4.22].

No aromatic carbonaceous deposit was observed (bands would have appeared at 3050 and 1585 cm^{-1} [4.21]).

The bands below 1200 cm^{-1} were due to skeletal vibrations e.g. asymmetric stretching, symmetric stretching and bending of SiO_4 and AlO_4^- at 1124 cm^{-1}, 837 cm^{-1} and 486 cm^{-1} respectively [4.14].

The carbonaceous deposits on SAPO-34 therefore appeared to be aliphatic. The C=C symmetric vibrations and C-OH bending are most likely due to adsorbed light olefins and methanol even though the spent catalyst was flushed with nitrogen at 400°C after the methanol conversion reaction. No aromatics were observed by Xu *et al* using *in situ* DRIFTS on SAPO-34 during methanol conversion, but they observed aromatics using MAS NMR spectroscopy [4.4].

4.4 CONCLUSIONS

The deposition of "coke" caused deactivation of the SAPO catalysts after 3 h of methanol conversion at a methanol WHSV of 0.5 h^{-1}. The formation of "coke" in SAPOs is probably enhanced by the large cavities at the channel intersections which facilitate the formation of bulky "coke" precursors. The Ni-SAPO

and SAPO-5 catalysts deactivated more rapidly than SAPO-34, possibly as the diameters of the pores were large enough to facilitate the formation of bulky "coke" precursors. The silicon modification increased the active lifetime of SAPO-34 to 18 h, possibly by decreasing the number of acid sites and hence "coke" formation on the surface of the catalyst. The catalytic lifetime of the silicon modified SAPO-34 was still much shorter than that obtained for H-ZSM-5 (112 h).

The "coke" deposition in SAPO-34 caused a rapid decrease in surface area during the first hour of methanol conversion, whereas the surface area of H-ZSM-5 was only significantly reduced after 112 h. The pore volume of SAPO-34 decreased rapidly in the first hour of reaction as "coke" formed in the large cavities. The pore volume of H-ZSM-5 also decreased rapidly during the first 5 hours as "coke" built up in the medium pores. After the initial decrease in pore volume in both the SAPO-34 and the H-ZSM-5 catalysts, the pore volume decreased very slowly, possibly due to steric factors affecting the formation of the "coke" precursors. The surface areas of SAPO-5 and Ni-SAPO were also greatly reduced during 5 h of methanol conversion. The silicon modification of SAPO-34 resulted in a decreased rate at which the "coke" was deposited and thus extended the active lifetime of the catalyst.

The deactivation of the catalyst due to "coke" deposition was decreased by diluting the methanol with water or nitrogen. The water competed with the olefins and oligomers for the strong acid sites, and thereby decreased the rate at which aromatization and

oligomerization reactions occurred. The nitrogen decreased the residence time of the products on the catalyst surface, reducing the probability of further reactions. The amount of "coke" deposited on the SAPO-34 increased with temperature (350°C to 400°C) and is related to the oligomerization and aromatization reactions which are favoured by high temperature.

Both the *in situ* and *ex situ* FTIR spectra of SAPO-34 used in methanol conversion reactions indicated that aliphatic and not aromatic "coke" was formed. The adsorbed species detected could have been methanol and initial products, rather than "coke". Further characterization of the "coke" is continued in chapter 5.

4.5 REFERENCES

4.1] Kaiser, S.W.; *Arab. J. Sci. Eng.*, 10, (1985), 361

4.2] Lewis, J.M.O.; Catalysis 1987; Ward, J.W. (ed), Elsevier, Science, Amsterdam, (1988)

4.3] Marchi, A.J. and Froment, G.F.; *Appl. Catal.*, 71, (1991), 139

4.4] Xu, Y., Grey, C.P., Thomas, J.M. and Cheetham, A.K.; *Catalysis Letters*, 4, (1990), 251

4.5] Das, J., Bhattacharya, A., Goswami, T.K. and Roy, S.K.; *J. Chem. Tech. Biotech.*, 50, (1991), 13

4.6] Anderson, M.W., Sulikowski, B., Barrie, P.J. and Klinowski, J.; *J. Phys. Chem.*, 94, (1990), 2730

4.7] Sayed, M.B. and Gooney, R.P.; *Aust. J. Chem.*, 35, (1982), 2483

4.8] Zubkov, S.A., Kustov, L.M. and Kazansky, V.B.; *J. Chem. Soc. Faraday Trans.*, 87(6), (1991), 897

4.9] Aronson, M.T., Gorte, R.T. and Farneth, W.E.; *J.Catal.*, 105, (1987), 455

4.10] Mirth, G. and Lercher, J.A.; *J. Catal.*, 124, (1990), 441

4.11] Kubelkouá, L. Nováková, J. and Nedomová, K.; *J. Catal.*, 124, (1990), 441

4.12] Bolis, V., Verdrine, J.C., van de Berg, J.P., Wolthuizen, J.P. and Derouane, E.G.; *J. Chem. Soc. Faraday Trans. I*, 76,(1980), 1606

4.13] Jentys, A., Rumplmayr, G. and Lercher, J.A.; *Appl. Catal.* 53, (1989), 299

4.14] Schukla, D.B. and Pandya, V.P.; *J. Chem. Tech. Biotechnol.*, 44, (1989), 147

4.15] Dong, Q.N., Anderson, J.R. and Mole, T.; *Appl. Catal.*, 72, (1991), 99

4.16] Bibby, D.M., Milestone, N.B., Patterson, J.E. and Aldridge, L.P.; *J. Catal.*, 97, (1986), 493

4.17] Stepanov, V.G. Paukshtis, E.A., Zaikovskii, V.I., Chesnokov, V.V., Ketchik, S.V. and Ione, K.G.; Zeolites for the Nineties, Jansen, J.C., Moscou, L. and Post, M.F.M. (Eds), 8th International Zeolite Conference proceedings, Amsterdam, (1988)

4.18] Guisnet, M. and Magnoux, P.; *Appl. Catal.*, 54, (1989), 1

4.19] Hočevar, S. and Levec, J.; *J. Catal.*, 135, 518, (1992)

4.20] Lewis, J.M.O.; *Catalysis Letters*, 199 (1987)

4.21] Eberly, P.E.(Jr), Kimberlin, C.N.(Jr), Miller, W.H. and Drushel, H.V.; *I & EC Process Design and Development*, 5 (2), (1966), 193

4.22] Schnabel, K.H., Schreier, E. and Peuker, C.; *Catal. Today*, 3, (1988), 513

CHAPTER 5 : DEACTIVATION OF CATALYSTS DURING METHANOL CONVERSION : CHARACTERIZATION OF THE "COKE"

5.1 INTRODUCTION

Magnoux *et al* [5.1] have described a process to analyse "coke" deposited on and within zeolite catalysts. The zeolite framework was dissolved in a 40 % aqueous HF solution to liberate the internal "coke". This internal "coke" was subsequently extracted with dichloromethane and analysed by G.C., H.P.L.C., ^{1}H-NMR and mass spectroscopy [5.1]. This treatment was shown not to change the nature of the carbonaceous compounds as 1-tetradecene and 9-methylphenanthrene impregnated on an inert solid were not broken down, and alkanes and alkenes were not isomerised during the HF treatment and dichloromethane extraction [5.1].

The "coke" deposited on the external and internal surfaces of the zeolite catalysts differed in composition. The soluble fraction of the external "coke" was dissolved in dichloromethane before the zeolite framework was destroyed with HF. The polyaromatic "coke" (greater than seven fused aromatic rings) on the surface of the zeolites was insoluble in dichloromethane, but was studied by electron microscopy. The internal "coke" was subsequently liberated by dissolving the framework in HF, extracted with dichloromethane, and analysed as above.

The nature of the carbonaceous product on SAPO-34 after methanol conversion was investigated in this study using the method described by Magnoux *et al* [5.1].

MAS ^{13}C-NMR was also used to study the carbonaceous deposit on SAPO-34 after methanol conversion as this method has been reported to give valuable information on the nature of the carbonaceous deposit on zeolites [5.2, 5.3, 5.4, 5.5 and 5.6]. The chemical shifts relative to tetramethylsilane (TMS) observed for the resonances of the various carbonaceous species are summarized in Table XIV [5.2, 5.3, 5.4, 5.5 and 5.6]. The carbon chains associated with aliphatics and alkyl aromatics are reported to resonate below 40 ppm [5.3]. Resonances in the 50-60 ppm region are reported to correspond to alkoxide groups which occupy but do not poison the active sites [5.6]. Aromatics are reported to resonate in the 100-150 ppm region [5.4]. A mixture of alkyl aromatics and polyaromatics are reported to be observed between 120 and 180 ppm [5.6].

TABLE XIV : CHEMICAL SHIFTS REPORTED FOR CARBONACEOUS SPECIES

CHEMICAL SHIFT* (ppm)	SPECIES
- 6.1	cyclopropane
-10.7	methane
0-40	aliphatics
50-60	methoxy groups
100-150	aromatics
120-180	alkyl aromatics
> 200	ketones

* = relative to tetramethylsilane

Derouane *et al* [5.3] have studied the carbonaceous residues on H-ZSM-5 and H-mordenite, produced during the conversion of methanol and ethylene, using ^{1}H-^{13}C cross-polarization MAS ^{13}C-NMR. On H-ZSM-5 they observed a broad aliphatic product distribution (propane, propene, *n*-butane, *iso*-butane and *iso*-pentane) with resonances between 11.4 and 31.7 ppm relative to tetramethylsilane. More *iso*-paraffins than linear chains were observed. A broad resonance peak from 125 to 145 ppm was observed and assigned to aromatics and olefins. No polycyclic aromatics were observed.

In H-mordenite less aliphatics (only propane, propene and *n*-butane) and more aromatics (including fused ring aromatics) were observed than over H-ZSM-5 [5.3]. Derouane *et al* suggested that the larger pore size facilitated the conversion of paraffins and olefins into aromatics, alkylated aromatics and fused ring aromatics. A resonance at 59.9 ppm was observed on both catalysts and was assigned to surface methoxy groups. These were produced by the alkylation of the acidic sites with methanol.

Carlton *et al* [5.4] also studied the carbonaceous deposits on H-ZSM-5 by ^{13}C-NMR following methanol conversion and found that the "coke" consisted of aliphatics, aromatics, ethers and ketones.

Anderson and Klinowski [5.5] studied the carbonaceous species on H-ZSM-5 after 35 min. of methanol conversion at 300°C and 370°C. They found that the predominant aromatic species deposited at 300°C were *o*-xylenes, *p*-xylenes, trimethylbenzenes and tetramethylbenzenes. The dominant aliphatic species at 300°C

were *iso*-butane and propane [5.5]. At 370°C more *m*-xylene and toluene were formed and less tetramethylbenzene. Penta- and hexa-methylbenzene were observed at 370°C. In the aliphatic region there were more branched alkanes and less linear alkanes than at 300°C. Methyl substituted benzenes, up to C_{11}, were observed in the gas phase at 370°C but not at 300°C. The larger species were able to leave the crystallite at 370° due to the increased effective channel diameter. The only trimethylbenzene observed in the gas phase was 1,2,4-trimethylbenzene (kinetic diameter 6.1 Å) whereas in the adsorbed phase 1,2,3- and 1,3,-trimethylbenzenes (kinetic diameters 6.4 and 6.7 Å respectively) were also observed. The channel dimensions of ZSM-5 are 5.6 Å x 5.3 Å respectively, but more space is available for the growth of substituted aromatics at the channel intersections. At the higher temperature (370°C) the effective channel dimensions may increase sufficiently via a "breathing motion" to allow the smaller substituted aromatics to diffuse out of the crystallite [5.7].

Anderson *et al* [5.2] used ^{13}C MAS-NMR spectra to study SAPO-34 after methanol conversion at different temperatures. The authors showed that branched aliphatics (up to 49 % selectivity) are formed inside SAPO-34, but were not observed in the gaseous product, so presumably these species could not leave the intracrystalline space even at temperatures as high as 370°C. Only 5-10 % of the C_3 products found in the adsorbed phase were observed in the gas-phase product, as branched hydrocarbons partially blocked the pore system, trapping the C_3 products.

5.2 EXPERIMENTAL

5.2.1 Mass spectroscopy after extraction

The framework of a sample (1.0 g) of the spent SAPO-34 was dissolved in HF (0.68 g, 40 % in water). The organics which were released from the catalysts were extracted with dichloromethane (4.26 g) and then analysed by G.C. mass spectroscopy.

A blank reaction was completed using 4.21 g dichloromethane to extract any trace organics in 0.78 g of HF. The dichloromethane and any trace organics were subsequently analysed by G.C. mass spectroscopy. No organics were observed in the dichloromethane. The external "coke" on SAPO-34 was also extracted from 0.1 g of spent SAPO-34, with 3.00 g of dichloromethane in an ultrasonic bath. The organics which were extracted by the dichloromethane were analysed by G.C. mass spectroscopy.

5.2.2 Solid state magic angle spinning - nuclear magnetic resonance

The carbonaceous deposits on the H-ZSM-5, SAPO-34 and Ni-SAPO were analysed by ^{13}C MAS-NMR spectroscopy using a Brüker AM300 MAS-NMR spectrometer.

5.3 RESULTS AND DISCUSSION

5.3.1 Mass spectroscopy after extraction

The organics which were extracted from SAPO-34 after HF dissolution, as determined by G.C. mass spectroscopy, are shown in Table XV.

TABLE XV : THE CARBON SPECIES EXTRACTED FROM SAPO-34 AFTER METHANOL CONVERSION

CARBON NUMBER	CARBON SPECIES
C_7	toluene
C_8	*o,m,p*-xylenes
C_9	trimethylbenzenes
C_{10}	tetramethylbenzene naphthalene
C_{11}	pentamethylbenzene methyl naphthalene
C_{12}	dimethyl naphthalene
C_{13}	trimethyl naphthalene
C_{14}	phenanthrene
C_{15}	pyrene

The relative amounts of the various species could not be determined without calculating response factors for each species. Methyl naphthalenes, dimethyl naphthalenes, trimethyl-naphthalenes, phenanthracene and pyrene are so large they could only have formed in the large ellipsoidal cavities of SAPO-34, or on the surface, and possibly caused pore blockage.

Only a trace of dimethyl heptane was detected by G.C. mass spectroscopy of the dichloromethane used to extract HF in the blank reaction. Traces of tetramethylhexane, ethyl-tetramethyldecane, trimethyl-octane and methyl-heptadecane were detected in the dichloromethane used to extract "coke" from the external surface of SAPO-34. The concentration of organic species detected in the dichloromethane (3.00g) used to extract "coke" before HF digestion of the catalyst was much less than in the dichloromethane (4.26g) used for extraction of "coke after HF digestion. The amount of "coke" deposited on the external surface of SAPO-34 was therefore small compared to that deposited on the internal surface and consisted of alkylated long chain paraffins as opposed to polyaromatics.

5.3.2 <u>Solid state magic angle spinning - nuclear magnetic resonance</u>

The MAS ^{13}C-NMR spectra of the spent SAPO-34, Ni-SAPO and H-ZSM-5 are shown in Fig 33. The amount of noise was inversely indicative of the amount of "coke" deposited, i.e. more "coke" was deposited on SAPO-34 after 5 h than on H-ZSM-5 after 112 h and Ni-SAPO after 5 h. The amount of "coke" on Ni-SAPO (as shown by C analysis in section (4.3.3) was shown to be less than that on SAPO-34.

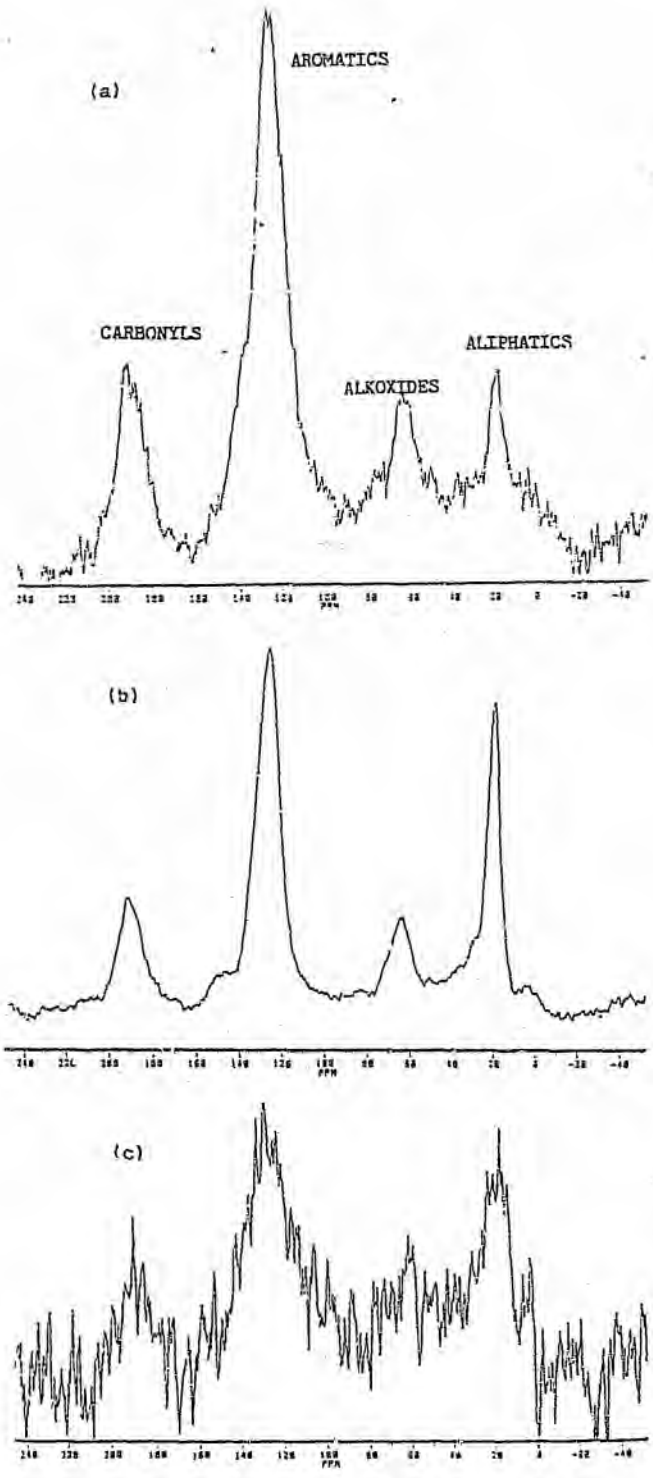


FIG 33 : MAS ^{13}C-NMR SPECTRA OF SPENT a) H-ZSM-5, b) SAPO-34 AND c) Ni-SAPO

The relative ratio of aliphatics (20-25 ppm) to aromatics (128-132 ppm) (as estimated from the peak heights) was the same for the "coke" on SAPO-34 and Ni-SAPO, but the ratio of aliphatics to aromatics of the "coke" formed on H-ZSM-5 was significantly lower. This could indicate that more aromatics formed on the surface and in the channels of H-ZSM-5 than on the surface and ellipsoidal cavities of SAPO-34 or Ni-SAPO-34. The aromatics could not have formed in the channels of SAPO-34 as the channel dimensions are too small (4.0 Å).

Carbonyls were observed at 190-195 ppm in all catalysts. Anderson and Klinowski assigned this peak to CO [5.5], but it could also have been due to the presence of ketones or aldehydes. Alkoxide groups were also observed in all the catalysts at 65 ppm due to methanol or DME [5.6].

5.4 CONCLUSIONS

Extraction of the carbonaceous deposits with dichloromethane after dissolution of the SAPO-34 framework with HF, and subsequent analysis by mass spectroscopy, showed that mainly substituted naphthalenes and polyaromatics (phenanthracene and pyrene) were formed on SAPO-34 during methanol conversion at 400°C. These large molecules could only have formed in the large ellipsoidal cavities of SAPO-34.

A small amount of "coke", consisting of alkylated long chain paraffins, was deposited on the external surface of SAPO-34.

MAS ^{13}C-NMR was used to show that the aromatic to aliphatic ratio of the "coke" on H-ZSM-5 was greater than on SAPO-34 or Ni-SAPO. This could indicate that aromatic "coke" formed on the surface and in the channels of H-ZSM-5 to a greater degree than on the surface and in the ellipsoidal cavities of SAPO-34 or Ni-SAPO. Aliphatic "coke" trapped in the small pores of SAPO-34 and Ni-SAPO were presumably not converted into aromatics due to steric constraints. They may, however, have contributed to the deactivation of the catalysts by occupying active sites and pore blockage.

5.5 REFERENCES

5.1] Guisnet, M. and Magnoux, P.; *Applied Catal.*, 54, (1989), 1

5.2] Anderson, M.W., Sulikowski, B., Barrie, P.J. and Klinowski, J.; *J. Phys. Chem.*, 94, (1990), 2730

5.3] Derouane, E.G., Gilson, J. and Nagy, J.B.; *Zeolites*, 2, (1982), 42

5.4] Carlton, L., Copperthwaite, R.G., Hutchings, G.J. and Reynhardt, E.G.; *J. Chem. Soc. Chem. Commun.*, (1986), 1008

5.5] Anderson, M.W. and Klinowski, J.; *J Am. Chem. Soc.*, 112, (1990), 10

5.6] Deroune, E.G.; Catalysis by Acids and Bases, Imelik *et al* (eds), Elsevier Science Publishers, Amsterdam (1985), 234

5.7] Deem, M.W.; Newsam, J.M. and Creighton, J.A.; *J. Am. Chem. Soc.*, 114, (1992), 7189

CHAPTER SIX : REGENERATION

6.1 INTRODUCTION

Hutchings *et al* [6.1] have studied the regeneration of zeolites using nitrous oxide and oxygen at high temperatures (450-500°C). They also used a 5 mole percent ozone in oxygen mixture at lower temperatures (200°C). Most (99.6 %) of the carbonaceous residue was removed using nitrous oxide at high temperatures, but this regeneration [illegible] is too expensive for industrial use. The ozone/oxyg [illegible] low temperature removed 96.8 % of the carbonaceous dep[illegible] is also expensive, but this method of regeneration [illegible] useful for catalysts that cannot be exposed to high temperatures.

H-ZSM-5 deactivated during methanol conversion and regenerated (i) using oxygen at 450-500°C and (ii) using a 5 mole percent ozone in oxygen mixture at 200°C, has been studied by ^{13}C MAS-NMR spectroscopy [6.1]. Most of the aromatic carbon was removed by the ozone/oxygen treatment, whereas both the aromatic and the aliphatic carbon was removed by the oxygen treatment at higher temperatures. Hutchings *et al* [6.1] proposed that the ozone/oxygen attacked the unsaturated centres of the aromatic carbon, forming oxygenated fragments. This was suggested by the broadening of the ether type resonance in the ^{13}C MAS-NMR spectrum. The high temperature oxygen treatment resulted in oxidation of the "coke" to carbon oxides and water. The high

temperature water vapour has been shown to cause dealumination and subsequent loss of activity [6.2, 6.3].

The choice of regeneration treatment, therefore, depends on the financial constraints, the extent to which the catalyst needs to be regenerated to regain its catalytic activity, and the sensitivity of the catalyst to high temperatures.

Kaiser [6.4] has reported that deactivated SAPO-34 can be regenerated in 2 h in a flowing stream of air at 500°C. He reported that SAPO-34 was regenerated 15 times in this manner without significant loss in crystallinity or selectivity of the catalyst, but the subsequent conversion of methanol was slightly lower.

6.2 EXPERIMENTAL

The ZSM-5, SAPO-34, SAPO-5, Ni-SAPO and TMSC-SAPO catalysts, used for the conversion of methanol as described in chapter 4, were regenerated. In this procedure, the catalyst was held at 550°C under a flowing stream of nitrogen for 1 h to remove any residual methanol. The nitrogen was then slowly replaced with air and the temperature was held at 550°C for a further hour. The catalyst was then held at 550°C for 15 hours under a flowing stream of oxygen, to oxidise the "coke" deposits, and then cooled under nitrogen. The organics released during regeneration were analysed by G.C.

6.2.1 Thermal gravimetric analysis during regeneration

A Setaram TG/DTA92 thermal gravimetric differential thermal analyser was used to study the weight loss during the regeneration of a portion (44.93 mg) of the SAPO-34 catalyst which had been deactivated during a five hour methanol conversion reaction at 350°C, with a methanol WHSV of 0.5 h^{-1}. The reference cell was filled with fresh SAPO-34 catalyst so that the weight loss due to water and excess template resident in the catalyst, as well as the effect of thermal ramping, would not influence the detection of weight loss due to "coke" constituents. Both the deactivated SAPO-34 and the reference SAPO-34 were heated to 550°C in 100 minutes under nitrogen and maintained at this temperature under nitrogen for 1 h. The nitrogen was then replaced with oxygen and the temperature maintained at 550°C for 45 minutes.

6.2.2 Gas-chromatography-mass spectroscopy of "coke" constituents

A sample of the deactivated H-ZSM-5, (deactivated during methanol conversion as described in chapter 4) was placed in a stainless steel reactor and heated to 550°C under a flowing stream of nitrogen. The organics that were released during heating procedure were channelled into a G.C. capillary inlet tube filled with Tenax 80/100 resin, which trapped the organics. The catalyst was maintained at 550°C for an hour and the organics which were released were similarly trapped in resin in another capillary inlet tube. The zeolite was then maintained at 550°C

while the nitrogen was substituted with oxygen. The organics which were released (in 1 h) were similarly collected in a capillary inlet tube. The organics which were in the resin were subsequently analysed by G.C. mass spectroscopy using a novel injection technique. The organics were desorbed from the resin, by heating the capillary inlet tube to 250°C, and condensed on the front of a DB-wax column by cooling the column with liquid nitrogen. The column was then slowly heated and the organics were analysed by G.C. mass spectroscopy.

Samples of SAPO-34, SAPO-5, Ni-SAPO and silicon-modified-SAPO-34 were regenerated and analysed in the same way.

A capillary inlet tube filled with the same resin was placed in the oven (at 100°C) with the silicon rubber tubing used between the catalytic reactor and the capillary inlet tube during regeneration. The organics released from the silicon tubing and trapped on the resin were analysed using the same method as above.

Two other capillary inlet tubes filled with resin were spiked with equal quantities of phenol, benzene, toluene and methylbenzene as follows; 1 g of each of these organic species were placed in a 400 ml gas pipette which was subsequently heated to evaporate the organics. The gaseous organics were released from the gas bomb into the two capillary inlet tubes simultaneously. These capillary inlet tubes were analysed as above.

6.2.3 Characterization of the catalysts after regeneration

Regenerated SAPO-34 was used to convert methanol into hydrocarbons under the same conditions described in section 4.2.1. The methanol conversion was stopped after ~ h as the catalyst had deactivated. The catalyst was regenerated and again used in the methanol conversion reaction. The catalyst was only active for 1.5 h.

The carbonaceous residues after regeneration were analysed by C and H analysis using a LECO 932 C,H,N analyser.

The surface areas of the fresh and regenerated ZSM-5, SAPO-34, SAPO-5, Ni-SAPO and silicon-modified SAPO-34 were measured on a Micromeretics Pulse Chemisorb 2700 as described in section (4.2.3).

All of the regenerated catalysts were analysed by XRD and XRF spectroscopy to determine if the methanol conversion and regeneration procedure had any affect on the crystallinity and composition of the cat lysts.

6.3 RESULTS AND DISCUSSION

6.3.1 Thermal gravimetric analysis

The thermal gravimetric differential thermal analysis (TG/DTA) spectrum of SAPO-34 during regeneration is shown in Fig 34. Most (62 %) of the weight loss during the regeneration procedure

occurred while the SAPO-34 was heated to 200°C under nitrogen. The amount of water that was desorbed (about 20 mass %) is consistent with the 2.7 mass % H reported in Table X.A sharp peak (26 % of the total mass loss) was observed as the oxygen was introduced, due to oxidation of the "coke" to carbon oxides and water. The remainder of the weight loss during the regeneration (12 %) occurred between 200 and 550°C. Gas chromatography analysis during regeneration confirmed that carbon oxides were released.

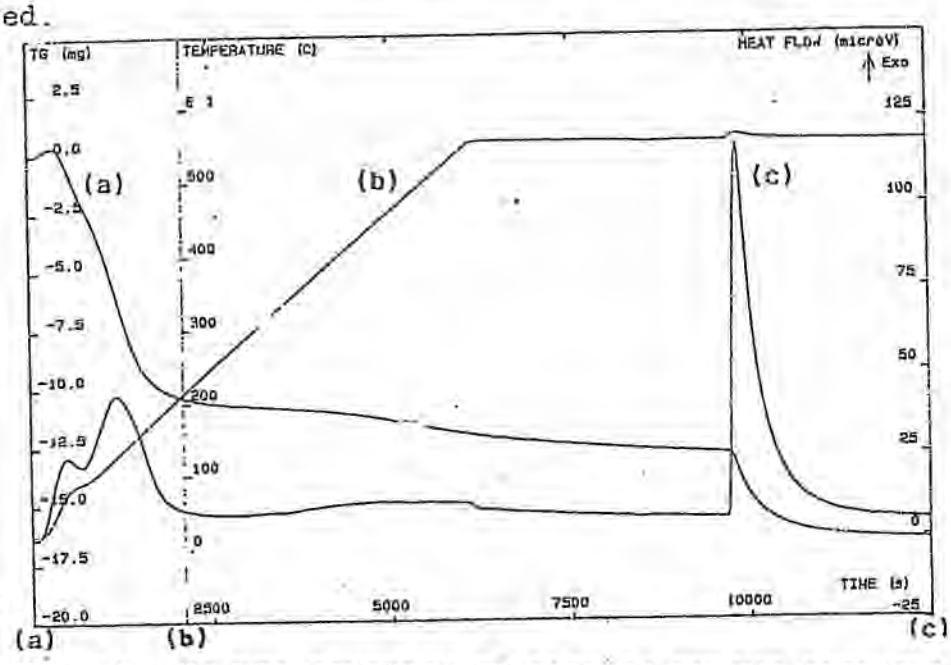
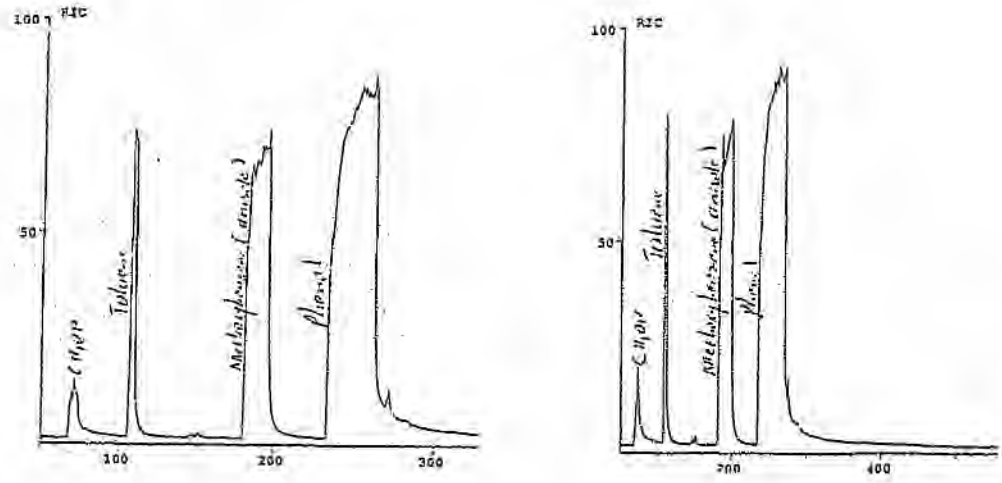


Fig 34 : TG/DTA SPECTRUM OF SAPO-34 DURING REGENERATION
a) MASS CHANGE, b) TEMPERATURE AND
c) DIFFERENTIAL OF MASS LOSS

6.3.2 Gas-chromatography-mass spectroscopy of "coke" constituents

The G.C. mass spectra of the two capillary inlet tubes spiked with equal quantities of methanol, toluene, methoxybenzene and

phenol are shown in Fig 35. No significant differences were observed in the two spectra which indicates that this technique is reproducible. The relative amounts of the four organic species trapped and/or detected in the capillary inlet tubes differed from the relative amounts released into the tubes, therefore resin retention factors and G.C mass spectroscopy response factors for every species would have to be determined before this technique could be used quantitatively. However, this technique was used qualitatively in this study to determine relative differences in the nature of the carbonaceous deposits on the various catalysts.



(a) (b)

FIG 35 : G.C. MASS SPECTRA OF THE ORGANIC SPECIES ON THE SPIKED CAPILLARY INLET TUBES. (a) FIRST CAPILLARY TUBE AND (b) SECOND CAPILLARY TUBE

The organics released from the silicon rubber tubing and absorbed onto the resin were identified as toluene, diethylphthalate, hexadecanoic acid, 2-butoxy-ethylbutylphthalate, hexadecanoic acid dioctylester and di-isooctyl phthalate. These organics were therefore ignored during all the other analyses.

The organics released from H-ZSM-5 and SAPO-34 during regeneration, which were trapped in the resin in the capillary inlet tubes and identified using G.C. mass spectroscopy, are shown in Table XVI and XVII respectively.

TABLE XVI : ORGANIC SPECIES RELEASED FROM H-ZSM-5 DURING REGENERATION

	Heating to 550°C under N_2	550°C for 1 h under N_2	550°C under O_2
C_5			phenol
C_7	toluene	toluene	toluene
C_8	ethylbenzene xylenes	xylenes	ethylbenzene xylenes
C_9	trimethylbenzene ethylmethylbenzene	trimethylbenzene	trimethylbenzene ethylmethylbenzenes
C_{10}	diethylbenzene tetramethylbenzene	naphthalene	diethylbenzene tetramethylbenzenes naphthalene
C_{11}		methylnaphthalene	methylnaphthalene
C_{12}		C_{12} hydrocarbon	dimethylnaphthalene
C_{14}		C_{14} hydrocarbon	C_{14} hydrocarbon

Some light aromatics were released and trapped during the thermal ramping under nitrogen. Under prolonged heating some bulky aliphatics and aromatics, including naphthalenes, were able to move out of the catalyst.

No carbon oxides, which are reported to be released during thermal oxidation [6.1], were trapped by the resin. During thermal oxidation of the "coke" more of the bulkier aromatics, including naphthalenes, were released.

The introduction of oxygen did not alter the type of organics released, but the oxidation of some of the "coke" may have opened some of the blocked pores, or increased the local temperature of the catalyst, so that more of the organic deposits were released from the catalyst.

A batch of H-ZSM-5 which had been used for methanol conversion for 5 hours at a methanol WHSV of 0.5 h^{-1} (as described in chapter 4) was also regenerated and analysed as above. The organics which were released were the same as those listed in Table XVI for the H-ZSM-5 which had been deactivated after 112 h of methanol conversion at a methanol WHSV of 0.5 h^{-1}. The major organic species formed during the first 5 hours were xylenes, trimethylbenzenes and tetramethylbenzenes whereas after 112 hours they were pentamethylbenzenes and hexamethylbenzenes. This analysis shows that, during "coke" formation on H-ZSM-5, the amount of substituted benzenes builds up and the degree of substitution increases. Large polyaromatic molecules may have been formed and broken up into smaller aromatics during the regeneration procedure.

TABLE XVII : ORGANIC SPECIES RELEASED FROM SAPO-34 DURING REGENERATION

	Heating to 550°C under N_2	550°C for 1 h under N_2	550°C under O_2
C_6	benzene	benzene	benzene
C_7	toluene	toluene	toluene
C_8	xylene	xylene	xylene
C_9	trimethylbenzenes	trimethylbenzenes	trimethylbenzenes
C_{10}	tetramethylbenzenes	tetramethylbenzenes	tetramethylbenzenes
C_{11}	pentamethylbenzenes	pentamethylbenzenes	pentamethylbenzenes
C_{12}	C_{12} aliphatic		
C_{15}		C_{15} aromatic	
C_{16}		C_{16} aromatic	

The major organic species released from SAPO-34 during regeneration and trapped in the capillary inlet tubes, were pentamethyl-benzenes, hexamethylbenzenes and propyltetramethyl-benzenes. The organics released from SAPO-34, therefore, do not differ significantly from those released form H-ZSM-5, although slightly larger molecules (C_{16}) appeared to have formed in the large cavities of SAPO-34. Bulky polyaromatics (trimethyl naphthalenes, phenanthrene and pyrene) were detected by G.C. mass spectroscopy when the SAPO-34 framework was destroyed in HF (section 5.3.1). These species may have been formed in the ellipsoidal cavities, but did not migrate out of the channels

without breaking down into smaller molecules or carbon oxides during regeneration.

The organics released from SAPO-5, Ni-SAPO and silicon-modified SAPO-34 during regeneration, are listed in Table XIII.

TABLE XIII : ORGANICS RELEASED FROM SAPO-5, Ni-SAPO AND SILICON-MODIFIED SAPO-34 DURING REGENERATION

	SAPO-5	Ni-SAPO	Si-modified SAPO-34
C_6	benzene	benzene, cyclohexane, C_6H_{10}, C_6H_{12}, C_6H_{14}	benzene
C_7	toluene	toluene, C_7H_{14}, C_7H_{16}, 3,3 dimethyl-1-pentene	toluene
C_8	xylenes octane	xylenes ethyl benzene	xylenes
C_9	trimethylbenzenes	trimethylbenzenes	trimethylbenzenes
C_{10}	tetramethylbenzenes 4-propyl heptane	tetramethylbenzenes	tetramethylbenzenes $C_{10}H_{20}$, methylnonane ethylmethylheptane trimethylheptane tetramethylhexane 4-propylheptane dimethyloctane
C_{11}	pentamethylbenzenes	pentamethylbenzenes	pentamethylbenzene
C_{12}	hexamethylbenzene	hexamethylbenzenes	hexamethylbenzene
C_{13}	trimethyl decane		trimethyldecanes $C_{13}H_{28}$
C_{14}	$C_{14}H_{16}$		tetramethyldecanes cyclotetramethyldecane
C_{15}	$C_{15}H_{22}$	$C_{15}H_{22}$	pentamethyldecane

The major organic species released from SAPO-5 were pentamethylbenzenes, hexamethylbenzenes and $C_{15}H_{32}$ hydrocarbons. The C_{11} to C_{13} species which were released from H-ZSM-5 and SAPO-34 were also released from SAPO-5, along with some bulkier hydrocarbons. These bulkier hydrocarbons are released from SAPO-5 as the diameter of the pores is larger than for H-ZSM-5 or SAPO-34.

The major organic species released form the deactivated Ni-SAPO were toluene, xylenes and trimethylbenzenes (C_7 to C_9). This indicates that either the incorporation of nickel into the framework decreased the size of the pores so that only light aromatics could migrate out of the catalyst during regeneration, or the metal assisted in the breakdown of carbonaceous deposits into smaller organic molecules during regeneration as suggested by Lewis *et al* [6.5]. The MAS ^{13}C-NMR spectrum of the "coke" on Ni-SAPO and SAPO-34 (section 5.3.2) showed that the same ratio of aromatics to aliphatics were formed on both catalysts. The latter explanation for the smaller molecules released during regeneration is thus probably correct.

The major organic species released from the silicon-modified SAPO-34 were in the same range as those released from SAPO-34 (C_{11} to C_{13}) suggesting that the size of the pores was not affected by the silicon treatment. The major organic species were xylenes, pentamethylbenzenes, hexamethylbenzenes and trimethyldecanes. Significantly more aliphatics and alkanes were observed, which indicates that the silicon modification may have decreased the rate of dehydrogenation and cyclization. This

would account for the longer catalytic lifetimes observed during methanol conversion compared to SAPO-34.

6.3.3 Characterization of the catalysts after regeneration

The equivalent conversions of methanol with reaction time over SAPO-34 and regenerated SAPO-34 are shown in Fig 36.

The reduced catalytic activity observed in SAPO-34 after regeneration shows that either the regeneration procedure may not have removed all of the "coke" deposits, or that the methanol conversion reaction or the regeneration procedure may have changed the catalyst framework. Dealumination is known to occur in aluminosilicate catalysts at high temperatures if water is present [6.2, 6.3]. Dealumination may change the catalyst acidity so that deactivation occurs at a faster rate.

C and H analysis of the catalysts after regeneration showed that 0.13 mass % C was still present in the Ni-SAPO after regeneration, while 0.14 mass % C was present in the H-ZSM-5 and SAPO-5, 0.17 mass % C in the silicon-modified SAPO-34 and 0.20 mass % C in the SAPO-3. The amount of carbonaceous residues in all of the regenerated catalysts were in the same order, so the extent of the regeneration process was not affected by the different pore structures or presence of Ni.

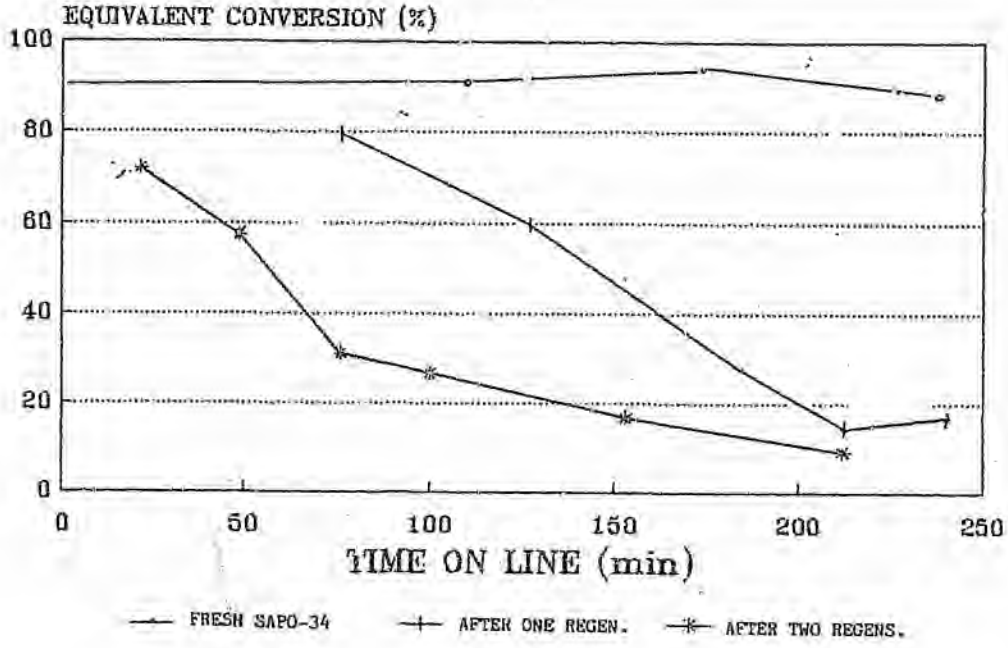


FIG 36 : A COMPARISON OF THE EQUIVALENT CONVERSION OF METHANOL OVER SAPO-34 AND REGENERATED SAPO-34

The surface areas of all the catalysts before and after regeneration are shown in Fig 37. The initial surface area was not regained after regeneration, which shows that either carbonaceous deposits were still present (which is not supported by the residual carbo after regeneration) or that the structure of the catalyst was altered during the reaction and / or regeneration process.

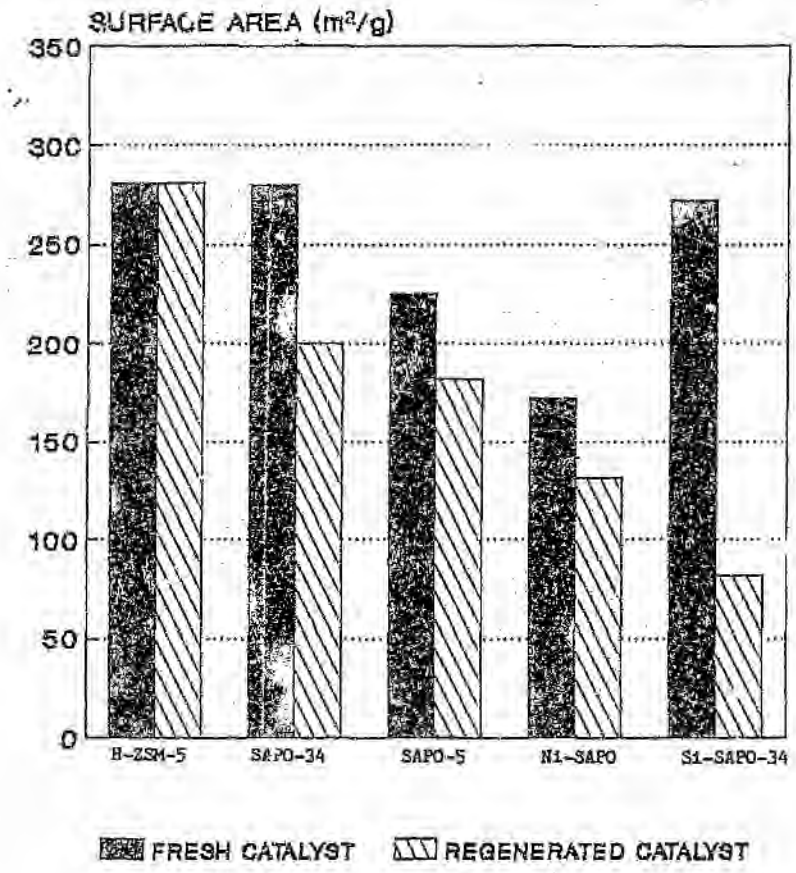


Fig 37 : A COMPARISON OF THE SURFACE AREAS OF THE CATALYSTS BEFORE THE METHANOL CONVERSION REACTION AND AFTER REGENERATION

The XRD patterns of the regenerated catalysts are shown in Figs 38 to 42. The crystallinity of SAPO-34 actually improved after methanol conversion and regeneration, whereas the crystallinity of H-ZSM-5, SAPO-5 and Ni-SAPO-5 were unchanged. This could

after calcination and it was removed during the methanol conversion or regeneration procedures. The XRD pattern of the regenerated trimethyl silicon chloride modified SAPO-34 was mainly that of silica, therefore the treatment resulted in the generation of some extra-framework silicon which migrated to the surface during the methanol conversion and regeneration procedures.

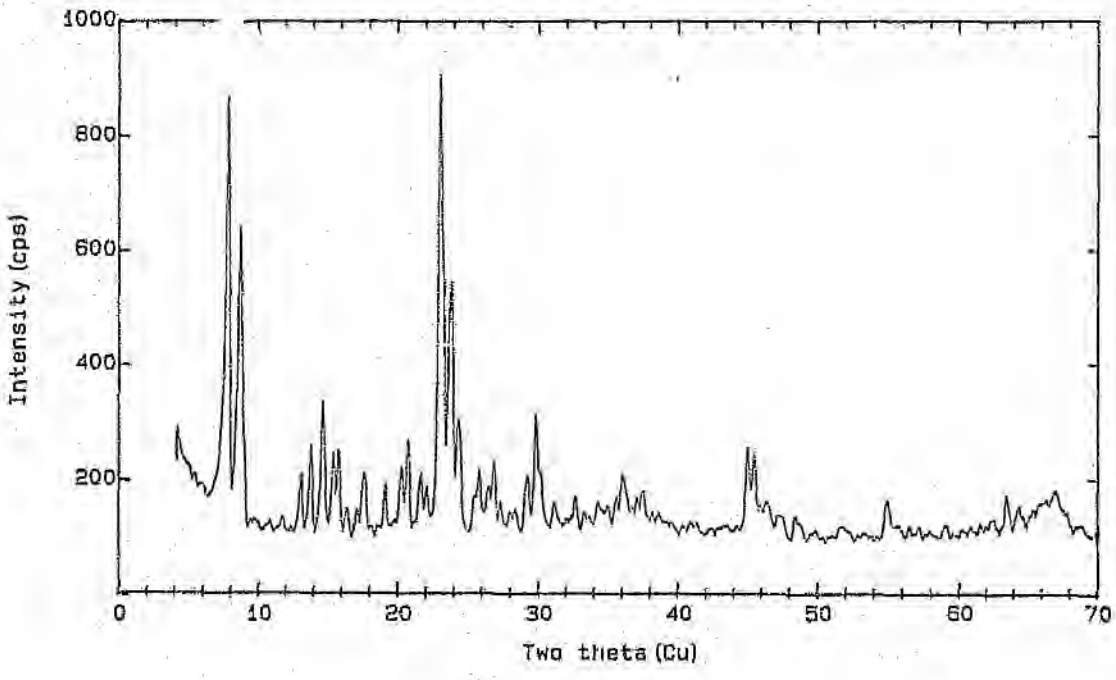


FIG 38 : XRD PATTERN OF REGENERATED H-ZSM-5

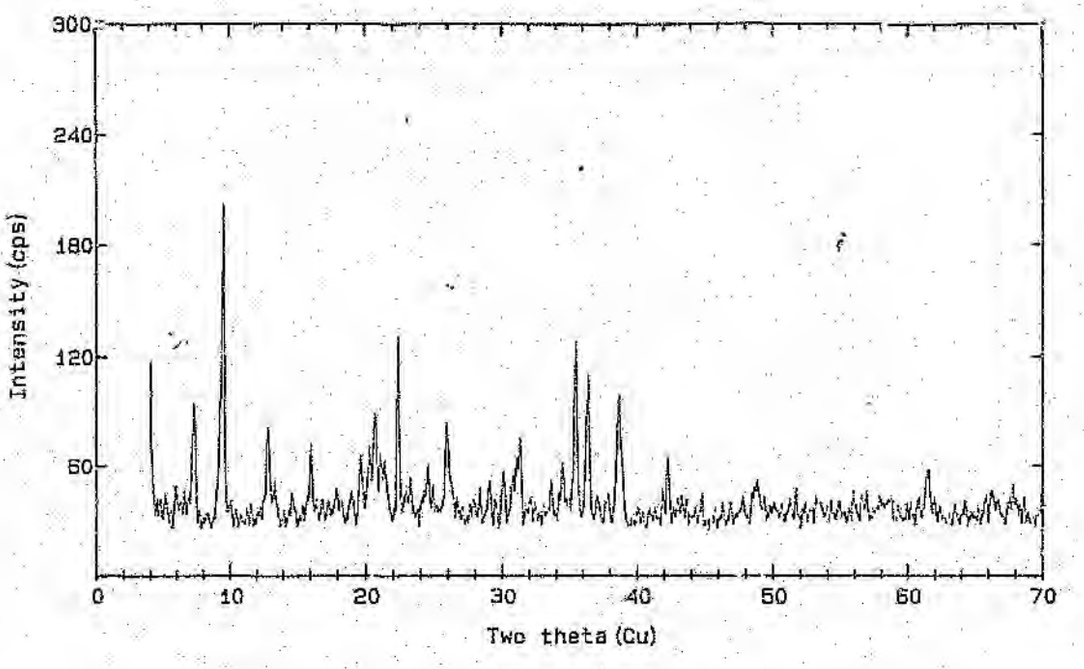


FIG 39 : XRD PATTERN OF REGENERATED SAPO-34

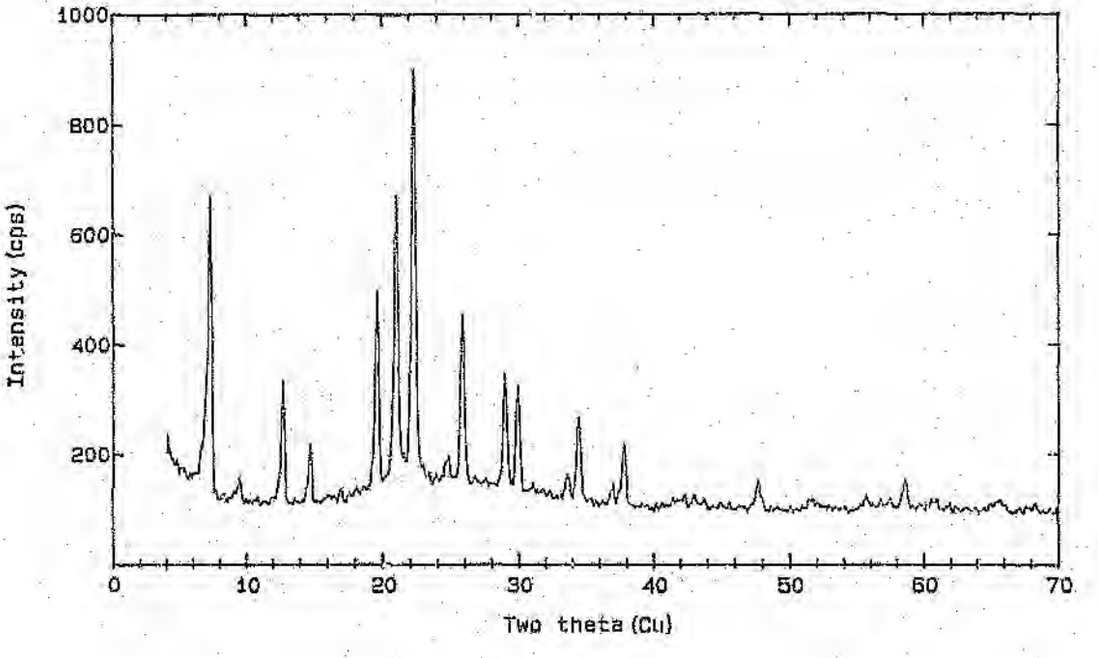


FIG 40 : XRD PATTERN OF REGENERATED SAPO-5

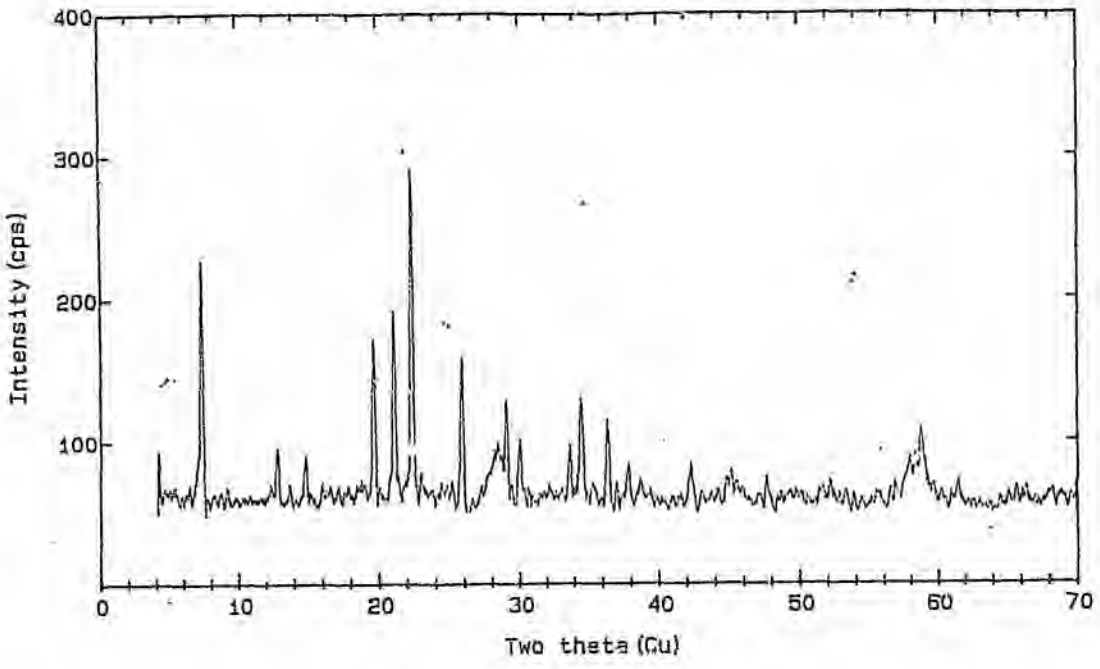


FIG 41 : XRD PATTERN OF REGENERATED Ni-SAPO

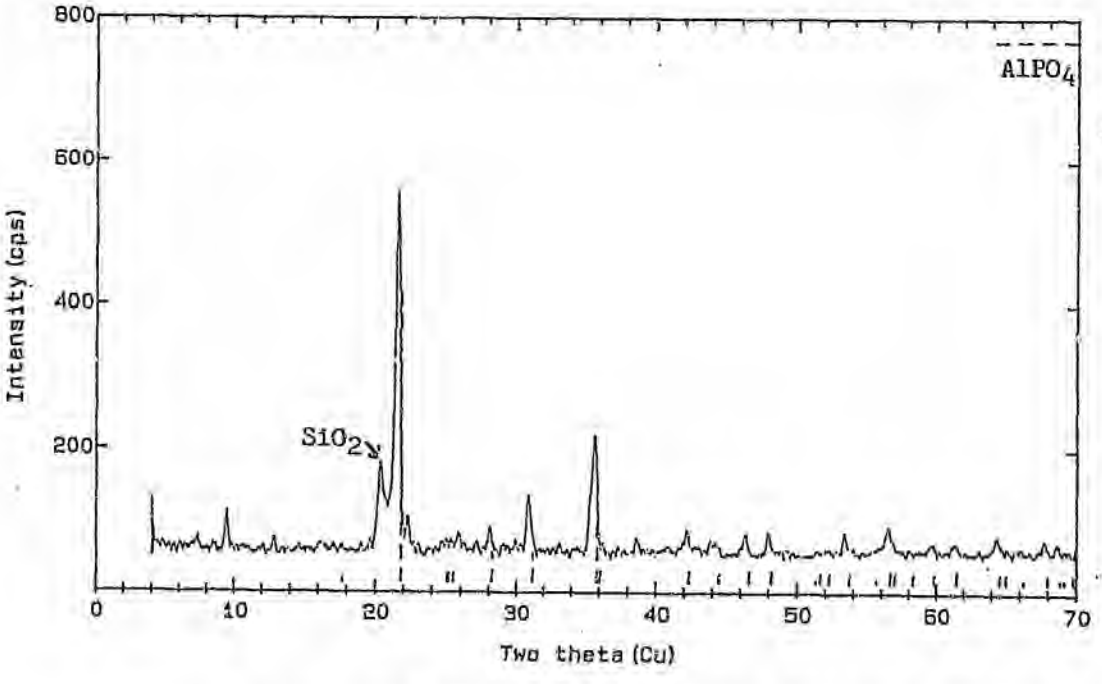


FIG 42 : XRD PATTERN OF REGENERATED SILICON-MODIFIED SAPO-34

XRF spectroscopy of the regenerated catalysts confirmed that some dealumination of SAPO-34, Ni-SAPO and silicon modified SAPO-34

occurred during the regeneration procedure. The change in Al : P : Si ratio of these catalysts, as well as for SAPO-5 which showed no dealumination, are shown in Table VIX.

TABLE XIX : XRF ANALYSIS OF THE FRESH AND REGENERATED CATALYSTS

	FRESH CATALYST	REGENERATED CATALYST
CATALYST	Al : P : Si mole ratio	Al : P : Si mole ratio
SAPO 34	1.00 : 0.86 : 0.27	1.00: 0.94 : 0.25
SAPO-5	1.00 : 0.93 : 0.22	1.00: 0.92 : 0.23
Ni-SAPO	1.00 : 0.75 : 0.19	1.00: 1.05 : 0.22
Si-SAPO	1.00 : 0.80 : 0.10	1.00: 0.95 : 0.20

The P : Al mole ratio of the regenerated catalysts increased in the SAPO-34, Ni-SAPO and Si-SAPO catalysts which shows that dealumination had occurred. The Si : Al ratio remained constant, but the silicon content was at the lower detection limit of the XRF spectrometer, so it was difficult to detect any slight changes.

6.5 CONCLUSIONS

Both thermal gravimetric analysis and G.C. mass spectroscopy showed that some light hydrocarbons were released from the deactivated catalysts during thermal ramping under nitrogen.

G.C. analysis showed that carbon oxides were released during regeneration when oxygen was introduced. G.C. mass spectroscopy

was used to show that bulky aliphatics and aromatics, including naphthalenes, were also released during the oxidative regeneration stage. The concentrations of these species were below the detection limit of the G.C. analysis technique, but a novel technique of trapping the organics in resin in capillary inlet tubes for G.C. mass spectroscopy analysis was successful.

The organics which were released from the catalysts during regeneration were related to the size of the pores to some extent as well as to the presence (SAPO catalysts) or absence of cavities (H-ZSM-5) at the channel intersections. The major organic species released from SAPO-34 were in the range C_{11} to C_{13}, whereas organics in the range of C_{11} to C_{15} were released from SAPO-5 due to its larger pores. H-ZSM-5 has medium size pores but no cavities, and the major species in the released organics were in the range of C_{11} to C_{12}. The major organics released from Ni-SAPO, on the other hand, were in the range C_7 to C_9 due to either weaker or fewer acid sites, or metal-assisted decomposition of the organics during regeneration. More aliphatic hydrocarbons were released from the silicon-modified SAPO-34 which may indicate that the rate of dehydrogenation and cyclization decreased as a result of the modification. The pore size was not affected significantly as the major species released were in the C_{11} to C_{13} range, as obtained with SAPO-34.

The catalytic activity of the regenerated SAPO-34 was lower than that of the fresh catalyst, possibly due to changes in the acidity arising from dealumination during regeneration [6.2, 6.3]. Dealumination of SAPO-34, Ni-SAPO and the silicon-modified

SAPO-34 was observed by determining the Al : P : Si ratio by XRF spectroscopy.

The SAPO-34 framework may also have been affected by dealumination during regeneration as the surface areas of the regenerated SAPO-34 were lower than for the fresh catalyst. All the regenerated catalysts were shown to have lower surface areas than the fresh catalysts.

The regeneration procedure was shown to be effective in the removal of "coke" as the amount of residual carbon in the catalysts after regeneration was shown to be between 0.13 and 0.20 mass %. This shows that 99.95 to 99.9 % of the carbonaceous deposits were removed from the catalysts during regeneration.

XRD spectroscopy was used to show that the crystallinity of the H-ZSM-5, SAPO-34, SAPO-5 and Ni-SAPO catalysts was not affected by using the catalysts for methanol conversion, or by regenerating the catalysts. The XRD pattern of the regenerated silicon modified SAPO-34 was mainly that of silica. The trimethyl silicon chloride treatment thus resulted in the formation of some extraframework silicon which may have migrated to the surface during the methanol conversion or regeneration procedures.

6.6 REFERENCES

6.1] Hutchings, G.J., Copperthwaite, R.G., Hunter, R., Jansen van Re' burg, L., Comninos, H. and Themistocleous, T.; *J. Chem, Soc., Faraday Trans. 1*, 85 (3), (1989), 633

6.2] Fyfe, C.A., Kennedy, G.J., Kokotailo, G.T. and De Schulter, G.T.; *J. Chem. Soc., Chem. Commun.*, (1984), 1093

6.3] Ryabov, Y.V., Echevskii, G.V., Antonova, N.V., Antsiburova, E.A., Kalinina, N.G., Poluboyarov, V.A., Erofeev, V.I. and Anufrienko, V.F.; *Kinetika i Katalis*, 28 (5), (1987), 1217

6.4] Kaiser, S.W.; *Arabian J. Sci.*, 10 (4), (1985), 361

6.5] Lewis, J.M.O., *J. Catal.*, 97, (1987), 199

CHAPTER SEVEN. : CONCLUSIONS

SAPO-34 and SAPO-5 catalysts were found to deactivate rapidly during methanol conversion reactions due to pore blockage by "coke" deposition. This is mainly due to the large ellipsoidal cavities in SAPO-34 and SAPO-5 which allow bulky "coke" intermediates to form, and the narrower pore networks which limit the diffusion of "coke" molecules out of the catalyst. The blockage of channel intersections limits the access of reactants to the acid sites, and of products out of the catalyst. The amount of "coke" deposited was not influenced by the strength of the acid sites as increasing numbers of strong acid sites were detected in SAPO-5, SAPO-34 and H-ZSM-5 whereas the amount of "coke" deposited during 5 hours of methanol conversion decreased from 8.3 % to 7.2 % to 3.3 % for the three catalysts respectively.

Modification of the SAPO-34 catalyst with silicon decreased the rate at which "coke" was deposited. The silicon treatment could have resulted in the occupation of strong acid sites on the surface of the catalyst, or within the large cavities by silicon atoms. This would decrease the rate of "coke" formation but not the rate of methanol conversion. The rate of "coke" formation was not decreased by the incorporation of Ni into the SAPO framework. The nature of the "coke" was affected by the nickel incorporation. The number and strength of acid sites may have decreased, which would have decreased the rate of alkylation and

aromatization reactions during "coke" formation, or the nickel could have facilitated the cracking of carbonaceous deposits.

Dilution of the methanol with nitrogen and / or water was shown to decrease the rate of "coke" formation. Water competed with the products for occupation of the acid sites, thereby retarding the rate of oligomerization and aromatization reactions which lead to "coke" formation. The nitrogen decreased the residence time of the reactants and products, thereby also decreasing the rate of "coke" forming reactions. The amount of "coke" deposited increased with the methanol WHSV and reaction temperature, as more methanol was converted into hydrocarbons and oligomerization and / or aromatization reactions occurred more rapidly.

Both *in situ* and *ex situ* FTIR analyses showed that the "coke" formed during methanol conversion on SAPO-34 was mainly aliphatic. Dissolving the catalyst framework in HF so that the carbonaceous deposits on SAPO-34 could be extracted with dichloromethane and analysed by G.C. mass spectroscopy, showed that aromatics were formed in addition to aliphatics, but to a lesser extent than with H-ZSM-5.

Trapping the carbonaceous deposits released during regeneration, in resin in G.C. capillary inlet tubes, and subsequent G.C. mass spectroscopy analysis, showed that the "coke" consisted mainly of substituted aromatics. The major carbonaceous species deposited in SAPO-34 were in range C_{11} to C_{13}, in H-ZSM-5 from C_{11} to C_{12} and in SAPO-5 from C_{11} to C_{15}. This was most likely due to the increasing channel size of SAPO-34, H-ZSM-5 and SAPO-5

respectively. Significantly different carbon ranges were obtained from the nickel modified SAPO-34 (C_7 to C_9), possibly due to changes in the number and strength of acid sites or due to the nickel facilitating cracking reactions of the "coke". A greater amount of aliphatic hydrocarbons were released from the silicon modified SAPO catalyst than in SAPO-34. The silicon modification probably decreased the rate of oligomerization and aromatization and hence the rate of deactivation.

The catalytic activity and surface area of the regenerated SAPO-34 was lower than that of the fresh catalyst. This was not due to residual carbon after regeneration as 97 % of the carbon was removed by regeneration. The increased rate of "coke" formation of the regenerated catalyst compared to the fresh catalyst was most likely due to steam dealumination of the SAPO framework during regeneration. XRF spectroscopy was used to show that dealumination had occurred, but XRD spectroscopy showed that the crystallinity of the SAPO-34 did not change after regeneration.

Considering the rapid deactivation of SAPO-34, SAPO-5 and even the nickel- and TMSC-modified SAPO-34, industrial application of these catalysts would require a circulating bed mode of operation. This would entail continuous regeneration of the catalyst in one part of the reactor while the rest of the reactor was used for methanol conversion.

APPENDIX 1 : SURFACE AREA CALCULATIONS

The surface area of the sample was calculated using a simplified version of the BET equation :

$$S = V\ A\ N \left[\frac{1 - P / P}{M} \right]$$

where S = surface area of sample

V = volume (at STP) of gas desorbed

A = Avogadro's number, 6.023×10^{23} molecules/g-mol

N = area of a solid covered by one atom of the adsorbed gas, i.e. 16.2×10^{-20} m^2 for a N atom

P = partial pressure of the adsorbing gas (nitrogen)

P = saturation pressure of the adsorbing gas, typically 15 mmHg above atmospheric pressure for N_2.

M = molar volume of a gas at standard temperature and pressure (STP), 22 414 cm^3/g-mol.

The Chemisorb 2700 was purged with a 30 % N_2 / 70 % He mixture and then calibrated with 1.00 cm^3 of nitrogen. At 22°C and 760 mm Hg pressure, the 1.00 cm^3 of nitrogen should result in a constant of 2.39 as calculated below, so the Chemisorb 2700 was adjusted to give this value before each set of analyses.

$$S = V\left[\frac{273.2\ K}{295.2\ K}\right]\left[\frac{638 mmHg}{760 mmHg}\right]\left[\frac{6.023\times10^{23} \times 16.2\times10^{-20}}{22.414\times10^{3}}\right]\left[1+\frac{0.30\times638 mmHg}{653 mmHg}\right]$$

$$= V[2.39]$$

APPENDIX 2 : PORE VOLUME CALCULATIONS

The equivalent liquid volume (V) of the 10 cm^3 of nitrogen gas used to calibrate the Pulse Chemisorb was determined as follows:

The temperature and pressure during the calibration (295 K and 638 mmHg) were taken into consideration as the equivalent liquid volume is recorded under standard conditions (273 K and 760 mmHg). The molar volume of liquid nitrogen is 34.670 cm^3 and gaseous nitrogen 22 414 cm^3, so a ratio of the two, 0.00155, was used to convert the gaseous volume of nitrogen into a liquid volume.

$$V = \left[\frac{273.2\ K}{295.2\ K}\right]\left[\frac{638\ mmHg}{760\ mmHg}\right]\left[0.00155\right]\left[10\ cm^3\right]$$

APPENDIX 3 : EQUIVALENT METHANOL CONVERSION

The equivalent conversion of methanol (MEOH) is defined as the percentage methanol converted to hydrocarbons, excluding dimethylether (DME). The equivalent conversion of methanol was calculated as follows :

$$\% \text{ MEOH eq. conv.} = \frac{\text{moles MEOH}_{in} - (\text{moles MEOH}_{out} + 64/44 \text{ moles DME}_{out}) \times 100}{\text{moles MEOH}_{in}}$$

The fraction 64/44 is the molar ratio of DME / methanol and the number of moles of methanol out includes both the methanol in the gas phase and in the liquid phase.

Author: Cornel Veronica May.
Name of thesis: The deactivation of silico-aluminophosphate catalysts during methanol conversion reactions.

PUBLISHER:
University of the Witwatersrand, Johannesburg
©2015

LEGALNOTICES:

Copyright Notice: All materials on the University of the Witwatersrand, Johannesburg Library website are protected by South African copyright law and may not be distributed, transmitted, displayed or otherwise published in any format, without the prior written permission of the copyright owner.

Disclaimer and Terms of Use: Provided that you maintain all copyright and other notices contained therein, you may download material (one machine readable copy and one print copy per page)for your personal and/or educational non-commercial use only.

The University of the Witwatersrand, Johannesburg, is not responsible for any errors or omissions and excludes any and all liability for any errors in or omissions from the information on the Library website.